Third-Order Nonlinear Optical Response in Organic Materials: Theoretical and Experimental Aspects

J. L. Brédas,*,† C. Adant,† P. Tackx,‡ and A. Persoons‡

Center for Research on Molecular Electronics and Photonics, Université de Mons-Hainaut, Place du Parc 20, B-7000 Mons, Belgium, and
Center for Research on Molecular Electronics and Photonics, Katholieke Universiteit Leuven, Celestijnenlaan 200D, B-3001 Leuven, Belgium

B. M. Pierce

Hughes Aircraft Company, Building R2, MS V518, P.O. Box 92426, Los Angeles, California 90009-2426

Contents

I. Introduction

As is exemplified by this issue of *Chemical Reviews*, nonlinear optical processes are being increasingly exploited in a variety of optoelectronic and photonic applications. For instance, the third-order nonlinear optical phenomenon of an optically-induced change in refractive index is fundamental to all-optical switching and computing, as well as phase conjugate adaptive optics.[1-3] The high-speed processing of data is essential to numerous technologies like computing and telecommunication systems. It is predicted that the future photonic switching office for telecommunications will operate 10 000 channels producing a combined bit-rate of 1 terabit/s or 10^{12} bit/s.[4] In contrast, the current electronic switching offices handle a combined bit-rate of less than 15×10^9 bit/s.[4] All-optical architectures have been designed that are well-suited for the serial and parallel processing of high bit-rate data streams.[1,2,5,6] It is obvious that the efficiencies of these nonlinear optical processes are dependent upon the material employed to couple the given combination of electrical and/or optical signals. The implementation of all-optical signal processing has been slow because of the lack of materials needed for the components in an optically-based signal processor.

Most of the nonlinear optical materials currently used in the fabrication of passive and active photonic devices are ferroelectric inorganic crystals.[3,7-10] For example, the potassium dideuterium phosphate (KDP) crystal is widely employed as a laser frequency doubler, the lithium niobate (LiNbO₃) crystal is virtually the exclusive material of choice for electrooptic modulators

that operate in the near-infrared spectral range, and the barium titanate (BaTiO₃) crystal is being investigated for applications involving phase conjugation. Although the crystal-growing technology for these materials is highly developed and their nonlinear optical susceptibilities are sufficient for most current photonic applications, they have features that are less than desirable. One such feature is the constraint of working with only single-crystalline materials. Another is the relatively slow optical switching time characteristic of photorefractive, ferroelectric inorganic crystals. As an example, the switching time for doped, single-crystalline BaTiO₃ is in the millisecond range at laser intensities of about 1 W/cm².[11] However, this switching time does decrease with increasing laser intensity. This limitation is not critical in applications involving parallel optical signal processing, but is important for serial processing. In conclusion, *new nonlinear optical materials are needed to extend the range of photonic applications made possible by the current set of ferroelectric inorganic crystals.*

Organic materials and inorganic semiconductors are prominent candidates as new nonlinear optical media. This review will focus on organics since these are materials whose development depends strongly on advances in synthetic, physical, and theoretical chemistry. The current progress in inorganic semiconductor materials relies heavily on the fabrication of multiple quantum well structures. It is likely that both types of materials will actually find different application niches. The organic materials are of major interest[12-23] because of their relatively low cost, ease of fabrication and integration into devices, tailorability which allows one to fine tune the chemical structure and properties for a given nonlinear optical process, high laser damage thresholds, low dielectric constants, fast nonlinear optical response times, and off-resonance nonlinear optical susceptibilities comparable to or exceeding those of ferroelectric inorganic crystals.

This contribution will cover the following topics. In section II, some of the material requirements for all-optical processing are presented. The discussion allows us to point out some of the characteristics that need to be fulfilled to optimize third-order nonlinear optical processes. Section III is devoted to an overview of the theoretical techniques that are used to calculate third-order polarizabilities. The goal there is not to go into computational details but to present the spirit which

† Université de Mons-Hainaut.
‡ Katholieke Universiteit Leuven.

Jean-Luc Brédas was born in Fraire, Belgium, in 1954. He obtained his M.Sc. (1976) and Ph.D. (1979) in Chemistry at the Facultés Universitaires Notre-Dame de la Paix in Namur, under the supervision of Jean-Marie André. After a postdoctoral stay (1980–1981) jointly at Allied Corporation with Ray H. Baughman and Ron R. Chance and at MIT with Bob Silbey, he went back to Namur as a Research Fellow of the Belgian National Fund for Scientific Research. He presented his Thèse d'Agrégation in 1986 at the Catholic University of Louvain. He was appointed professor of chemistry and head of the Laboratory for Chemistry of Novel Materials at the University of Mons-Hainaut in 1988 and became full professor in 1990. He has spent extended stays in particular at MIT, IBM San Jose, Exxon Corporate Research Center, Linköping University, and University of California at Santa Barbara. He is currently Director, together with André Persoons, of the Center for Research on Molecular Electronics and Photonics and Chairman of the Department of Materials in Mons. He shares with his research group his interest in the theoretical determination of the electronic structure of conjugated oligomers and polymers, with applications in the fields of conducting and semiconducting polymers, nonlinear optics, and polymer surfaces and interfaces. His other interests include music (both classical and rock), soccer (as a player), and volleyball (as a spectator).

Christine Adant was born in Mons, Belgium, in 1968. She received her M.Sc. degree from the University of Mons-Hainaut in 1990. She is currently working on her Ph.D. in Mons under the supervision of Jean-Luc Brédas. Her main research interests lie in the understanding, on the basis of quantum chemistry calculations, of the relationship between the structural and electronic properties of organic molecules and their third-order nonlinear optical properties.

Peter C. E. Tackx was born in Turnhout, Belgium, in 1967. He studied Physical Chemistry at the Catholic University of Leuven and received his M.Sc. degree in 1989 with a study of second-order nonlinear optical properties of organic molecules. He just presented his Ph.D. Thesis, working in the laboratory of Chemical and Biological Dynamics under the direction of André Persoons. His main interest is the third-order nonlinear optical properties of organic molecules, studied with phase-conjugate interferometry.

André Persoons was born in 1940 in Leuven, Belgium, where he received his education from kindergarten to University obtaining his Ph.D. in Chemistry at the Catholic University of Leuven in 1965 under the guidance of Prof. J. C. Jungers. After a research stay at the Max-Planck Institute für Physikalische Chemie in Göttingen in 1968, where he worked with Leo De Maeyer on instrumental techniques for the study of fast reactions, he returned to the University of Leuven and founded, together with Leo De Maeyer, the Laboratory for Chemical and Biological Dynamics. He became full professor at the K. U. Leuven in 1977 and extraordinary professor at the K. U. Brussel in 1987. He has been visiting professor, as a JSPS fellow, at the University of Hiroshima, Japan. Recently he founded, together with Jean-Luc Brédas, the Center for Research on Molecular Electronics and Photonics. His research group is currently working on nonlinear optical properties of organic and polymeric materials with a strong focus on development of new experimental techniques. Apart from being a lover of literature and an avid book and art collector, he is, together with his wife Martha, breeding golden retrievers in his free time.

guides the approaches followed for *organic compounds of medium to large size*. We should stress that at the present time, very accurate calculations (*i.e.*, allowing for quantitative estimates) of third-order polarizabilities can only be performed on atoms or very small molecules. For the kind of organic molecular or macromolecular compounds which are being investigated for actual applications and for which theoretical guidance is highly desirable, the very size of the systems precludes the possibility of predicting absolute hyperpolarizability values. Therefore, one has to rely mostly on trends obtained on series of chemically-related compounds. In that section, we also discuss the physical origin of the third-order response in conjugated materials on the basis of simple models as well as the connection between the microscopic hyperpolarizabilities and the macroscopic electric susceptibilities. The following section contains a practical description of the major experimental techniques used to probe the third-order nonlinear responses. For each technique, emphasis is placed on the type of nonlinear optical response that is probed, the time scales for the response, and the possibilities of obtaining the phase characteristics. Finally, section V deals with an overview of the organic

Brian M. Pierce was born in Los Angeles, CA, in 1955. He received his B.S. degree with highest honors (1978) in chemistry and mathematics from the University of California at Riverside, and his Ph.D. degree from University of California at Riverside under the direction of Prof. Robert R. Birge. He has been with the Hughes Aircraft Company since 1983, and is currently a Senior Project Engineer in the Electromagnetic Systems Laboratory of the Radar Systems organization. In 1988, he was a guest professor in the Laboratory for Applied Mathematical Physics at the Technical University of Denmark. His principal research interests are the theoretical design and development of nonlinear dielectric materials for device applications.

materials that are being considered for third-order nonlinear optical processes; there also the aim is much more to provide guidelines than a comprehensive list.

II. Material Requirements

The components central to most all-optical signal processors are waveguide devices that switch or control optical beams through phase shifts resulting from light-induced changes in the refractive index of the material comprising the waveguide. Such devices include the $1/2$ beat-length directional coupler, the 1 beat-length directional coupler, the distributed feedback grating, the Mach–Zehnder interferometer, the mode sorter, and the prism coupler.[5,6] The phase shift for an optical beam at wavelength λ is related to the light-induced change in refractive index in the following manner:

$$\Delta\phi(\lambda,I) = \frac{2\pi l \Delta n(\lambda,I)}{\lambda} \quad (1)$$

where $\Delta\phi(\lambda,I)$ is the phase shift as a function of the radiation wavelength and light intensity, l is the interaction length, and $\Delta n(\lambda,I)$ is the change in the real part of the refractive index as a function of λ and I. High optical power densities on the order of MW/cm^2 are generally needed to induce $\Delta n(\lambda,I)$'s large enough so that phase shifts of π radians can be achieved over propagation lengths of at least 10^{-3} cm.[5,6] The minimum light-induced phase shifts required for an all-optical waveguide device can vary from 0.5π to 7π depending on the type of device and the origin of the light-induced change in refractive index.[5,6] One should consult ref 6 for a more detailed description of all-optical waveguide devices and the different phase shifts required by these devices.

The 10^{-6}-cm^2 cross-sectional areas typical of fiber and channel-guided wave structures make it possible to obtain power densities on the order of MW/cm^2 using lasers with modest peak powers of <1 W. Candidate materials for these waveguide structures should have:

(i) high susceptibilities for light-induced changes in refractive index so that the optical power density can be kept as low as possible; (ii) small linear and nonlinear absorption coefficients in order that the optimal propagation lengths can be achieved and that the photoinduced heating is minimized; and (iii) sub-picosecond lifetimes for the change in refractive index. These features are quantified by the figures of merit defined below.

A more detailed discussion of the light-induced change in the real refractive index must begin with the real relative permittivity of the material and its dependence on the applied electric field(s):

$$\epsilon(\lambda,E) = 1 + 4\pi\chi(\lambda,E) \quad (2)$$

where $\chi(\lambda,E)$ is the real electric susceptibility of the medium as a function of λ and the electric field. This susceptibility determines the extent to which the medium is polarized by an applied electric field(s). Note that the units for eq 2 are electrostatic units (esu), with the permittivity of free space, ϵ_0, set equal to $1/4\pi$.

The $\chi(\lambda,E)$ has linear and nonlinear components that result from the expansion as a Taylor series in powers of E:

$$\chi(\lambda,E) = \chi^{(1)}(\lambda) + (1/2!)\chi^{(2)}(\lambda)E + (1/3!)\chi^{(3)}(\lambda)E^2 + \underset{\cdots}{} \quad (3)$$

where $\chi^{(2)}(\lambda)$ and $\chi^{(3)}(\lambda)$ are the real second- and third-order nonlinear electric susceptibilities. If one replaces $\chi(\lambda,E)$ in eq 2 with the expression given in eq 3 and defines the linear component of the real permittivity as

$$\epsilon^{(1)}(\lambda) = 1 + 4\pi\chi^{(1)}(\lambda) \quad (4)$$

then eq 2 becomes

$$\epsilon(\lambda,E) = \epsilon^{(1)}(\lambda)\left(1 + \left[\frac{4\pi}{\epsilon^{(1)}(\lambda)}\right][1/2\chi^{(2)}(\lambda)E + 1/6\chi^{(3)}(\lambda)E^2 + ...]\right) \quad (5)$$

Recall that the real refractive index, $n(\lambda,E)$, can be taken to be equal to the square root of $\epsilon(\lambda,E)$ for most low-loss dielectric materials. The use of the binomial expansion to evaluate the square root of the sum in eq 5 yields the following approximation of $n(\lambda,E)$:

$$n(\lambda,E) \cong n_0(\lambda) + \left[\frac{2\pi}{n_0(\lambda)}\right][1/2\chi^{(2)}(\lambda)E + 1/6\chi^{(3)}(\lambda)E^2 + ...] \quad (6)$$

where $\epsilon^{(1)}(\lambda) = n_0(\lambda)^2$. The expansion can be truncated after the first two terms because the sum, $((\chi^{(2)}(\lambda)/2)E + (\chi^{(3)}(\lambda)/6)E^2 + ...)$, is taken to be much less than 1.

In the case of applied electric field(s) varying in time, the electric field components of eq 6 are replaced by temporal averages:

$$n[\lambda,E(t)] \cong n_0(\lambda) + \left[\frac{2\pi}{n_0(\lambda)}\right][1/2\chi^{(2)}(\lambda)\langle E(t)\rangle + 1/6\chi^{(3)}(\lambda)\langle E(t)^2\rangle + ...] \quad (7)$$

For a plane sinusoidal electromagnetic wave, the $\langle E(t)^2\rangle$ term is related to the intensity of the wave, $I(t)$, by the following expression (in esu):

$$\langle E(t)^2\rangle = 4\pi[I(t)/c] \quad (8)$$

where c is the speed of light. The *contribution of*

nonresonant electric-field-induced polarization of the material to the light-induced change in real refractive index is defined by the term in the expression for $n[\lambda, E(t)]$ that is proportional to the light intensity, $I = I(t)$:

$$\Delta n_{ep}(\lambda, I) = \frac{8\pi^2}{cn_0(\lambda)} \frac{\chi^{(3)}(\lambda)}{6} I \qquad (9)$$

(where the subscript ep refers to electric-field induced polarization). The nonlinear refractive index defined by eq 9 is generally given as

$$n_2(\lambda) = \frac{8\pi^2}{cn_0(\lambda)} \frac{\chi^{(3)}(\lambda)}{6} \qquad (10)$$

The subscript 2 in $n_2(\lambda)$ is employed because this nonlinear refractive index is associated with the square of the applied electric field. This response is also known as the quadratic electrooptic response or the optical Kerr effect. It is emphasized that the above two equations are only appropriate for a *Taylor series* expansion of $\chi(\lambda, E)$, where the expansion coefficient of $(1/3!)$ is not incorporated into the definition of $\chi^{(3)}(\lambda)$, in which case one deals with a *power series*.

The *nonresonant* electric-field-induced polarization of the material can occur through several different processes, each with a characteristic time scale. For instant, the polarization of electrons is the fastest with response times ranging from 10^{-15} to 10^{-14} s. Successively slower polarization responses are those involving ionic or atomic displacements, the reorientation of molecules or domains, and the bulk phenomenon of electrostriction. Another contribution to the light-induced change in real refractive index for the material is that resulting from the light-induced heating of the material, or the thermooptic effect. This effect is related to the linear and nonlinear absorptivities of the material at λ, and the change in real refractive index is given here as $\Delta n_{th}(\lambda, I)$. Thus, the total change in refractive index proportional to the light intensity can be expressed as

$$\Delta n(\lambda, I) = \Delta n_{ep}(\lambda, I) + \Delta n_{th}(\lambda, I) \qquad (11)$$

In order to achieve the high processing speeds required for optical devices that exploit the intensity-dependent refractive index, it is desirable that the relatively long-lived thermooptic contribution is minimized and the rapid electronic polarization component of $\Delta n_{ep}(\lambda, I)$ is maximized.

A useful figure of merit that defines the optical switching performance of a third-order nonlinear optical material is

$$F(\lambda) = \frac{\chi^{(3)}(\lambda)}{\alpha'(\lambda) \tau} \qquad (12)$$

where $\chi^{(3)}$ is the third-order electric susceptibility which determines the third-order nonlinear optical response, α' denotes the sum of the linear and nonlinear absorptivity, and τ is the lifetime of the third-order nonlinear optical response. It is assumed here that the attenuation of light due to scattering is insignificant compared to the intrinsic absorption by the material. Thus, the larger the magnitude of $\chi^{(3)}(\lambda)$, the lower the light intensities required to induce switching; the lower the

linear *and* nonlinear absorptivity, the longer the propagation length possible for a phase shift for a given $\chi^{(3)}$ and the lower the probability of thermal effects overwhelming the response; the shorter the lifetime, the faster the serial processing speed of the switch. In the case of serial all-optical signal processing, it is very desirable that τ be sub-picosecond.

Although the figure of merit given in eq 12 is effective in illustrating the important material properties needed to achieve efficient all-optical switching, it is not dimensionless and it does not explicitly separate the impact of linear and nonlinear absorption. Stegeman has defined dimensionless figures of merit that are more suitable for evaluating materials.[6] The starting point for deriving these figures of merit is the approximate expression for intrinsic linear and nonlinear absorption:[6]

$$\alpha'(\lambda) \simeq \alpha_0 + \beta_2 I + \beta_3 I^2 \qquad (13)$$

where α_0 is the linear, one-photon absorption coefficient at λ; β_2 is the nonlinear, two-photon absorption coefficient at λ; and β_3 is the nonlinear, three-photon absorption coefficient at λ. The expression for $\alpha'(\lambda)$ is approximate because nonlinear absorption processes of higher order than 3 are neglected. The three absorption coefficients give rise to three figures of merit.[6]

The first figure of merit results from a dominant linear, one-photon absorption such that $\alpha_0 \gg \beta_2 I + \beta_3 I^2$, and $1/\alpha_0 > d$, where d is the propagation length. If a normalized phase shift for this case is defined as $W = \Delta\phi/2\pi$, then

$$W = \frac{n_2(\lambda) I}{2\alpha_0 \lambda} > 1 \qquad (14)$$

is needed to switch, for example, a 1 beat-length directional coupler. Note that we assume for all three figures of merit that $\Delta n(\lambda, I)$ is defined solely by $n_2(\lambda) I$, i.e., the candidate nonlinear optical material is a Kerr medium whose refractive index changes linearly in response to the light intensities of interest.

The second figure of merit results from a dominant two-photon absorption such that $\beta_2 I \gg \alpha_0 + \beta_3 I^2$, and $(1/\beta_2 I) > d$. If the inverse of the normalized phase shift for this case is defined as $T = 2\pi/\Delta\phi$, then

$$T = \frac{2\beta_2 \lambda}{n_2(\lambda)} < 1 \qquad (15)$$

is needed to switch, for example, a 1 beat-length directional coupler. In contrast to W, the T figure of merit has no dependence on the light intensity I. This is due to the fact that both β_2 and $n_2(\lambda)$ are associated with the square of the light intensity.

The third figure of merit results from a dominant three-photon absorption such that $\beta_3 I^2 \gg \alpha_0 + \beta_2 I$, and $(1/\beta_3 I^2) > d$. If the inverse of the normalized phase shift for this case is defined as $V = 2\pi/\Delta\phi$, then

$$V = \frac{2\beta_3 I_{sw} \lambda}{n_2(\lambda)} < 1 \qquad (16)$$

is needed to switch, for example, a 1 beat-length directional coupler. The I_{sw} term is the switching intensity of the device of interest. For the majority of devices, I_{sw} is inversely proportional to the device length, and so it is possible to reduce the V figure of merit by constructing longer devices, thereby reducing the

Table 1. Summary of Properties That Characterize the Optical Switching Performance of Several Candidate Nonlinear Optical Materials (from Ref 6)

material	n_2 (cm^2/W)	α_0 (cm^{-1})	W^a	T^b	$W/(1 + T)^c$	λ (nm)
		Semiconductors				
GaAs	$<-3 \times 10^{-13}$	1.0	<2.8	>17	<0.06	1064
AlGaAs (790 nm)^d	-4×10^{-12}	18	2.5	0.9	0.77	810
AlGaAs (750 nm)^e	2×10^{-13}	0.1	8	<0.3	>2.35	1560
		Organics				
PTS (crystal)^f	-2×10^{-12}	0.8	40	4	0.25	1064
poly-4BCMU^g	5×10^{-14}	<0.2	>2.5	<1.0	>0.71	1310
DANS (polymer)	8×10^{-14}	<0.2	>4.0	~ 1	>0.80	1060
	8×10^{-14}	<0.2	>5.0	~ 0.2	>2.50	1310
DEANST (20% solution)	6×10^{-14}	$<10^{-2}$	>40	<1	>0.98	1064
DAN (crystal)	5×10^{-12}	3	26			630
	-10^{-12}					1320
DAN2 (polymer)	2×10^{-13}	<1	>2	<1	>0.67	1064
		Inorganic Oxide Glasses				
SiO$_2$	2×10^{-16}	10^{-6}	$>10^3$	$\ll 1$	$\gg 1$	>1064
RN (Corning)	1.3×10^{-14}	0.01	13	<0.1	>5.65	1064

^{a} Goal for W is >1. ^{b} Goal for T is <1. ^{c} Goal for $W/(1 + T)$ is > 1. ^{d} AlGaAs with a 790-nm bandgap. ^{e} AlGaAs with a 750-nm bandgap. ^{f} Reference 24. ^{g} Reference 62.

switching power.[6] Fortunately, due to the very small magnitude of β_3, the V figure of merit is generally insignificant. One can continue to define figures of merit for four-photon and higher order absorption, but this has not been seen to be necessary because of the low absorption coefficients.

In summary, the combined effect of the three figures of merit for switching a 1 beat-length directional coupler is given by

$$1 < \frac{\Delta\phi}{2\pi} = \frac{W}{(1 + WT + WV)} \qquad (17a)$$

or since WV is usually much less than WT,

$$1 < \frac{\Delta\phi}{2\pi} = \frac{W}{(1 + WT)} \qquad (17b)$$

Measured values of $n_2(\lambda)$, α_0, W, T, and $W/(1 + WT)$ at different wavelengths for several candidate nonlinear optical materials are presented in Table 1.[6] These candidate materials are classified as semiconductors, organics, or inorganic oxide glasses. Recall that the T term contains the measured two-photon absorption coefficient, β_2. It is assumed in this table that $I = 1$ GW/cm^2, which corresponds to a 200-W laser peak power focused into a channel waveguide with a cross-sectional area of 10^{-7} cm^2. All materials in Table 1 were measured to have switching times on the order of picoseconds and less.

The two materials with the best figures of merit that meet the goals for W (>1), T (<1), and $W/(1 + WT)$ (>1) are the SiO$_2$ and Corning RN inorganic oxide glasses. The reason for this result is the very low absorptivity of these glasses compared with the organics and semiconductors. Of course, the intrinsic nonlinearities of the organics and semiconductors, as reflected in the values of $n_2(\lambda)$, are higher than those for the glasses. In the case of the organics presented in Table 1, the material with the best figure of merit is the DANS [(dimethylanilino)nitrostilbene] doped polymer with a value of >2.50 for $W/(1 + WT)$ at 1310 nm. All the other organics have values of $W/(1 + WT)$ less than 1. The figures of merit for the semiconductors in Table 1 are not much better than those for the organics. The semiconductor with the best figure of merit is AlGaAs

(750 nm) with a value of $W/(1 + WT)$ of >2.35 at 1560 nm. The GaAs figures of merit make it a very unlikely candidate for all-optical waveguide device applications.

Improvements in the properties of both organics and semiconductors are needed if they can be used effectively in all-optical signal processing applications. It must be borne in mind that the linear and nonlinear absorptivities for a material and the $n_2(\lambda)$ are not independent of each other. For example, the real and imaginary components of the complex linear refractive index are related through the Kramers–Kronig transform. Generally, the larger the magnitude of $n_2(\lambda)$, the greater the magnitudes of the linear and nonlinear absorption coefficients. This relationship is seen in the data presented in Table 1.

The optical requirements for the third-order nonlinear optical materials critical to optical signal processing are defined well by the figures of merit described above. It is also desirable that the saturated change in refractive index is very high with a value >0.01, and that the optical damage threshold exceeds 1 GW/cm^2 peak power. In addition to these optical requirements, the materials should be mechanically tough, environmentally resistant, formable into thin-films and coatings, and possess a wide operational temperature range.

III. Theoretical Aspects

A. General Concepts

The necessary starting point is Maxwell's equations which govern all electromagnetic phenomena depending on electric and magnetic fields $\mathbf{E}(\mathbf{r},t)$ and $\mathbf{B}(\mathbf{r},t)$:

$$\nabla \times \mathbf{E} = -\frac{1}{c}\frac{\partial \mathbf{B}}{\partial t}$$

$$\nabla \times \mathbf{B} = \frac{1}{c}\frac{\partial \mathbf{E}}{\partial t} + \frac{4\pi}{c}\mathbf{J} \qquad (18)$$

$$\nabla \cdot \mathbf{E} = 4\pi\rho$$

$$\nabla \cdot \mathbf{B} = 0$$

It is often possible to expand the charge density ρ and

the current density $\mathbf{J}$ into a series of multipoles. The charge density and the current density take then the form

$$\rho = \rho_0 - \nabla\cdot\mathbf{P} - \nabla(\nabla\cdot\mathbf{Q}) + \dots$$

$$\mathbf{J} = \mathbf{J}_0 + \frac{\partial\mathbf{P}}{\partial t} + c\,\nabla\times\mathbf{M} + \frac{\partial}{\partial t}(\nabla\cdot\mathbf{Q}) + \dots \quad (19)$$

where $\mathbf{P}$ is the electric dipole polarization, $\mathbf{Q}$ the electric quadrupole polarization, and $\mathbf{M}$ the dipole magnetization. In many instances, the magnetic dipole and the higher-order multipoles can be neglected, which leads to the so-called *electric dipole approximation*. Note that the electric dipole polarization $\mathbf{P}$ is a local function of the electric field. In this case, two of Maxwell's equations are rewritten as

$$\nabla\times\mathbf{B} = \frac{1}{c}\frac{\partial}{\partial t}(\mathbf{E} + 4\pi\mathbf{P}) + \frac{4\pi}{c}\,\mathbf{J}_{\mathrm{dc}}$$

$$\nabla\cdot(\mathbf{E} + 4\pi\mathbf{P}) = 0 \quad (20)$$

where $\mathbf{J}_{\mathrm{dc}}$ is the dc current density and $\mathbf{E} + 4\pi\mathbf{P}$ is the displacement $\mathbf{D}$.

The electric dipole polarization $\mathbf{P}$ is a complicated nonlinear function of the electric field $\mathbf{E}$, which describes the response of the medium to the field. The convention for the electric field used throughout this paper is the electric dipole component of the summation:

$$\mathbf{E}(\mathbf{r},t) = Re\sum\nolimits_{\mathrm{w,k}}{}^1\!/_2[\mathbf{E}(\omega,\mathbf{k})e^{i(\omega t - \mathbf{k}\mathbf{r})} + \mathrm{c.c}] \quad (21)$$

where $\mathbf{k}$ is the wavevector for the field at angular frequency ω, and c.c. is the complex conjugate of $\mathbf{E}(\omega,\mathbf{k})e^{i(\omega t - \mathbf{k}\mathbf{r})}$. In the case of a given ω and k, the dielectric dipole component is

$$\mathbf{E}(t) = |\mathbf{E}(\omega,\mathbf{k})|^1\!/_2[e^{i\omega t} + e^{-i\omega t}] \quad (22)$$

When the electric field is not too large, the polarization as a function of $\mathbf{E}$ can be expanded as a power series of $\mathbf{E}$. Fourier transforming the dependence of $\mathbf{E}$ on $\mathbf{r}$ (position) and t (time) to a dependence on $\mathbf{k}$ and $\omega = 2\pi\nu$ leads to the following general expression[25] where reference to $\mathbf{k}$ is dropped since $\mathbf{P}$ is a local function of the field ($\mathbf{P}_0$ denotes the possible permanent polarization):

$$\mathbf{P}(\omega) = \mathbf{P}_0 + \chi^{(1)}(\omega)\cdot\mathbf{E}(\omega) + \chi^{(2)}(\omega=\omega_i+\omega_j+\omega_k)\cdot\cdot\mathbf{E}(\omega_i)\mathbf{E}$$

$$(\omega_j) + \chi^{(3)}(\omega=\omega_i+\omega_j+\omega_k)\cdot\cdot\cdot\mathbf{E}(\omega_i)\mathbf{E}(\omega_j)\mathbf{E}(\omega_k) + \dots \quad (23)$$

The $\chi^{(n)}$ terms correspond to tensors of order $(n+1)$; they represent the electric susceptibilities of order n of the medium and fully characterize its linear and nonlinear optical properties. We recall that the linear dielectric constant $\epsilon^{(1)}(\omega)$ is related to the first-order susceptibility by

$$\epsilon^{(1)}(\omega) = 1 + 4\pi\chi^{(1)}(\omega) \quad (24)$$

It is important to bear in mind that, within the electric dipole approximation, because of symmetry relations, all electric susceptibilities of even orders vanish when centrosymmetry is present; quadratic responses can thus be obtained only in noncentrosymmetric media while there is no such constraint on the cubic response. (Note that quadratic responses can sometimes be observed in centrosymmetric media, due to the presence of significant magnetization effects.[26])

Physically, the electric susceptibilities are related to the microscopic structure of the medium. In organic compounds, it is therefore useful to address the nonlinear optical response at the molecular level. It then becomes possible to determine the relationship between the molecular architecture and the optical properties, which is essential in order to design materials with optimal characteristics. The evolution of the dipole moment as a function of electric field is the fundamental molecular parameter that needs to be evaluated (μ_0 is the possible permanent dipole moment):

$$\mu(\omega) = \mu_0 + \alpha(\omega)\cdot\mathbf{E}(\omega) + \beta(\omega=\omega_i+\omega_j)\cdot\cdot\mathbf{E}(\omega_i)\mathbf{E}(\omega_j) +$$

$$\gamma(\omega=\omega_i+\omega_j\omega_k)\cdot\cdot\cdot\mathbf{E}(\omega_i)\mathbf{E}(\omega_j)\mathbf{E}(\omega_k) + \dots \quad (25)$$

Here, α, β, and γ are tensors that correspond to the first-, second-, and third-order polarizabilities. We describe at the end of this section how it is possible to pass from the microscopic to the macroscopic quantities.

B. Quantum-Chemical Evaluation of Molecular Polarizabilities

In the context of quantum-chemical calculations, there are three main approaches which are followed. We do not intend to describe these methods in detail since they have already been largely documented in the literature but it is instructive to point out their main characteristics.

1. Derivative and Time-Dependent Techniques

The first type of techniques are derivative techniques which rely on the fact that the static first- (second-, third-) order polarizability tensor components can be obtained as first- (second-, third-) order derivatives of a given dipole moment component μ_i with respect to the field:

$$\alpha_{ij}(0) = \left(\frac{\partial\mu_i}{\partial\mathbf{E}_j}\right)_{\mathbf{E}\to 0}$$

$$\beta_{ijk}(0) = \left(\frac{\partial^2\mu_i}{\partial\mathbf{E}_j\partial\mathbf{E}_k}\right)_{\mathbf{E}\to 0} \quad (26)$$

$$\gamma_{ijkl}(0) = \left(\frac{\partial^3\mu_i}{\partial\mathbf{E}_j\partial\mathbf{E}_k\partial\mathbf{E}_l}\right)_{\mathbf{E}\to 0}$$

Note that the dipole moment itself is the negative first-order derivative of the molecular total energy U_{tot} as a function of electric field (Stark energy):

$$U_{\mathrm{tot}}(\mathbf{E}) = U_{\mathrm{tot}_0} - \mu_0\cdot\mathbf{E} - \frac{1}{2!}\alpha\cdot\cdot\mathbf{EE} - \frac{1}{3!}\beta\cdot\cdot\cdot\mathbf{EEE} -$$

$$\frac{1}{4!}\gamma\cdot\cdot\cdot\mathbf{EEEE} + \dots \quad (27)$$

$$\mu_i(\mathbf{E}) = -\frac{\partial U_{\mathrm{tot}}(\mathbf{E})}{\partial\mathbf{E}_i} \quad (28)$$

The molecular polarizability of order n can therefore be evaluated as the nth-order derivative of the dipole moment or the $(n+1)$th-order derivative of the total energy.

Evaluation of the derivatives can be carried out numerically or analytically within the coupled Hartree–

Fock scheme. A numerical procedure is used in the finite-field approach, originally proposed by Cohen and Roothaan,[27] where the molecular Hamiltonian explicitly includes an electric-field-dependent term:

$$H = H_0 - \mu E \qquad (29)$$

Several Hartree–Fock self-consistent-field or post-Hartree-Fock calculations need to be performed for different numerical values of the electric field. A numerical differentiation of the total energy or dipole moment as a function of the different field values is then performed at the limit of vanishing field. The electric-field values are usually chosen to be on the order of 10^{-3} atomic unit (1 atomic unit of electric field is equal to 5.14×10^{11} V/m). They constitute the result of a compromise; in order to boost the precision of the derivation, it is best to deal with large field strengths but too large fields lead to difficulties in achieving convergence of the self-consistent-field procedure.

The finite-field technique is now routinely exploited for large molecules at the Hartree–Fock *ab initio*[28] and semiempirical[29] levels. It is being used within calculations including the treatment of electron correlation; finite-field second-order Møller–Plesset calculations have been very recently reported on paranitroaniline.[30] The MOPAC package has popularized the use of the finite-field approach[29] with the AM1 (Austin Model 1) or PM3 Hamiltonians. We stress that the AM1 finite-field method has been largely applied with a good deal of success to the evaluation of the static (zero photon frequency) second-order (β components) nonlinear optical response of conjugated molecules.[31-34] It has also been tested for the third-order response, in particular by Matsuzawa and Dixon.[34]

In the analytical coupled perturbed Hartree–Fock technique, the derivation is carried out analytically at the end of a usual self-consistent-field calculation following the general methodology of Dykstra for gradients of the total energy.[35] This method has been extensively developed at the Hartree–Fock *ab initio* level mainly through the work of Dupuis and co-workers, and of Karna, Prasad and co-workers.[36-38] In that context, using extended and diffuse basis sets, it is by now possible to obtain reliable third-order molecular polarizability *trends* in molecules containing up to 20 carbon or equivalent atoms. However, the absolute calculated values often remain 5–10 times smaller than the experimental values which is a consequence of (i) the neglect of correlation effects and (ii) the fact that the calculations refer to gas-phase values while the measurements are carried out in condensed phase.

A second type of technique is the time-dependent Hartree–Fock (TDHF) method[39-43] which, in contrast to the derivative techniques which can only provide static polarizability components, allows for the calculation of the dynamic components. The TDHF method solves the wave function of the ground electronic state in the presence of the oscillating electric field; it is a variational method for the calculation of both static and dynamic linear and nonlinear polarizabilities.

At this stage, we would like to comment on three issues which impacts on the overall quality of *ab initio* third-order polarizability results. A first issue is the *choice of the basis functions* used for the calculations. Our experience is that, for second-order polarizabili-
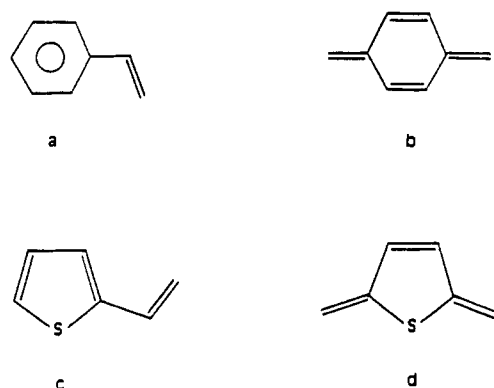

Figure 1. Molecular structure of (a) styrene, (b) 3,6-dimethylene-1,4-cyclohexadiene (quinodimethane), (c) 2-ethenylthiophene, and (d) bismethylidene-2,5-thiocyclopentene.

ties, split-valence basis sets perform rather well for trends.[44-46] However, they are far from being sufficient for the description of third-order nonlinear optical responses. Several studies of the basis set effects have been reported on molecules of medium to large size.[47-48] They all point to the fact that a set of *diffuse* functions must be added to an extended basis set, the use of conventional polarization functions having no significant impact.

Recently, we have studied[49] at the *ab initio* level as a function of basis set, the third-order static response in aromatic and quinoidic molecules: styrene, 2-ethenylthiophene, and their quinoid counterparts, see Figure 1. The basis sets taken into account were (i) the standard 3-21G and 6-31G* split valence basis sets; (ii) a Dunning double-ζ valence basis set augmented with p and d semi-diffuse functions denoted DZSD (ζ_d for C atoms equal to 0.20, ζ_d (S) = 0.15, and ζ_p (H) = 0.10); (iii) the 3-21G basis set extended by two different combinations of diffuse functions: a basis set labeled 3-21G+pd ($\zeta_{p,d}$ for C atoms equal to 0.05, $\zeta_{p,d}$ for S equal to 0.03) and a basis set labeled 3-21G+sp+sd (ζ_s = 0.021 and ζ_d = 0.087 on C atoms; ζ_s = 0.014 and ζ_d = 0.051 on S atoms, ζ_s = 0.02 and ζ_p = 0.045 on H atoms). The static longitudinal γ_{zzzz} components are reported in Table 2. [The z axis connects the 1–4 (2–5) positions of the benzene (thiophene) compounds.] Note that is of major interest to analyze the evolution of the longitudinal component because, in long chains, it totally dominates the $\langle \gamma \rangle$ response.

The results in Table 2 are fully consistent with previous studies of basis set effects on large conjugated molecules. The third-order polarizabilities of all aromatic and quinoid compounds considered in our study are extremely sensitive to the addition of diffuse functions. For instance, for the styrene and 2-ethenylthiophene molecules, γ_{zzzz} goes respectively from 11.4 $\times 10^{-36}$ and 10.4 $\times 10^{-36}$ esu with the 3-21G basis set to 25.7 $\times 10^{-36}$ and 22.5 $\times 10^{-36}$ esu with the 3-21G+pd basis set. Note that the 3-21G+pd and 3-21G+sp+sd basis sets provide very similar results. On the other hand, as often mentioned in previous studies,[47-48] the 3-21G and 6-31G* basis sets underestimate the third-order polarizabilities values. Particularly in the quinoid compounds, the γ_{zzzz} components *are calculated to be negative when using the small basis sets.* Improving the basis set quality makes the γ_{zzzz} value of the quinoid compounds become larger; this means that the absolute γ_{zzzz} value first decreases, passes by zero, and then

Table 2. Ab Initio CPHF Third-Order Polarizabilities of Quinodimethane, Bismethylidene-2,5-thiocyclopentene, Styrene, and 2-Ethenylthiophene as a Function of the Basis Set (from Ref 49)[a]

	3-21G	6-31G*	DZSD	3-21G +pd	3-21G +sd+sp
γ_{zzzz}	−12.66	−12.39	2.09	16.73	16.77
$\langle\gamma\rangle$	−0.66	−0.43	5.17	14.79	15.30
γ_{zzzz}	−4.45	−4.78	5.62	15.19	14.07
$\langle\gamma\rangle$	0.40	0.57	4.60	12.40	11.53
γ_{zzzz}	11.42	12.49	19.21	25.66	25.09
$\langle\gamma\rangle$	2.29	2.54	6.12	12.44	12.69
γ_{zzzz}	10.38	10.98	16.48	22.51	21.24
$\langle\gamma\rangle$	2.12	2.29	5.50	12.36	11.75

[a] The calculated values are expressed in electrostatic units (α in 10^{-24} esu and γ in 10^{-36} esu).

increases. Taking a basis set such as 3-21G+pd would leave us with the impression that the aromatic compounds have a larger γ_{zzzz} component than their quinoid counterparts.

It is interesting to note that we have also carried out AM1 finite-field calculations on the same compounds. The results are comparable to those obtained at the *ab initio* level with the 6-31G basis set. The quality of the AM1 calculations for other systems can thus be expected to be on the order of that of a relatively small basis set *ab initio* calculation. However, we should stress that smaller basis sets perform better, in a relative sense, in the case of longer chains.[48a]

Another issue is the *influence of electron correlation*. The effect of correlation is undoubtedly large in an absolute sense. For instance, in the case of *p*-nitroaniline, the static γ value has been evaluated at both Hartree–Fock *ab initio* and second-order Møller–Plesset levels, using a large basis set.[30] The γ value jumps from 7.8 × 10^{-36} to 15.6 × 10^{-36} esu when correlation is taken into account, *i.e.*, about a 100% increase (the latter theoretical result remains, however, three times as small as the experimental estimates due to the neglect of solvent effects). Nevertheless, we can expect that in a series of chemically-related compounds, correlation effects will not significantly affect the trends, which is our prime interest.

A third issue, as we already indicated above, is related to the fact that *the calculations are generally carried out on isolated molecules. This complicates the comparison with results of measurements performed in the condensed phase.* We have recently evaluated explicitly the solvent dependence of the molecular polarizabilities of *p*-nitroaniline and *trans*-retinal, using a self-consistent reaction field approach.[50] The results we have obtained as a function of solvent dielectric constant are in very good agreement with the available data. Such an approach thus appears very promising and paves the way toward obtaining quantitative *ab initio* estimates of static components on medium-size molecules.

2. Perturbation Techniques

Another set of techniques is based on the perturbation expansion of the Stark energy of the molecule as a function of electric field. The perturbation is usually introduced via a summation over electronic states (SOS, sum over states), although in some instances one simply performs the summation over self-consistent-field molecular orbitals. The SOS expression for the third-order microscopic nonlinear optical response reads (in a power series context)[51]

$$\gamma_{ijkl}(-\omega_\sigma;\omega_1,\omega_2,\omega_3) = \frac{1}{6}\left(\frac{\hbar}{2\pi}\right)^{-3}\sum_{\text{perm}}\left[\sum_{m,n,p(\neq r)}\right.$$

$$\frac{\langle r|\mu_i|m\rangle\langle m|\overline{\mu}_j|n\rangle\langle n|\overline{\mu}_k|p\rangle\langle p|\mu_l|r\rangle}{(\omega_{mr}-\omega_\sigma-i\Gamma_{mr})(\omega_{nr}-\omega_2-\omega_3-i\Gamma_{nr})(\omega_{pr}-\omega_3-i\Gamma_{pr})} -$$

$$\left.\sum_{m,n(\neq r)}\frac{\langle r|\mu_i|m\rangle\langle m|\mu_j|r\rangle\langle r|\mu_k|n\rangle\langle n|\mu_l|r\rangle}{(\omega_{mr}-\omega_\sigma-i\Gamma_{mr})(\omega_{nr}-\omega_3-i\Gamma_{nr})(\omega_{nr}+\omega_2-i\Gamma_{nr})}\right]$$

(30)

where $\langle r|\mu_i|m\rangle$ is the electronic transition moment along the ith Cartesian axis for the molecule-fixed coordinate system, between the reference state described by wave function $\langle r|$ and excited state $\langle m|$; $\langle m|\overline{\mu}_j|n\rangle$ denotes the dipole difference operator equal to $\langle m|\mu_j|n\rangle - \langle r|\mu_j|r\rangle\delta_{mn}$; ω_{mr} (times $\hbar$) is the energy difference between state m and reference state r; ω_1, ω_2, ω_3 are the frequencies of the perturbating radiation fields; $\omega_\sigma = \omega_1 + \omega_2 + \omega_3$ is the polarization response frequency; Γ_{mr} is the damping associated to the excited state m; $\sum_{\text{perm}}$ indicates a summation over the 24 terms obtained by permuting the frequencies.

The SOS technique presents a number of advantages. A first one is that it allows for *an easy implementation of the frequency dependence of the response*, as can be observed from the above expression of γ. This is important in order to produce theoretical results that compare more directly to experiment, as the measurements are carried out at optical frequencies. A second

attractive feature is that the states entering the perturbation procedure can explicitly contain *the effect of electron correlation*, for instance through a configuration interaction calculation. The third, and maybe most useful advantage in terms of the analysis of the nonlinear optical response, is that it allows one to obtain *a physical picture as to which excited states play a significant role in the response.*

The sum-over-states approach has been widely applied on the basis of simple tight-binding or Hückel Hamiltonians, semiempirical π-electron Pariser–Parr–Pople or all-valence electron Hamiltonians, or pseudopotential valence effective hamiltonians (VEH).[52-58] In particular, the INDO (intermediate neglect of differential overlap)[59] and CNDO (complete neglect of differential overlap) semiempirical techniques coupled to single or single and double configuration interaction have often been exploited. An elegant diagrammatic valence-bond approach has also been introduced by Soos and co-workers;[55] this method allows one to carry out a full configuration interaction calculation of the nonlinear optical coefficients at the Pariser–Parr–Pople level (it is, however, currently limited to about 14 π-electron systems).

3. Coupled-Oscillator Techniques

An approach generally more popular within the physics community is to consider the medium as composed of a set of coupled anharmonic oscillators.[25,60-64] The resonant frequencies of these oscillators correspond to electronic transition frequencies. The application of an external oscillating field induces the electrons to oscillate about their equilibrium positions. At low electric field strengths, this motion is harmonic and gives rise to the linear polarization response. The nonlinear polarization response becomes significant at high electric field strengths, where the anharmonicity of the electron oscillators must be taken into account. Thus, the linear and nonlinear polarization response of a material consisting of an assembly of molecular units can be reduced to solving the equations of motion for coupled anharmonic oscillators driven by an electric field. The oscillators corresponding to the monomer units in a conjugated π-electron polymer like polyacetylene are considered very strongly coupled, while the oscillators corresponding to hydrogen-bonded molecules in a molecular crystal are more weakly coupled. This coupling is also influenced by the oscillating frequency of the external electric field; a resonant frequency promotes stronger coupling, and an off-resonant frequency results in weaker coupling.

The application of the coupled oscillator approach to conjugated polymer chains has been recently considered by Mukamel and co-workers.[60-62] In the case of a polydiacetylene derivative (4-BCMU),[62] these authors have obtained a very nice correlation between the results of their coupled anharmonic oscillator method (on the basis of a Pariser–Parr–Pople Hamiltonian with single configuration interaction) and those of careful frequency-dependent experimental data.

Note that the anharmonic oscillators describe the motions of electron–hole pairs (exciton states), electrons (conduction band states), and holes (valence band states) as well as nuclear motions. An interesting piece of work would be to compare and relate the charac-

teristics of the anharmonic oscillators which play an important role in the nonlinear optical response of a system, to those of the important excited states appearing in an SOS approach.

C. Origin of the Third-Order Nonlinear Optical Response

A first essential feature to emphasize is that conjugated oligomers and polymers possess a strong electron-phonon coupling. This means that there exists a very close relationship between the electronic structure and the geometric structure. Any modification in the electronic structure, for instance following a *resonant* photoexcitation process, results locally in a fast ($\sim 10^{-13}$ s time scale) relaxation of the molecular geometry, which can eventually lead to the formation of nonlinear excitations such as solitons, polarons, bipolarons, or polaron–excitons.[65-67] In turn, the geometry modifications alter the electronic structure and there occur major shifts in oscillator strengths that can induce a highly nonlinear optical response. In this context, strong similarities exist between the effects of doping and photoexciting conjugated polymers.

The geometric relaxations that are induced upon photoexcitation originate in the redistribution of the π-electron densities in the excited state. In a conjugated system, the pattern of single-like and double-like carbon–carbon bonds is actually imposed by the π-electron densities. To illustrate this feature, we take the simple case of a polyene molecule. If, in the first place, we assume the exclusive presence of the σ-framework, all the carbon–carbon bond lengths would be roughly equal and amount to ca. 1.50–1.51 Å (Figure 2a). When the π electrons are added, the π-electron wave function in the ground state (the 1 A_g state) is such that there is a regular alternation of large and small π densities on the bonds. This results in an alternation of double and single bonds, the external bonds being double (Figure 2b). In the first one-photon optically-allowed state (the $1B_u$ state), the π-electron wave function is deeply modified. It can be depicted as leading to a shift in the π-bond density maxima and minima from one bond to the next (Figure 2c). This process takes place instantaneously; the geometry relaxations which follow the change in π-electron wave function and π-bond densities, occur more slowly, approximately in the 10^{-13} s range as mentioned above. *It is precisely the instantaneous shift in π-electron densities occurring upon excitation over the whole molecule which explains the large and fast polarizabilities of π-electron networks.* As can be observed from Figure 2c, these shifts lead to strong charge separation. Note that throughout this process, the σ-framework remains nearly unaltered.

The above discussion calls for the following remarks. Off-resonance processes can be described on the basis of virtual excitations. They take place in femtosecond time scales due to the instantaneous polarization of the π-electron cloud and have thus a purely electronic origin. On the contrary, resonant processes involve actual absorptions of photons and are dependent on excited-state lifetime (they also induce thermal effects). However, in conjugated polymers, very fast multiphonon deexcitation pathways (which originate in the strong electron–phonon coupling) lead to recovery times which
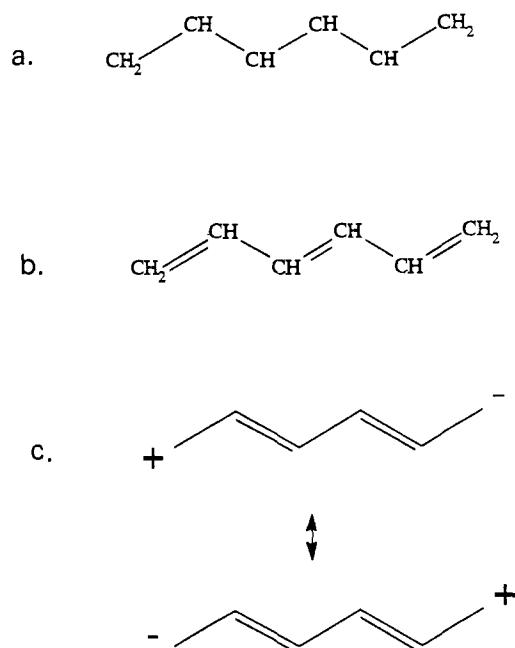
Figure 2. Patterns of single-like and double-like carbon–carbon bonds in the case of a polyene molecule: (a) in the ground state, considering exclusively the σ framework, (b) in the ground state, taking into account of all σ and π electrons; and (c) in the $1B_u$ state.
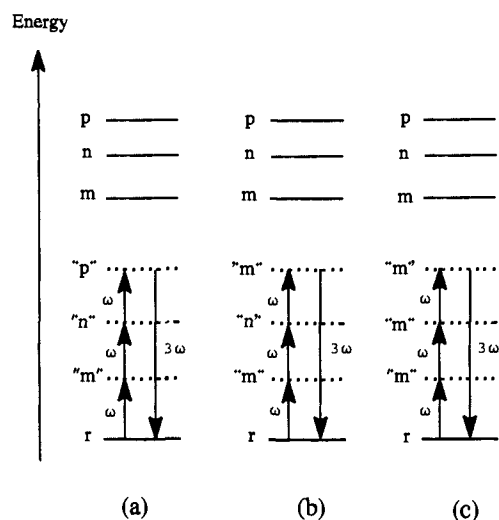

Figure 3. Illustration of the *positive* channel contributions in the case of (off-resonance) third-harmonic generation $\gamma \cdot (-3\omega;\omega,\omega,\omega)$. The states in quotes refer to the primary stationary state contributing to the virtual state. The channels of the type in part c appear exclusively in noncentrosymmetric systems.

in some instances can be as fast as picosecond time scales.[68–69]

In contrast to the situation in conjugated systems, in saturated compounds, there occur *localized* σ–σ^* excitations with the consequence that there is no charge separation over the whole molecule. This is the reason why the polarizabilities of saturated compounds can be very well described on a purely additive basis, *i.e.*, by simply adding the polarizabilities of the individual groups forming the molecule. As a result, there appears a linear chain-length dependence of the polarizability; for instance, if we consider the series of alkanes, the polarizability of octane is simply about twice that of butane. Furthermore, the σ-framework can be altered upon excitation of $^1\sigma\sigma^*$ states leading more readily to photochemistry.

In inorganic ferroelectric crystals, the polarization due to an external electric field comes from setting the cations and anions in motion, *i.e.*, from phonon processes. The charge separation is rather localized and the response time is inherently limited by vibrational time scales. This rationalizes the fact that conjugated organics usually possess larger and faster nonlinear optical responses than inorganics.

It is now useful to go back to the sum-over-states expression for γ (see eq 30). This expression contains two sets of summations over excited states, starting from a reference state $|r\rangle$ which is usually, but not necessarily, the ground state. For each term in the summations, the numerator contains a product of four transition or state dipole moments (state dipoles exclusively appear in noncentrosymmetric compounds); the denominator consists of a product of three energy differences between excited states and the reference state. The first set of summations (globally multiplied by a positive sign and referred to as positive channels) has terms which involve three excited states. The excitations are as follows: the system leaves reference

state $|r\rangle$ for excited state $|m\rangle$; from $|m\rangle$, it evolves to excited state $|n\rangle$ and then to excited state $|p\rangle$, before returning to the reference state. These excitations can be depicted diagramatically as in Figure 3 depending on whether some of the excited states are the same (for instance $|m\rangle$ is equal to $|p\rangle$) or the molecule is centrosymmetric or not.

The second set of summations (globally multiplied by a negative sign and referred to as the negative channels) deals with terms involving only two excited states since the reference state also corresponds to the intermediate state. The excitations then lead from $|r\rangle$ to excited state $|m\rangle$ before returning to $|r\rangle$; there occurs then another excitation from $|r\rangle$ to $|n\rangle$ and then back to $|r\rangle$. The corresponding diagrams are illustrated in Figure 4.

From this description, we can make the following remarks that indicate the requirements for a given term (channel) to make a significant contribution to γ:

(i) It is necessary that all excitation or deexcitation steps be allowed by selection rules. This implies that in highly symmetric molecules, only a few channels may contribute. For instance in the case of polyene oligomers, the symmetry is C_{2h} and the π-states possess either A_g or B_u symmetry; if the reference state has A_g symmetry, this implies that the $|m\rangle$ and $|p\rangle$ states must have B_u symmetry and the $|n\rangle$ state, A_g symmetry.

(ii) The higher the excited states involved in the channel, the lower their expected contribution because of the energy terms in the denominator.

(iii) Significantly contributing channels will be those which consist of excitations involving large transition dipole moments.

(iv) When one of the optical frequencies used to excite the compound, their multiple, or their linear combination matches one of the excitation energies, resonance enhancement of the response occurs and there appears a peak in the imaginary part of γ. Bear in mind that upon resonance, there occurs an actual absorption of photons, which leads to higher optical damage, thermal effects, and response times limited by the lifetime of
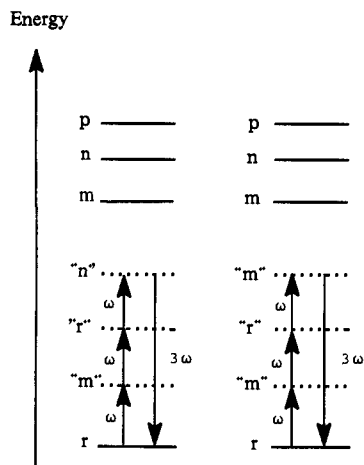
Figure 4. Illustration of the *negative* channel contributions in the case of (off-resonance) third-harmonic generation γ-$(-3\omega;\omega,\omega,\omega)$. The states in quotes refer to the primary stationary state contributing to the virtual state.

the excited state. Therefore, in most cases, one avoids working with an optical frequency that is on resonance. These remarks allow us to understand the physical basis of the so-called three-state model, as worked out for instance by Kajzar and Messier,[70] Pierce,[23] Garito,[52] and Dirk and Kuzyk.[71] In this model, one describes the γ response as predominantly coming from three states: the ground state, a first low-lying excited state which is strongly (one-photon optically) allowed from the ground state, and a second excited state, strongly accessible from the first excited state. The summations over excited states in eq 30 being then reduced to single terms, we are left with only two channels (one positive and one negative) in the case of a centrosymmetric compound; a third channel adds on in noncentrosymmetric situations. These channels are shown in Figure 5. Accordingly, the expression for γ simply becomes

$$\gamma_{iiii} = \frac{1}{6}\left[\frac{M_{rm}^{2}M_{mn}^{2}}{E_{rm}^{2}E_{mn}} - \frac{M_{rm}^{4}}{E_{rm}^{3}} + \frac{M_{rm}^{2}\,\Delta\mu_{rm}^{2}}{E_{rm}^{3}}\right] \quad (31)$$

where M_{rm} $[E_{rm}]$ is the electronic transition moment [transition energy] between reference state $|r\rangle$ and excited state $|m\rangle$, and $\Delta\mu_{rm}$ is the dipole moment difference between excited state $|m\rangle$ and reference state $|r\rangle$ $(\mu_{m} - \mu_{r})$. This three-state model constitutes the direct extension at the third-order level, of the two-state model which has been abundantly exploited for describing the second-order nonlinear optical response of conjugated systems[72] (note that a two-state model has also been used for γ[71,73] but it is often too limited to provide much insight). We can factor the (M_{rm}^{2}/E_{rm}) ratio out of each of the three terms above. Doing so is informative since this ratio is proportional to the linear polarizability coming from π electrons. Then, γ can be written as

$$\gamma \propto \alpha_{\pi} \times \left[\frac{\Delta\mu_{rm}^{2} - M_{rm}^{2}}{E_{rm}^{2}} + \frac{M_{mn}^{2}}{E_{rm}E_{mn}}\right] \quad (32)$$

In the case of conjugated organic compounds, the third-order polarizability can thus be seen as the product of the linear polarizability by the nonlinear term in brackets, which has been referred to by Meredith and co-workers as corresponding to an anharmonicity factor.[74]

(a)   (b)   (c)
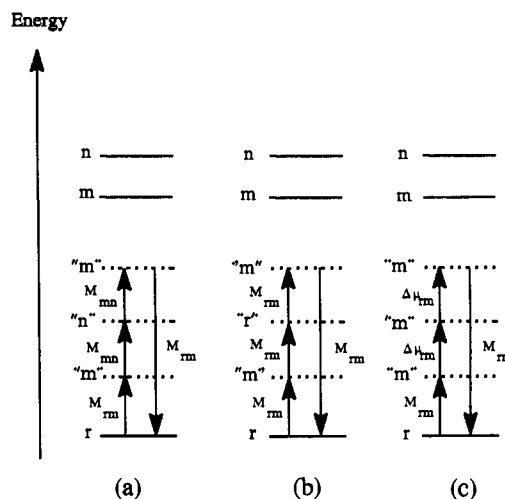
Figure 5. Illustration of the three channels contributing to (off-resonance) third-harmonic generation in the context of the three-state model. The states between quotes refer to the primary stationary state contributing to the virtual state. The channels of the type in part c appear exclusively in noncentrosymmetric systems. The M_{ij} transition dipoles or $\Delta\mu_{ij}$ state dipole differences between states i and j are indicated.

To illustrate the three-state model, we can take the example of *all-trans* polyenes; there, the ground state is the $1A_g$ state. It is very strongly coupled to the first one-photon optically-allowed state, the $1B_u$ state. Note that, at least for chains longer than butadiene,[75] $1B_u$ is not the lowest-lying singlet excited state; it usually lies above the $2A_g$ state which, for symmetry reasons, cannot be accessed in a one-photon process from the ground state. As we depicted earlier, $1B_u$ leads to a coherent shift of the π-electron densities from one bond to the next (Figure 2c). The $1B_u$ level is itself connected via a large transition dipole moment to a higher-lying A_g state, denoted the mA_g state (for instance, in the case of octatetraene, a number of calculations indicate the mA_g state is the $6A_g$ state).[76,77] The mA_g state has been shown by Garito and co-workers to produce a further charge separation within the molecule with respect to $1B_u$, from one-half of the molecule to the other half.[76] As the length of the polyene chain gets longer, the number of mA_g states contributing to γ gets larger. Mazumdar and co-workers[78] have shown that this "band" of A_g states is close to the $1B_u$ state and lies below the conduction band threshold.

The recent availability of experimental nonlinear optical spectra taken over a wide range of frequencies and with a combination of measurement techniques, makes it possible to test in detail the validity and limits of the simple three-state model. To explain some of the features in the experimental spectra of conjugated polymers, Mazumdar and co-workers have worked out a more complex model based on four essential states.[78,79] In this model, they consider that some significant contributions are coming from type a diagrams in Figure 3, since it is necessary to take account of a series of nB_u states which are strongly accessible from the mA_g states. Careful analysis of their theoretical results has allowed Mazumdar and co-workers to show that these nB_u states correspond to the bottom of the conduction band. We have recently found from INDO/SD-CI SOS calculations that the same picture holds in the case of oligothiophenes.[80] The four-essential-state model has
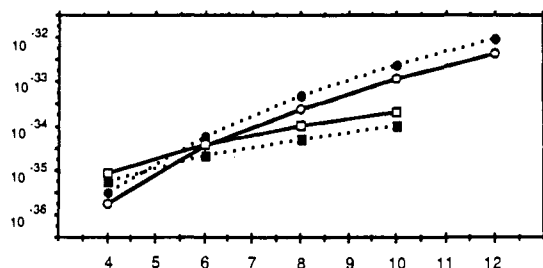
Figure 6. Evolution of the positive (solid line) and negative (dashed line) channel contributions to the INDO/SDCI static γ_{zzzz} component (in esu) as a function of the number of π electrons in polyenes (squares) and symmetric cyanine cations (circles) (adapted from ref 82).

been successfully applied to polydiacetylenes and polyalkylthiophenes by Mazumdar, Stegeman, Kajzar, and their co-workers.[79,81]

We mentioned previously the very detailed theoretical and experimental work of Mukamel and Stegeman and co-workers:[62] They probed over a wide frequency range the third-harmonic generation and nondegenerate four-wave mixing spectra of the 4-BCMU polydiacetylene. From their analysis based on coupled anharmonic oscillators, they found that about 17 levels are necessary to take account of all the details (resonances) in the experimental spectra; these levels are difficult to interpret but we may expect them to correspond to the ground state, the $1B_u$ state, and series of mA_g and nB_u states. To summarize, we can say that the three-state and four-essential-state models provide useful starting points from which to analyze in more detail the origin of the third-order optical nonlinearities.

The γ expression (eq 30) contains positive and negative terms. It has been shown that in polyenes the positive channels dominate: the static γ values are therefore positive, in agreement with experimental data. We should stress, however, that the positive and negative contributions are usually of the same order of magnitude and thus nearly cancel each other:[23,82] for instance, in the case of octatetraene, an extended sum-over-states calculation indicates that the positive channel contributions to γ_{zzzz} amount to about 20×10^{-36} esu and the negative channels to about 15×10^{-36} esu, resulting in a net static γ_{zzzz} value of 5×10^{-36} esu. In the case of cyanine dyes, on the other hand, the negative contributions are dominant, which is mostly a result of the low first optical transition; the static γ value is then negative,[23,82] which means that the polarizability decreases at high electric-field values. It is important to realize that, in absolute value terms, the static third-order nonlinear optical response is larger in a cyanine dye than in the polyene with the same number of π electrons.[23,82] (Note that a negative sign of γ can be an advantage since this results in self-defocusing of incident light, thereby increasing the optical damage threshold.) Figure 6 illustrates the evolution of the positive and negative channel contributions to γ_{zzzz} as a function of the elongation of the polyene and cyanine dye chains.[82] Similar results have also been discussed by Dirk, Kuzyk and co-workers.[71] Furthermore, we must point out that a complete analysis of the evolution of the value and sign of γ when passing from the polyene limit to the cyanine limit has recently been made by Marder and co-workers.[83,84] We will go back to this topic in more detail in section V.

In the previous examples, we have dealt with centrosymmetric systems. Within the three-state model, only the first two terms to the right of eq 31 contribute. In a noncentrosymmetric case, for instance a polyene end-capped by a donor group and an acceptor group, the relaxation of the selection rules and the appearance of the third term of eq 31 result in an increase in the static γ value. This third term is directly proportional to (i) the square of the difference in state dipole moment between the ground state and first excited state, $\Delta\mu$, and (ii) the square of the transition dipole. Note that at the limit of long chains, the term $\Delta\mu$ tends to decrease;[85,86] the end groups then play a negligible role, as should be expected. An increase in the γ value by push-pull substitution of short polyenes has been shown by Garito and co-workers,[87] Zyss and co-workers,[88] and Meyers and Brédas.[89] Optimization of this third term in the case of push-pull thiazole azo dyes has also been recently addressed by Dirk et al.[90]

In conjugated compounds, the question of *saturation of the nonlinear optical response as a function of chain length* is of importance, namely in order to evaluate the best compromise between nonlinear optical efficiency and packing density. Early on, Flytzanis and co-workers have shown, from simple tight-binding calculations, that the larger the electronic delocalization along the chain, the slower the saturation regime is reached.[91] To evaluate the saturation, the γ values are usually expressed as a function of a power of the chain length:

$$\gamma \propto N^{a(N)}$$

$$\log \gamma \propto a(N) \log N$$

where N can correspond to the number of monomer units along the chain (it might alternatively consists of the physical length of the chain or the number of π electrons). In the Hückel-type calculations carried out by Flytzanis, the power value was found to be equal to 5.[91] Actually, the power value is itself dependent on the chain length, a feature which is not always properly pointed out. Saturation is reached when the power value tends to 1, *i.e.*, when we enter a purely additive regime.

A number of theoretical studies have been devoted to chain-length saturation in the case of polyenes; the results consistently indicate that the saturation sets in after about 50–60 carbons.[56,92–94] We have recently investigated the saturation behavior in oligothiophenes;[80] the γ/N values are reported as a function of N in Figure 7. The curve of Figure 7 is typical of what is usually obtained in conjugated compounds. It can be divided into three parts: (i) the γ response first picks up significantly with extension of chain length, which means that the power value strongly increases; (ii) the power value then enters a regime where it stays nearly constant; for the oligothiophenes, it is the case for a number of thiophene rings between 3 and 6–7; we calculate the power value in this regime to stay around 3.7; in these first two parts of the curve, polarization and delocalization of the π-electron cloud over the whole chain plays an essential role; (iii) finally, the power value starts decreasing, which indicates the beginning of the saturation regime; saturation in oligothiophenes is calculated to occur after about 7–8 rings,[80] a result
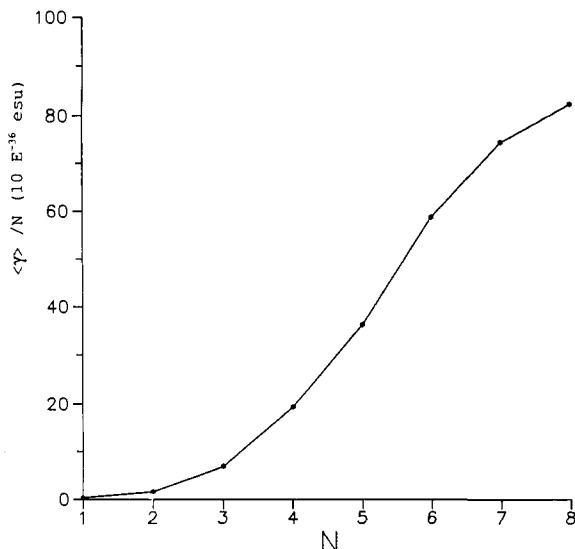
Figure 7. Illustration of the evolution of the average value of the INDO/MRDCI static third-order polarizabilities of thiophene oligomers as a function of the number N of thiophene rings (adapted from ref 80).

which is in excellent agreement with the experimental data of Prasad and co-workers,[95] Meijer and co-workers,[96] and Kajzar and co-workers.[97]

The initial strong increase of γ with chain length in conjugated oligomer chains clearly points out the fact that quasi-one-dimensional systems present a topology that favors charge separation over a long distance and thus contributes to increase the induced polarization.[91] In that case, the longitudinal γ_{zzzz} component totally dominates the third-order response. In systems of higher dimensionality, despite the fact that other components start playing a role, the overall γ value tends to shrink. An illustrative example comes from the comparison between a $C_{60}H_{62}$ polyene and the C_{60} fullerene.[98] The γ value is calculated to be about 2 orders of magnitude larger in the former $(8 \times 10^{-32}\ \text{esu})$ than in the latter $(2 \times 10^{-34}\ \text{esu})$: charge separation can go over about 60 Å in the polyene while charge separation is at most 10 Å in the fullerene.

A final aspect we want to stress in this section relates to the recent indication by Taliani and co-workers[99,100] and Garito and co-workers[101,102] that a strong enhancement of the nonlinear optical response can be obtained when working in the excited state. This means that the reference state in the sum-over-states expression (eq 30) is no longer the ground state but is a low-lying excited state which can be optically pumped. The enhancement comes from the following features: (i) the energy differences appearing at the denominators tend to be smaller (ii) and there appear many more channels that contribute significantly (in other words, the application of a modified three-state model where the reference state is an excited state, would be inadequate). Taliani and co-workers[99,100] have investigated the picosecond degenerate-four-wave mixing response at 1.064 μm of a polythiophene film simultaneously pumped at 532 nm (*i.e.*, across the bandgap). A strong enhancement by 1 order of magnitude was found, which was interpreted as the contribution to the cubic response due to the preparation of photoexcited polarons.[99,100] In a similar context, Mc Branch *et al.* have evaluated the sign and magnitude of the

nonlinear n_2 refraction index in poly(3-hexylthiophene) when pumping across the bandgap. The n_2 term was found at 1.064 μm (1.17 eV) to be complex with a negative real component: $n_2 \approx (-5 + 7i) \times 10^{-5}$ (MW/cm^2)$^{-1}$;[103] this is related to the appearance of a photoinduced polaron absorption peak in the gap below 1.17 eV. Garito and co-workers have considered the concept of excited-state enhancement both theoretically[101] and experimentally.[102] They have examined the γ response of a dioxane solution of α,ω-diphenylhexatriene molecules pumped into the $2A_g/1B_u$ states. The γ response at 1064 nm was measured to be on the order of 100 times as large as the response in the ground state and reaches about 10^{-32} esu.[102]

We have carried out INDO/SD-CI calculations on diphenylhexatriene using either the $1A_g$ or the $1B_u$ state as the reference state in the sum-over-states expression (and keeping the ground-state geometry).[104] The results are fully consistent with the experimental data. We calculate an average third-order polarizability in the ground state equal to 38×10^{-36} esu, to be compared to a $1B_u$ excited state value of -1.2×10^{-32} esu. The different excited states and the most important channels playing a significant role in the nonlinear response have been analyzed. The third-order polarizability of diphenylhexatriene in the ground state is dominated by three channels (the $1A_g$-$1B_u$-$10A_g$-$1B_u$-$1A_g$ and $1A_g$-$1B_u$-$7A_g$-$1B_u$-$1A_g$ positive channels and the $1A_g$-$1B_u$-$1A_g$-$1B_u$-$1A_g$ negative channel) which constitute about 90% of the γ_{zzzz} dominant component. The microscopic description for the nonlinear optical processes originating from the $1B_u$ excited state is drastically different. The $2A_g$ and the $9B_u$ states play here a significant role. The $2A_g$ state is involved in three channels ($1B_u$-$2A_g$-$1B_u$-$2A_g$-$1B_u$; $1B_u$-$10A_g$-$1B_u$-$2A_g$-$1B_u$; and $1B_u$-$7A_g$-$1B_u$-$2A_g$-$1B_u$) that lead to a very large negative contribution to γ. The very small transition frequency ω_{rm} between the $1B_u$ and $2A_g$ states increases considerably the contribution of the first of these processes and provides a large negative static longitudinal γ_{zzzz} component. (This is in contrast to the ground-state static γ value which is positive.[101,102,104]) We note that similar theoretical results have recently been obtained by Medrano and Dudis in the case of unsubstituted polyenes.[105]

D. From γ to $\chi^{(3)}$

For each microscopic species in the material, for instance a molecule, we can relate each element of the tensor for the macroscopic third-order electric susceptibility $\chi^{(3)}_{IJKL}$ to the microscopic third-order coefficient c_{IJKL} by[14]

$$\chi^{(3)}_{IJKL} = N f_I(\omega_1)\, f_J(\omega_2)\, f_K(\omega_3)\, f_L(\omega_4)\, c_{IJKL} \qquad (33)$$

In this formula, the subscripts, I, J, K, L refer to axes in the laboratory-fixed coordinate system; N is the species number density; and $f_I(\omega_i)$ is the local field factor at radiation frequency ω_i. The local field factor at *optical frequencies* for a pure liquid can be estimated by the expression derived by Lorentz:[106]

$$f_I(\omega_i) = [n(\omega_i)^2 + 2]/3 \qquad (34)$$

where $n(\omega_i)$ is the index of refraction for the liquid at frequency ω_i. The local field is the actual electric field

acting on the microscopic species in the material. This field is defined by the product $f_I(\omega_i)E(\omega_i)$, where $E(\omega_i)$ is the external electric field applied to the bulk material. The electronic polarizability of the bulk material, as expressed through $n(\omega_i)$, therefore acts to amplify the magnitude of $E(\omega_i)$ at the site of the microscopic species. It should be emphasized that Lorentz's local field factor is an approximation since it considers the species to occupy a *spherical cavity* in the material and the local environment of the species is treated as a continuum. Also note that the indices of refraction used in the local field approximations for optical frequencies are generally assumed to be independent of the applied electric field.

The microscopic third-order nonlinear coefficient c_{IJKL} in laboratory-fixed coordinates is related to the molecule-fixed coordinate system by

$$c_{IJKL} = \sum_{ijkl} \phi_{Ii}\phi_{Jj}\phi_{Kk}\phi_{Ll}\gamma_{ijkl} \qquad (35)$$

in which ϕ_{Ii} is the direction cosine between the laboratory-fixed I axis and the molecule-fixed i axis, and γ_{ijkl} is an element of the molecular third-order polarizability tensor.

In isotropic liquids, we have to average over all directions and we obtain an orientationally averaged third-order polarizability:

$$\langle\gamma\rangle = \langle c_{IJKL}\rangle = \sum \langle\phi_{Ii}\phi_{Jj}\phi_{Kk}\phi_{Ll}\rangle\gamma_{ijkl} \qquad (36)$$

The symmetry of the molecule determines which of the 81 total elements in the third-order polarizability tensor are nonzero. For example, if the molecules in the liquid belong to the orthorhombic point group, there are 21 nonzero γ_{ijkl} elements:[107] γ_{iiii}, where $i = x, y, z$, and γ_{iijj}, γ_{ijij}, γ_{ijji}, γ_{ijii}, γ_{jjii}, γ_{iiij}, where $i, j = x, y; i, j = x, z$; and $i, j = y, z$. Kleinman showed[108] that the γ_{ijkl} element of the third-order polarizability tensor is identical with respect to any rearrangement of the indices of this element for the *static* case, i.e., $\gamma_{ijkl}(0;0,0,0)$:

$$\gamma_{xxyy} = \gamma_{xyxy} = \gamma_{yxyx} = \gamma_{xyyx} = \gamma_{yyxx} = \gamma_{yxxy} \qquad (37)$$

Although this relationship rigorously holds only for $\gamma_{ijkl}(0;0,0,0)$, it can be used in the analysis of the *nonresonant* $\gamma_{ijkl}(-\omega_p;\omega_1,\omega_2,\omega_3)$.

If we apply Kleinman's symmetry rule to the 21 nonzero elements, we are left with the following independent elements of the tensor:

$$\gamma_{xxxx}, \gamma_{yyyy}, \gamma_{zzzz}, 6\gamma_{xxyy}, 6\gamma_{xxzz}, 6\gamma_{yyzz} \qquad (38)$$

In degenerate four-wave mixing experiments (with the same polarization for all the beams), we measure the macroscopic third-order susceptibility $\chi^{(3)}_{xxxx}(-\omega;\omega,\omega,-\omega)$. If one calculates the different direction cosines[109] of eq 35, we obtain the following expression for an isotropic liquid of the orthorhombic point group:

$$\langle\gamma\rangle = \frac{1}{5}(\gamma_{xxxx} = \gamma_{yyyy} + \gamma_{zzzz} + 2\gamma_{xxyy} + 2\gamma_{xxzz} +$$

$$2\gamma_{yyzz}) \qquad (39)$$

Experimentally, only the averaged third-order polarizability is accessible for amorphous materials, which is the sum of different γ_{ijkl} elements. However, in the case of single crystals, it is possible to determine individual elements of the third-order polarizability tensor.

Table 3. Nonresonant $\chi^{(3)}$ Values for the Reference Materials Used in Different $\chi^{(3)}$ Measuring Techniques

technique	material	argument	λ (nm)	$\chi^{(3)}_{xxxx}$ $(10^{-14}$ esu)
DFWM	CS_2	$\omega = \omega + \omega - \omega$	532	680^{239}
OKG	CS_2	$2\omega = \omega - \omega + 2\omega$	1064	844^{232}
THG	BK-7 glass	$3\omega = \omega + \omega + \omega$	1910	5.8^{158}
				$\chi^{(2)}_{xxx}$ $(10^{-9}$ esu)
EFISHG	α·quartz	$2\omega = \omega + \omega$	1064	$2.3^{111,\ 240}$

IV. Measuring Techniques for Third-Order Susceptibilities

We now provide a general description of the main techniques for measuring the third-order susceptibilities or polarizabilities and a survey of their applications to organic compounds. It should be stressed that it is very difficult to compare the nonlinear optical response of organic systems examined with different techniques. First of all, the laser wavelength is very important. As we detailed in the previous section, the third-order susceptibility is strongly frequency (wavelength) dependent, and close to an absorption band, there occurs resonance enhancement. The repetition frequency and the pulse duration of the laser are of equal importance. Different nonlinear mechanisms give different contributions to the third-order susceptibility: molecular orientation, electrostriction, atomic alignment, change in population equilibrium (redistribution of the ground-state population among the degenerate sublevels) and electronic excitation.[110] In fact, the pure electronic nonlinearity is the parameter that one should compare. In order to avoid all the other dynamic nonlinearities occurring on time scales greater than picoseconds, one needs (in certain techniques) a short pulse duration (picoseconds) and a low repetition rate. Note that different resonance enhancements take place in different techniques. For instance, in third-harmonic generation, we can have ω, 2ω, and 3ω resonances. In electric-field-induced second-harmonic generation, there is a possible one-photon (ω) and two-photon (2ω) enhancement of $\chi^{(3)}$. When we are using a degenerate four-wave mixing process, there can be a resonance enhancement at ω and 2ω. If we probe a species which absorbs in the UV region (for instance, around 250 nm) and we are measuring at a wavelength of 1064 nm, there will be a resonance enhancement of the $\chi^{(3)}$ value when we are using third-harmonic generation, but not when we are using the other two techniques. If organic thin and thick films are compared, one should always account for the thickness of the film and the weight percentage of the active component in the film.

It must be borne in mind that all measurements are made relative to a reference material and different techniques require different reference materials. In third-harmonic generation, the reference material is usually glass, while in degenerate four-wave mixing, it is often carbon disulfide. Given that there are different values for the same reference materials in the literature, care should be taken and one should mention the value for the reference if one compares different samples. In Table 3, we present a list of the best nonresonant $\chi^{(3)}$ values for the reference materials used in the different $\chi^{(3)}$ measuring techniques. The reference value for $\chi^{(3)}$-$(-3\omega;\omega,\omega,\omega)$ of BK-7 glass is the one reported by Heflin,

Table 4. Conversion between MKS and Gauss Units[a]

quantity	MKS	Gauss	$N_{Gauss} = QN_{MKS}$ Q
length, l	m	cm	100
mass, m	kg	g	1×10^3
force, F	N	dyn	100×10^3
energy, U	J	erg	10×10^6
charge, q	C	statcoulomb	2.998×10^9
potential, V	V	statvolt	3.336×10^{-3}
$\chi^{(1)}$	none	none	79.58×10^{-3}
$\chi^{(2)}$	m/V	cm/statvolt	2.387×10^3
$\chi^{(3)}$	m²/V²	cm²/statvolt²	71.62×10^6

[a] Note that for the physical quantities collected here, the Gauss units and electrostatic units (esu) are equivalent.

Cai, and Garito.[158] These authors analyzed six independent measurements of $\chi^{(3)}(-\omega_4;\omega_1,\omega_2,\omega_3)$ for BK-7 glass taken by means of four separate third-order processes, that give consistent values to better than 10%. Each value has been converted into the convention for $\chi^{(3)}(-3\omega;\omega,\omega,\omega)$. Until a careful absolute measurement of $\chi^{(3)}(-3\omega;\omega,\omega,\omega)$ is performed, they recommend to use the value in Table 3 as the standard reference value. The reference value for $\chi^{(2)}(-2\omega;\omega,\omega)$ of α-quartz that is used in EFISHG was measured by SHG relative to a KDP crystal.[111]

In order to ease the comparison between the susceptibility or polarizability values reported in the literature, we present in Table 4 the conversion between MKS and Gauss units for relevant physical quantities. We note that the main second-order and third-order nonlinear optical processes and techniques have been recently elegantly reviewed by Prasad and Williams[14] and Kajzar and Messier.[16] An important remark is that it should be obvious that dispersion measurements are vital for understanding the origin and features of third-order optical responses. For this reason, more and more research groups are moving into this direction. Van Herzeele[112] has for instance described a picosecond laser system which is continuously tunable from 0.6 up to 4 μm. This system is based on a mode-locked high-power Nd:YLF laser which synchronously pumps a dye laser and seeds a Nd:YLF regenerative amplifier; it has demonstrated its versability in various related $\chi^{(2)}$ and $\chi^{(3)}$ studies of both organic and inorganic materials. Other examples will be provided in section V.

A. Third-Harmonic Generation

Third-harmonic generation (THG) is a special case of frequency mixing. The nonlinear polarization $P_i(3\omega)$ responsible for this effect is given by

$$P_i(3\omega) = \chi^{(3)}_{ijkl}(-3\omega;\omega,\omega,\omega)E_j(\omega)E_k(\omega)E_l(\omega) \quad (40)$$

Harmonic generation is a coherent process: it occurs almost instantaneously through purely electronic interactions that do not depend on the population of the excited state. Dynamic nonlinearities (associated with the electric-field-induced displacement of nuclei) are not probed by third-harmonic generation and there is no information on the time response of the optical nonlinearity. The third-harmonic signal can be resonantly enhanced near one-photon or multi-photon absorption bands of the material.

1. Theory

The THG intensity $I_{3\omega}$ is calculated by solving the wave equation with $P_i(3\omega)$, and is approximately given by[113]

$$I_{3\omega} = \frac{(3\omega)^2}{n_{3\omega} \, n_\omega^3 \, c^4 \, \epsilon_0^2} \frac{\sin^2[\Delta k(l/2)]}{[\Delta k(l/2)]^2} |\chi^{(3)}|^2 \, l^2 \, I_\omega^3 \quad (41)$$

In this formula, n_ω is the index of refraction at frequency ω, ϵ_0 is the permittivity of free space, l is the interaction length, and Δk is the wave vector mismatch:

$$\Delta k = k_{3\omega} - 3k_\omega = 3\omega \frac{(n_{3\omega} - n_\omega)}{c} \quad (42)$$

Relation 41 predicts a dependence of the third-harmonic intensity on the wave vector mismatch for a medium of constant interaction length l. $I_{3\omega}$ shows a symmetrically-damped oscillatory behavior around $\Delta k = 0$. The damped oscillations result when, due to phase mismatch, the harmonic field gets out of phase with the polarization that drives it as the wave propagates through the medium. Phase matching is difficult to achieve because of dispersion of the refractive indices. In the absence of phase matching, one can optimize third-harmonic generation by adjusting the interaction length. This can be done by rotating the sample (Maker fringe method) or by translation of a wedge-shaped sample. A useful concept in this regard is that of the coherence length l_c which is defined as

$$l_c = \pi/\Delta k \quad (43)$$

The translation of a wedge-shaped sample produces a sinusoidal behavior and the interaction length variation between two consecutive maxima for $I_{3\omega}$ is $2l_c$.

2. Experimental Technique

A typical experimental arrangement for third-harmonic generation utilizes a Q-switched Nd:YAG laser with nanosecond pulses at a low repetition rate.[114] Because there is no time response information available and because of the pure electronic nature of third-harmonic generation, the pulse width of the laser is not crucial, as long as there is no decomposition of the sample. The wavelength of the laser should be selected very carefully. Since most organic materials absorb in the UV, one should always take a wavelength with its third harmonic out of the UV spectrum. This can be done by pumping a dye laser and a Raman shifter with the frequency-doubled output of the Nd:YAG laser.

After the selection of the wavelength, the laser beam is split in two parts, one to generate the third-harmonic signal in the sample and the other to generate the third-harmonic signal in the reference (glass in general). For non-phase-matched THG, the path length of the sample and the reference is varied and the third-harmonic signal is monitored as a function of the interaction length l to obtain the fringes. From these fringes, one can determine the coherence length (of sample and reference). The third-order susceptibility $\chi^{(3)}$ can be crudely estimated from the third-harmonic signals (for the same input intensity in sample and reference):

$$\frac{I_{3\omega,sample}}{I_{3\omega,reference}} = \left(\frac{\chi^{(3)}_{sample}}{\chi^{(3)}_{reference}}\right)^2 \left(\frac{l_{c,reference}}{l_{c,sample}}\right)^2 \quad (44)$$

The derivation of the third-order susceptibility from

THG experiments is much more complex in practice. Since all media (including air and the glass walls of the cell) present a third-order nonlinear effect, one has to be extremely careful in the analysis of third-harmonic data. It is possible to eliminate some of the effects (e.g., by working in vacuum chambers) to avoid the complex interference pattern one does otherwise obtain.

3. Historic Survey

Terhune, Maker, and Savage reported in 1962 the efficiency of third-harmonic generation in calcite under index-matched conditions.[115] They placed their samples near or at a focus of the laser beam. Since the $\chi^{(3)}$ is usually small and the laser intensity is often limited by optical damage in crystals, the conversion efficiency for the third-order nonlinear process is small. In addition, phase matching is very difficult to achieve in crystals. It has therefore found little practical application.

Third-harmonic generation can also occur in gases.[116] In spite of the low atomic or molecular density in gases, one can observe the third-order nonlinearity. As Harris and Miles pointed out,[117] $\chi^{(3)}$ can be resonantly enhanced much more easely in gases because of the sharp transitions. Also, the limiting laser intensity in gases is orders of magnitude higher than in condensed matter. It is even possible to have phase-matched THG when there is anomalous dispersion ($n(\omega) > n(3\omega)$ due to the absorption band) for one gas and normal dispersion ($n(\omega) < n(3\omega)$) for a buffer gas that compensates the difference of refractive indices at ω and 3ω. This has been demonstrated in many cases.[118-123]

In 1973 and 1974, Hermann, Ricard, and Ducuing investigated by THG the third-order polarizability of long-chain organic molecules such as β-carotene in solution.[124,125] In 1976, Sauteret et al.[126] measured the third-order susceptibilies of one-dimensional conjugated polymer crystals (polydiacetylenes) and found values comparable to those of inorganic semiconductors. A method for the determination of third-order nonlinear susceptibility in organic liquids was developed in 1983,[114,127,128] and a series of organic molecules in solution were studied.[129,130] The same technique was applied to measure the third-order nonlinearity in Langmuir-Blodgett and spin-coated films of for instance polysilanes,[131-135] polygermanes,[136] polythiophenes,[137] polydiacetylenes,[138,139] polyacetylenes,[140] poly(azomethines),[141] polybenzobisthiazoles, -oxazoles, -imidazoles[73a,142] and ladder polymers.[143,73b] Frazier et al. were among the first to investigate metal-contain ing organic polymers (1987).[144] A good review paper on organometallic materials for nonlinear optics was written by Nalwa in 1991.[145] Dispersion of the THG signal has been studied in trans-β-carotene,[146] polyacetylene,[147] polythiophenes,[148] and polydiacetylene.[62] Garito and co-workers have investigated the excited-state enhancement of optical nonlinearities in linear conjugated molecules.[102,149] Phthalocyanine thin films were examined by Sasabe and co-workers.[150] Hoshi et al. and Neher et al. have studied the nonlinear optical properties of fullerenes by THG.[151,152]

B. Electric-Field-Induced Second-Harmonic Generation (EFISHG)

This third-order technique gives second-harmonic generation according to the following nonlinear polarization:

$$P_i(2\omega) = \chi^{(3)}_{ijkl}(-2\omega;\omega,\omega,0)E_j(\omega)E_k(\omega)E_l(0) \quad (45)$$

As in the case of third-harmonic generation, EFISHG probes the purely electronic part of the third-order nonlinearity, which provide an instantaneous response. It does not measure dynamic nonlinearities and does not provide any information on the time response of the nonlinearity.

1. Theory

When we use the wave equation and the nonlinear polarization of eq 45, we obtain the following approximate expression for the SHG intensity:

$$I_{2\omega} = \frac{8\pi(2\omega)^2}{n^2_\omega n^2_{2\omega} c^2 \epsilon_0^2} \frac{\sin^2[\Delta k(l/2)]}{[\Delta k(l/2)]^2} |\chi^{(3)}|^2 \, l^2 \, I_\omega^2 \quad (46)$$

The phase mismatch Δk is given as

$$\Delta k = 2\omega \frac{(n_{2\omega} - n_\omega)}{c} \quad (47)$$

The EFISHG signal has contributions both from second- and third-order nonlinearities. For solutions, the microscopic third-order polarizability γ^0 of the dissolved molecules, derived from the macroscopic third-order susceptibility is given by

$$\gamma^0 = \langle \gamma \rangle + \frac{\mu \cdot \beta_{vec}}{5kT} \quad (48)$$

where $\mu \cdot \beta_{vec}$ is the scalar product of the dipole moment vector with the vector part of the second-order polarizability tensor and $\langle \gamma \rangle$ is the scalar orientationally averaged part of the third-order polarizability tensor. For centrosymmetric structures ($\mu = 0$), the EFISHG signal is caused by the third-order polarizability. By changing the interaction length l, the second-harmonic intensity can be optimized. This is done by translation of a wedge-shaped cell. A sinusoidal fringe pattern of second-harmonic intensity versus optical path length is obtained. The spacing between two maxima on the fringe pattern is twice the coherence length l_c.

2. Experimental Technique

A typical EFISHG setup uses a Nd:YAG laser with a wavelength of 1064 nm, a pulse duration of a few nanoseconds, and a low repetition rate (10 Hz). When the material to be studied is absorbing at 532 nm, a different wavelength should be selected. This can be done by dye-lasers and Raman shifters. The cell is wedge-shaped with electrodes at the top and the bottom of the cell. The necessary static electric field is generated by applying a high voltage (10 kV) to the electrodes. A pulsed rather than a dc source is used to minimize problems associated to electrolysis of the sample or polarization of the electrodes. The cell is mounted on a translation stage that can be driven laterally with respect to the laser beam to observe the fringes associated with phase mismatch between the

nonlinear polarization propagating with wave vector $\mathbf{k}_\omega$ and the second-harmonic field propagating with $\mathbf{k}_{2\omega}$ through the medium. A reference arm is also constructed with a sample of quartz to avoid errors due to laser beam intensity fluctuations.

The third-order susceptibility of the solution can be approximately estimated according to Levine and Bethea:[153,154]

$$\chi^{(3)} = \frac{(n_{2\omega}^L + n_\omega^G)\, l_c^G}{(n_{2\omega}^G + n_\omega^G)\, l_c^L} \chi_G^{(3)} + \frac{(n_{2\omega}^L + n_{2\omega}^G)d_{11}l_c^Q}{(n_{2\omega}^Q + n_\omega^Q)E_0 l_c^L}\left(\frac{e^A I_{2\omega}^L}{I_{2\omega}^Q}\right)^{1/2}$$ (49)

where L stand for the liquid solution, G for the glass window of the cell, and Q for the reference quartz; n_ω is the refractive index at frequency ω; l_c is the coherence length determined by the phase mismatch; E_0 is the applied electric field; A is the attenuation coefficient due to absorption of harmonic light; and $I_{2\omega}$ is the observed peak intensity of the harmonic light. The second-order polarizability of quartz is twice the value of its nonlinear coefficient d_{11}.

3. Historic Survey

Only the pure electronic third-order polarizability of centrosymmetric molecules is directly accessible by the EFISHG technique. It is clear that for this reason it is a limited technique. Levine and Bethea measured the γ of benzene with EFISHG in 1975.[153] In 1987, Kajzar and Messier[155] and in 1988 LeMoigne et al.[156] applied this technique on symmetrical polydiacetylenes. In 1991, Persoons et al. compared the EFISHG γ values of symmetrical diphenylpolyenes with the γ values obtained by nonlinear interferometry based on degenerate four-wave mixing.[157] Dispersion measurements in conjugated linear chains by EFISHG and THG were also performed.[158]

C. Degenerate Four-Wave Mixing (DFWM)

In a degenerate four-wave mixing process, there is an interaction between three beams to generate a fourth beam of the same frequency. The expression for the induced nonlinear polarization corresponding to the generated field is

$$P_i(\omega) = \chi_{ijkl}^{(3)}(-\omega;\omega,\omega,-\omega)E_j(\omega)E_k(\omega)E_l^*(\omega)$$ (50)

The degenerate four-wave mixing process derives its contributions from both the real and the imaginary parts of $\chi^{(3)}$. It is a convenient method for measuring both electronic and dynamic nonlinearities and for obtaining their time response.

1. Theory

The physical description of degenerate four-wave mixing can, in principle, be treated in a similar manner as that for harmonic generation, except that in this process three spatially distinguishable waves of the same frequency interact to generate a fourth wave of the same frequency, but with a different propagation direction. The starting point of the analysis is the wave equation and the nonlinear polarization in relation 50. The equation can be solved using slowly varying envelope approximation (which considers that the features of the pulse (the envelope and instantaneous phase) vary

little during an optical period) and assuming that there is no pump beam depletion. The wave equation also yields the phase-matching requirement:

$$\mathbf{k}_1 + \mathbf{k}_2 + \mathbf{k}_3 + \mathbf{k}_4 = 0$$ (51)

There are two common geometries. The first one is the forward-wave geometry in which all the incident beams are propagating in the same direction. The other one is the backward-wave geometry in which two beams are counterpropagating (forward pump beam E_f and backward pump beam E_b) and the third beam (probe beam E_p) is incident at a small angle θ with respect to E_f. In this geometry $\mathbf{k}_f = -\mathbf{k}_b$ so that the phase-matching condition requires for the signal beam $\mathbf{k}_s = -\mathbf{k}_p$. The signal is then generated counterpropagating to the probe beam and the phase-matching condition is automatically satisfied.

The process of degenerate four-wave mixing in the backward-wave geometry is synonymous with optical phase conjugation (OPC).[159] A probe beam incident on a phase conjugate mirror (i.e., a medium illuminated by E_f and E_b) retraces itself. The reflected beam is called the phase conjugate beam; it corrects every distortion of the probe beam when it retraces it. The efficiency of the DFWM/OPC is described by the reflectivity $R = I_{opc}/I_p$. The solution of the wave equation is given by

$$I_{opc} = \frac{\omega^2}{4c^2 n^2}|\chi^{(3)}|^2\, l^2\, I_f I_b I_p$$ (52)

This result is valid under the assumption that there is no linear or nonlinear absorption, no pump depletion, and low reflectivity. If the three input beams are derived from the same fundamental beam, then it is clear that the phase conjugate signal shows a cubic dependence on the fundamental intensity. One of the advantages of phase conjugation by degenerate four-wave mixing is that reflectivities higher than 100% can be achieved, has been demonstrated in a number of instances.[160-163] The energy of the phase conjugate beam is retrieved from the pump beams.

2. Experimental Technique

The choice of the laser source is very important in this case. Dynamic nonlinearities are possible and even a weak absorption can give dominant thermal nonlinearity (thermally induced refractive index change). This is often the case with long laser pulses (nanoseconds). If electronic susceptibilities are to be measured, one should use picosecond (or even subpicosecond) pulses. The laser system often consists of a mode-locked continuous-wave Nd:YAG laser which is frequency doubled and compressed to pump a dye laser. It is possible to amplify these dye laser pulses by another Nd:YAG laser, which result in subpicosecond pulses with high power. One can also use a mode-locked Nd:YAG laser and select pulses of the pulse train at low repetition rate. This results in 1064-nm pulses of 200 ps at 10 Hz.

The fundamental laser beam is split into a forward pump beam and a probe beam. If we place the nonlinear sample to be studied in front of a mirror, the backward pump beam is created by reflection of the forward pump beam on this mirror. The probe beam is directed on the sample under a small angle with these pump beams.

This method is called the back-reflection method. In the counterpropagating mode, the backward pump beam is not created by reflection of the forward pump beam, but by splitting the pump beam in two with a beamsplitter and directing these beams with mirrors in a counterpropagating way. The use of delay lines is necessary, because the pulses are very short and there has to be a good temporal overlap between the three input beams. The intensity of the phase conjugate signal is measured and compared with a reference (usually CS_2). The $\chi^{(3)}$ value is obtained approximately by using the following equation in the case of a nonabsorbing sample:

$$\frac{\chi^{(3)}_{\text{sample}}}{\chi^{(3)}_{\text{reference}}} = \left(\frac{n_{\text{sample}}}{n_{\text{reference}}}\right)^2 \frac{l_{\text{reference}}}{l_{\text{sample}}} \left(\frac{I_{\text{sample}}}{I_{\text{reference}}}\right)^{1/2} \quad (53)$$

where n_i is the refractive index and l_i is the path length in medium i. For an absorbing sample, one has to include an exponential factor accounting for the loss. Although in some cases and with some lasers, focusing is necessary, in general one can observe the optical phase conjugate signal without focusing. This means that fewer problems are encountered with the decomposition and photodegradation of organic molecules because the energies are lower than in third-harmonic generation.

To accurately measure the $\chi^{(3)}$ value of organic molecules nonlinear interferometers have been developed.[157,164-173] In this case, one arm of the interferometer consists of the sample cell, and the other arm is the reference. In this way, it is possible to measure the sign and the magnitude of the real and imaginary parts of $\chi^{(3)}$.

These techniques provide valuable information on the different nonlinear processes that contribute to the intensity-dependent refractive index.[174-177] It is also possible to obtain the time response of the nonlinearity[110] and, with this information in hand, the mechanism of optical nonlinearity can be identified. The technique is highly sensitive because the signal is a phase-matched nonlinear response. The main disadvantage is that picosecond pulses and a good control over the experimental conditions are required.[157]

3. Historic Survey

In 1977, Hellwarth was the first to demonstrate the generation of a phase conjugate wave by degenerate four-wave mixing.[107,159] In the same year, Yariv and Pepper calculated the reflectivity of this phase conjugate wave.[178] The reflectivity in absorbing media was calculated a few years later.[179-182] Third-order susceptibilities of organic thick films of polyacetylenes and conjugated aromatic heterocyclic polymers have been measured by Rao et al.[183,184] Maloney et al. used picosecond optical phase conjugation to study conjugated organic molecules.[185] Prasad and co-workers measured the third-order polarizability of a series of organic oligomers and polymers [polyphenylenes, polythiophenes and oligothiophenes, polyacetylenes, and poly(N-vinylcarbazoles)].[95,176,186,187] The third-order nonlinear optical properties of an organic dye (perylenetetracarboxylic dianhydride) were studied by sub-picosecond degenerate four-wave mixing at 602 nm by Samoc and Prasad.[188] The third-order nonlinearities of metal dithiolate complexes in solution were measured

by Maloney and Blau[189] and Winter et al.[190] The polydiacetylene polymers were studied in solution[191-193] and in thin films.[194-196] Thin films of polymers of poly(phenylacetylene) were investigated by Bubeck et al.[197] and LB films of an absorbing dye by Du and Chen.[198] In 1991, Davey et al. used an experimental method called forced light scattering from laser-induced gratings, a technique which may be viewed as a degenerate four-wave mixing process in the forward direction, to investigate the third-order nonlinear properties of transition-metal complexes containing diacetylene and phenylacetylene systems.[199] The review paper on organometallic materials for nonlinear optics also contains degenerate four-wave mixing data.[145] Picosecond degenerate four-wave mixing at 598 nm was performed on side-chain methacrylate copolymers incorporating 4-amino-4'-nitrostilbene, 4-oxy-4'-nitrostilbene and functionalized silicon phthalocyanine chromophores.[200] Ladder-type polymers were also studied by four-wave mixing.[201] Recently, Zhang et al. studied the third-order optical nonlinearities in C_{80} and C_{70} toluene solutions by using time-delayed degenerate four-wave mixing technique with 30-ps pulses at 532 nm for both parallel- and cross-polarization configurations.[202] Picosecond DFWM experiments due to Taliani and co-workers on polythiophene films pumped at 532 nm have shown the influence of excited-state enhancement processes; these have also been demonstrated on diphenylhexatriene by Rodenberger et al.[102,203]

D. Self-Focusing and Defocusing

These special cases of self-action are derived from the intensity dependence of the refractive index of the medium. There is only one input beam that provides the three input photons for the interaction. The nonlinear polarization is created at the same frequency as the incident beam:

$$P_i(\omega) = \chi^{(3)}_{iikk}(-\omega;\omega,-\omega,\omega)E_i(\omega)|E_k(\omega)|^2 \quad (54)$$

It is called self-action because the nonlinear polarization induced by the incident beam changes the propagation or other properties of the same incident beam. This effect does not give any time response information. Even weakly absorbing samples and a long interaction length provide large refractive index changes derived from thermal effects. These problems are more serious with longer pulse lengths (nanoseconds).

1. Theory

The intensity-dependent refractive index responsible for self-action (self-focusing, self-defocusing, and self-phase modulation) is

$$n(\lambda) = n_0(\lambda) + n_2(\lambda)\,I \quad (55)$$

where I denotes the intensity of the wave and n_0, the linear refractive index. The nonlinear refractive index coefficient n_2 is given by eq 10 (in which it is important to note that n_2 and $\chi^{(3)}$ have the same sign if n_0 is a real quantity). Self-focusing occurs as a combined effect of a positive n_2 and a spatial variation of the laser beam intensity (more intense in the center than at the edges). This results in a larger refractive index of the nonlinear medium in the center of the beam. The medium acts

as a positive lens and focuses the beam. Self-defocusing happens when n_2 is negative. The nonlinear polarization creates a negative lens which defocuses the beam.

2. Experimental Technique

Self-focusing and defocusing were observed in atomic vapors by Grischkowsky.[204,205] There are two important measuring techniques for $\chi^{(3)}$ which use self-action: the optical power limiter (OPL) and the z-scan. The first of these techniques was developed by Soileau et al. in 1983.[206] The basic concept is to use self-focusing and intensity-dependent absorption to make a passive optical device with high transmission for low input power, but with low transmission for high input power. In this technique, the laser beam is focused in the sample with high n_2. For low input powers the transmitted light is focused through a pinhole on a detector. As the power is increased, self-focusing becomes important and the transmitted laser beam is no longer focused through the pinhole; the power after the pinhole decreases. Beyond a certain critical input power P_c, many other nonlinear processes give rise to a leveling off of the transmitted power. Marburger has solved the nonlinear equation for the case of a spatial Gaussian beam.[207] This equation directly relates P_c to n_2:

$$P_c = \frac{3.72c\lambda^2}{32\pi^2 n_2} \qquad (56)$$

where c is the speed of light and λ, the laser wavelength. From the determination of the critical power, one can calculate n_2 and therefore the $\chi^{(3)}$ value of the medium.

Van Stryland and co-workers developed the z-scan method in 1989.[208] It is a highly sensitive single-beam experimental technique for the determination of both the sign and magnitude of n_2. A Gaussian beam is focused in a nonlinear sample and the transmitted power is measured with a photodiode and a pinhole placed in the far field as a function of the sample position z. The sample is moved through the focus of the beam. In the neighborhood of the focus, the laser intensity is very high and self-focusing or defocusing can occur. The resultant plot of transmittance through the aperture yields a dispersion-shaped curve from which n_2 can be calculated. This method is very sensitive on the beam quality: it must be Gaussian TEM_{00}. Because it requires a high power density and a long interaction length, this method is not very useful for thin polymeric films.

A serious problem for both techniques is the dielectric breakdown and sample damage at the power densities needed for these self-focusing experiments. It is a good screening method for transparent (visible range) liquid samples.

3. Historic Survey

The first demonstration of an OPL used CS_2 as a nonlinear medium.[209] The first organic materials studied with this technique were liquid crystals.[210,211] Frazier et al. measured in 1987 the nonlinearity of palladium polyyne films with OPL.[144] The third-order nonlinearity of ferrocene in the molten form and in solution was investigated with the same technique in 1988 by Winter, Oliver, and Rush.[212] The optical limiting behavior of semiconductors was studied by Van

Stryland and co-workers[213,214] and the dispersion and two-photon absorption characteristics of these materials by Sheik-Bahae et al.[215] They also measured CS_2 and BaF_2 with the z-scan in 1990.[216] In 1991, Soileau et al. demonstrated the z-scan technique for a solution of chloroaluminum phthalocyanine at 532 nm.[217] In the same year, Perry et al. also investigated the excited-state absorption and optical limiting behavior of metallophthalocyanines with the z-scan.[218] Recently, the optical limiting performance of C_{80} and C_{70} solutions were studied.[219] The resonant third-order nonlinearity of polythiophene thin films was investigated by the z-scan in 1992;[220] the results indicated that the negative nonlinearity at 532 nm is resonantly enhanced (at the one-photon transition) and is associated to the saturation of the absorption. Sheik-Bahae et al. developed in 1992 a two-color z-scan method[221] to measure nondegenerate nonlinearities at frequency ω_p in the presence of light at frequency ω_e; an interesting work describing two-color dispersion and dynamical z-scan measurements has been reported by Qian and Wang.[222]

E. Optical Kerr Gate (OKG)

This effect is the optically-induced birefringence caused by a nonlinear phase shift. The nonlinear polarization corresponds to

$$P_i(\omega) = \chi_{ijkl}^{(3)}(-\omega;\omega,\omega,-\omega)E_j(\omega)E_k(\omega)E_l(\omega) \qquad (57)$$

Evolution of the birefringence and hence the response time of $\chi^{(3)}$ can be probed. There are various mechanisms (electronic deformation, molecular reorientation, molecular libration, molecular redistribution, electrostriction, thermal change) that are responsible for the change of nonlinear refraction index in the OKG and each mechanism has different strengths and response times.

1. Theory

When an intense linearly-polarized laser pulse penetrates a Kerr active medium, the optical electric field generates a nonlinear polarization in the medium. The difference between the molecular nonlinear polarization parallel and perpendicular to the laser electric field results in an observed optical birefringence δn:

$$\delta n = \delta n_\parallel - \delta n_\perp \propto (\pi/n_0)(\chi_{XXXX}^{(3)} - \chi_{XXYY}^{(3)}) \qquad (58)$$

This optically-induced birefringence can be probed by a weaker, linearly-polarized probe pulse of the same or different frequency. Delaying this probe pulse gives the time response information. The relative transmitted signal of the probe beam through the Kerr gate as a function of the delay time between probe and orienting pump pulse is

$$I_t(\tau) = \int_{-\infty}^{+\infty} \langle E_{probe}^2(t-\tau) \rangle \sin^2\left[\frac{\pi l}{\lambda}\delta n\right] dt \qquad (59)$$

and in the case of a nonresonant electronic nonlinearity

$$\delta n = n_2 I_{pump} \qquad (60)$$

From a measurement of the intensity at $t = 0$ (peak value), the value of n_2 can be determined. It is clear from eq 58 that the value of $\chi_{XXXX}^{(3)}$ can be obtained only when $\chi_{XXYY}^{(3)}$ is relatively small. In an isotropic medium, for an off-resonance purely electronic non-

linearity, the $\chi^{(3)}_{XXYY}$ component is one-third of the $\chi^{(3)}_{XXXX}$ component; the latter can then be directly measured.

The optically-induced birefringence is small and requires high power density, very stable laser sources, a high polarization ratio, a long interaction length, and an isotropic medium. This method is best used for liquid samples.

2. Experimental Technique

A picosecond laser pulse is split in a strong orienting pump pulse and a weak probe pulse. The probe pulse can be delayed. Both beams are linearly polarized. To retrieve the optical birefringence information, the probe beam passes through an analyzer (cross polarizer). The intensity of the probe beam transmitted through the Kerr cell is measured as a function of the delay between pump and probe.

3. Historic Survey

The optical Kerr gate is based on the theory of the optical Kerr effect which was first derived by Buckingham (1956).[223] The traditional electrooptical Kerr effect[224] uses a dc electric field from a voltage source, instead of a light source to induce the birefringence. Mayer and Gires (1963)[225] and Maker et al. (1964)[226] used a Q-switched ruby laser to generate high-power laser pulses to observe the first optical Kerr effect in the nanosecond region. Different components of the third-order nonlinear susceptibility tensor were measured in 1968 by Veduta and Kirsanov.[227] Later, Duguay and Hansen (1969)[228] and Shimizu and Stoicheff (1969)[229] applied mode-locked Nd:glass lasers to generate picosecond laser pulses for constructing a 10-ps resolution Kerr gate. Hermann et al. used this method to study β-carotene glass.[124] The optical Kerr effect was used in 1974 by Wong and Shen to investigate the behavior of field-induced molecular alignment in isotropic nematic substances.[230] Ippen and Shank (1975)[231] achieved a 2-ps time-resolved Kerr shutter with a subpicosecond mode-locked dye laser. In 1979, Ho and Alfano measured the nonlinear refractive indices of a series of organic liquids.[232] A good review paper on picosecond Kerr gate appeared in 1984 by Ho.[233] The OKG was applied by Kobayashi and co-workers in 1988 to study the relaxation of the optical Kerr effect in CS_2 and nitrobenzene.[234]

In 1989, Guha et al. used the OKG to measure the third-order polarizability of platinum polyynes.[235] While Yang et al. used it to investigate thiophene-based polymers and polysilanes,[236] Charra and Nunzi studied in 1991 the relaxation of one- and two-photon excitations in a polydiacetylene red form by the same technique.[139] The resonance-enhanced third-order susceptibility of a diluted β-carotene solution in dodecane was measured by time-resolved optical Kerr effect in 1992.[237] The third-order optical nonlinearities of metallotetrabenzoporphyrins and a platinum polyyne dissolved in tetrahydrofuran were measured by using picosecond and nanosecond laser pulses.[238]

V. Organic Third-Order Optical Materials

In this section, we present an overview of the properties of the main types of organic conjugated
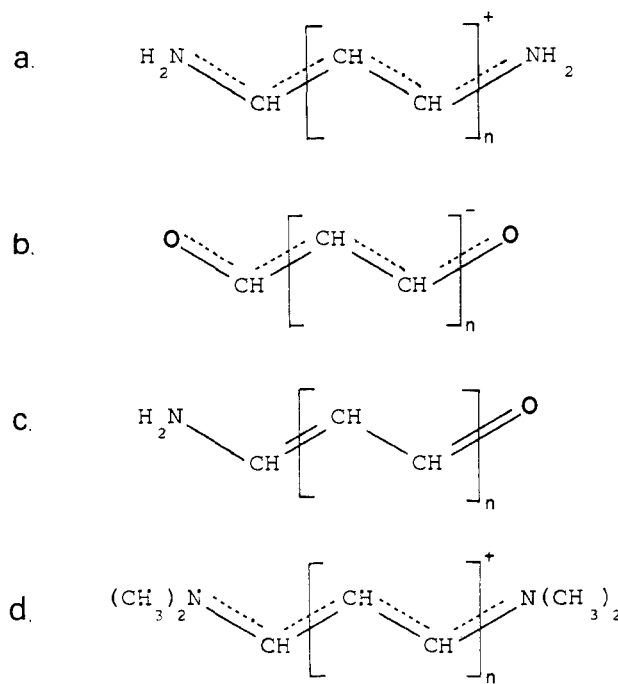
Figure 8. Molecular structures of (a) cyanine cations, (b) oxopolyeneolate anions, (c) merocyanine dyes, and (d) streptocyanines.

compounds which are being considered for third-order optical applications. We realize that the list of systems we discuss is not exhaustive, and we apologize in advance for any important works that have been missed by this review; however, we are confident that the essential parameters which influence the third-order nonlinear optical response of organic compounds are described in such a way that it also allows for a good understanding of other organic materials not covered here.

We first describe the optical response of simple polyenes and cyanine dyes and illustrate the importance of one major ingredient of the optical response, i.e., the molecular geometry and more precisely, the degree of carbon–carbon bond-length alternation along the chain; we then discuss the infinite polyene chain limit, all-trans-polyacetylene. Next, we mention polydiacetylenes but only briefly since these polymers have already been the subject of a number of recent reviews.[241,242] We then consider a wide class of oligomeric and polymeric compounds which are based on aromatic rings. These include polyarylenes [such as polythiophene and polyaniline), poly(arylenevinylenes) (such as poly(p-phenylenevinylene) and poly(thienylenevinylene)], and poly(arylenemethines). The issue of aromaticity vs quinoidicity of the rings is addressed in detail. The next sets of compounds correspond to ladder-type polymers and to polysilanes, the latter being prototypical of σ-conjugated materials. Finally, we deal with the influence of the extension of the π-electron system to form two-dimensional structures such as phthalocyanines or three-dimensional structures such as fullerenes.

A. Polyenes and Cyanine Dyes

Approximations of the SOS expression for γ reveal that candidate molecules for third-order nonlinear optical applications should also have large linear polarizabilities, or equivalently through the Kramers–

Kronig transform, large one-photon absorptivities.[82,92] Hans Kuhn in his classic 1949 paper[243] grouped the most important organic molecules that absorb visible and near-IR light into three categories, see Figure 8: (i) symmetric polymethines, e.g., cyanine cations and oxopolyeneolate anions, (ii) polyenes and related compounds, e.g., merocyanine dyes, and (iii) porphyrins and phthalocyanines. The conjugated π-electron bonding networks found in these molecules are the principal reason for their strong absorption of visible and near-IR light. It should therefore not be surprising that the organic molecules with the largest linear and nonlinear *electronic* polarizabilities measured to date fall into one of the above categories.[12,15,17,19,20] In this part, we will concentrate on the polyene and polymethine quasi-one-dimensional π-bonding networks exemplified by the linear *all-trans* polyenes and linear cyanine cations.

The symmetric polymethine-like molecules are distinguished by a π-electron bonding network with *attenuated* alternation of the π-electron bond orders in the ground electronic state, while the polyene-like molecules have a *pronounced* π-electron bond-order alternation in the ground electronic state. The attenuated alternation for the symmetric polymethines results from a π-electron ground state that can be described as a resonance hybrid of two equivalent structures, e.g., for the symmetric cyanine cations:

$$^{+}H_2N{=}CH{-}(CH{=}CH)_n{-}NH_2 \leftrightarrow$$
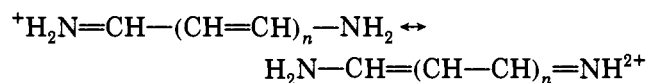
$$H_2N{-}CH{=}(CH{-}CH)_n{=}NH^{2+}$$

The pronounced bond-order alternation in the polyene-like molecules results from a π-electron ground state that is described by a single structure, e.g., the $^{+}H_2N{=}CH{-}(CH{=}CH)_n{-}O^-$ structure for the merocyanines in a vacuum is not equivalent to the more stable $H_2N{-}CH{=}(CH{-}CH)_n{=}O$ structure.

In free-electron theory, the potential energy of a π electron in a symmetric polymethine can be represented by a constant value because of the π-electron density delocalization associated with the resonance hybrid; in a polyene-like molecule the potential energy of the π-electron can be described by a periodic function with the crests and troughs of the function coinciding with the double and single bonds.[243] An important consequence of these different potential energy functions is that the energy separation between the highest occupied molecular orbital (HOMO) and the lowest unoccupied molecular orbital (LUMO) would go to zero with increasing chain length for symmetric polymethines, but converges to a finite value with increasing length for polyenes. In other words, symmetric cyanines would appear to become metallic in the limit of infinite length, while the polyenes resemble semiconductors in this limit.[244,245] It should be stressed, however, that AM1 semiempirical calculations indicate that symmetric cyanine dyes with 14 or more π electrons are likely to undergo a Peierls-type distorsion toward a bond-alternated geometric structure.[246] This result is not surprising since it can be expected that, as chain length grows, the electronic overlap between the two amino end groups sharply diminishes; as a consequence, the electronic structure becomes primarily determined by the central polyenic sequence, which favors bond-length alternation.

The free-electron/Hückel theoretical picture described above is in agreement with experimental and theoretical studies of the *linear* optical properties of *short* symmetric polymethines (cyanines) and polyene-like molecules. For example, there is the experimental observation that λ_{max} for the first one-photon allowed $S_0 \rightarrow {}^1\pi\pi^*$ transition increases linearly with chain length for short symmetric *all-trans*-polymethine cations with terminal dimethylamino groups (streptocyanines),[247] but reaches a limiting value in the case of *all-trans*-α,ω-dialkylpolyenes[248] and (dimethylamino)merocyanines,[247] $(CH_3)_2N{-}CH{=}(CH{-}CH)_n{=}O$. Also, the linear static polarizabilities of symmetric cyanine cations have been measured[74] and calculated[245,246,249,250] to be larger than those for *all-trans* linear polyenes of comparable methylation, length, and number of π-electrons.

One would thus also expect the nonlinear optical properties of symmetric polymethines (cyanines) to be different from those of polyene-like molecules. Third-harmonic generation measurements of the nonresonant electronic component of the third-order polarizability at $\omega = 1.91\ \mu m$ for a variety of symmetric cyanine dyes in the condensed phase yielded $\gamma(-3\omega;\omega,\omega,\omega)$ values with both *negative and positive signs*, while the measurements for a selection of polyenes yielded only positive $\gamma(-3\omega;\omega,\omega,\omega)$ values;[74] for streptocyanines, the magnitudes of the measured $\gamma(-3\omega;\omega,\omega,\omega)$'s met or exceeded those for $\alpha,\alpha,\omega,\omega$-tetramethylpolyenes of comparable size and number of π-electrons.[74] The THG measurements at $\omega = 1.85\text{--}2.15\ \mu m$ for the polycrystalline powder of a symmetric cyanine dye with terminal quinoline rings determined $|\gamma(-3\omega;\omega,\omega,\omega)|$ to be greater than that of the well-studied PTS polydiacetylene system.[251] Recent studies by Dirk, Kuzyk, and their co-workers of the third-order nonlinear optical properties for a set of *zwitterionic* polymethine dyes, the squaryliums, also emphasize the importance of this class of nonlinear optical molecules;[71b,252] Garito and co-workers have recently discussed theoretically the appearance of negative γ values in squaraines.[253]

We now describe some of the results that we have recently obtained on bond-alternating polyenes and symmetric cyanines with no bond alternation via an INDO/SDCI approach.[77,82] In the case of polyenes, a large number of contributions have already been reported.[48,55,57,60-62,92,149,254-256] We note that the INDO technique has been very successful in calculating nonresonant $\gamma(-2\omega;\omega,\omega,0)$ values for ethylene, linear polyenes, and benzene that are in excellent agreement with the γ values measured for these molecules in the gas phase.[53] The chosen geometries are such that in the case of the polyenes, a degree of bond-length alternation $\Delta r = 0.11$ Å ($r_{C=C}$, 1.35 Å; r_{C-C}, 1.46 Å) is picked. For the symmetric cyanine dyes with no bond alternation, the r_{C-N} and r_{C-C} bond lengths are set at 1.351 and 1.362 Å, respectively; note that this constitutes an approximation since *ab initio*[246] geometry optimizations on symmetric cyanines indicate the presence of a residual bond alternation in the middle of the molecule which increases with increasing chain length. A more thorough discussion of the influence of *molecular geometry* on the γ values will be provided below.

Figure 9 presents the evolution of the static γ values as a function of the extension of the π-system. All the
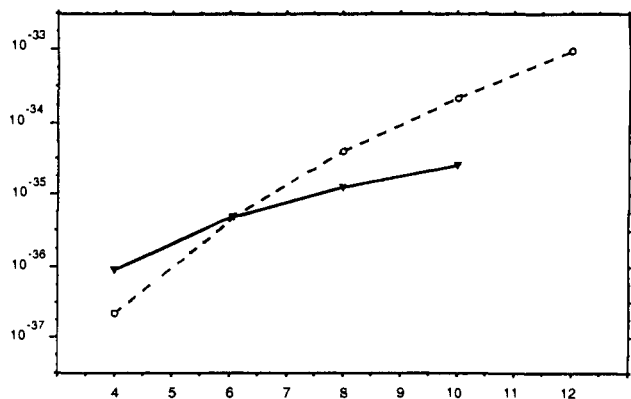
Figure 9. Evolution of the INDO/SDCI static γ values (in esu) of cyanine cations (dashed line) and polyenes (solid line) as a function of the number of the π electrons (adapted from ref 82).

γ values are negative for the cyanines and positive for the polyenes. We observe that for very short chains containing only four π-electrons, the polyene γ is larger in absolute terms than the symmetric cyanine γ. However, the evolution of γ with chain length is much stronger for the cyanine series, so that very quickly (beyond six-π-electron chains), the cyanines present the largest static γ values. Over the range of chain lengths considered in Figure 9, the polyene γ values evolve as a 3.9 power of the number of π-electrons while the corresponding power for the cyanines is 7.6. The 12 π-electron cyanine reaches a calculated static γ of about -1000×10^{-36} esu. As we discussed above, we can expect that in long chains, polyenes and cyanines lead to the same hyperpolarizabilities due to the decreasing influence of the cyanine amino end groups.

It is important to investigate the nature of the excited states which play a major role in the γ response. In

Figure 10, we plot the most significant transition dipole values. As was already pointed out by Garito and co-workers in the case of polyenes,[92] we observe that both type of compounds considered here present large transition dipoles between the $1A_g$ ground state and the $1B_u$ state and between the $1B_u$ state and a higher lying mA_g state; the precise value of m depends on the oligomer length; for instance in the case of octatetraene, $m = 6$.[77,82,92] (The description of these states has been provided in section III.) Furthermore, Mazumdar and co-workers have also shown[79] (and we have now been able to confirm that result[257]) that each significant mA_g state possesses a very large transition dipole with a high-lying nB_u state.[79] In the long polyenes, these nB_u states correspond to conduction band states. In the case of the short cyanines, two mA states do play an important role in contrast to the shortest polyenes where a single mA_g state is significant. As chain length increases, however, more mA states start contributing, also as a result of band formation. (At this stage, it is useful to note that our INDO/SDCI calculations[53,77,82] on the linear polyenes indicate that the mA_g state is not bound between the $1B_u$ and $2B_u$ states. This is at first sight in contradiction to the results of Mazumdar and co-workers;[78,79] however, these authors do use the electron–hole symmetry approximation and label their states accordingly, referring only to B_u states with ionic character. This approximation is not used in our calculations, where the hopping terms in the Hamiltonian are not constrained to nearest neighbors.)

1. Molecular Geometry

It is of utmost importance to investigate the influence of molecular geometry on the γ response. Early studies on polyenes focused on the relationship between the degree of bond-length alternation Δr and the α and γ polarizabilities. At the *ab initio* Hartree–Fock level,
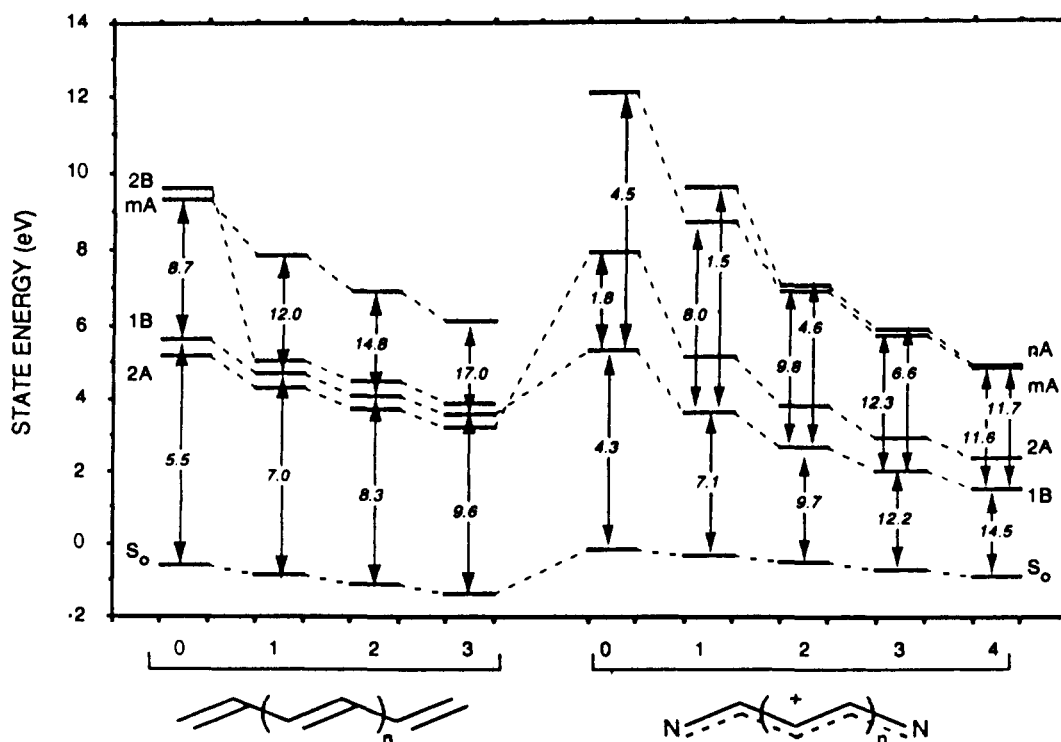
Figure 10. Most significant transition dipole moments (in D) of linear polyenes and symmetric cyanine cations as a function of chain length (adapted from ref 82).
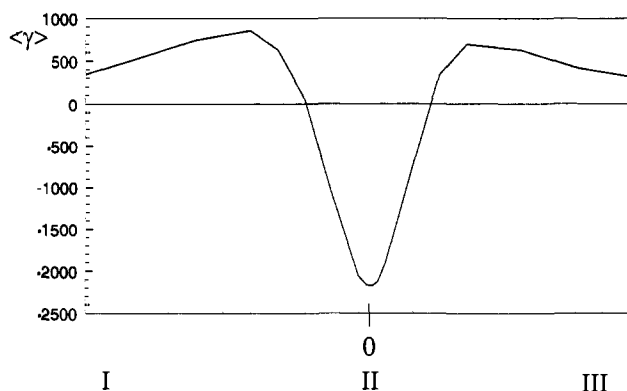
Figure 11. Evolution of the INDO/SDCI-SOS static γ value (in esu) for a three double-bond polyene end-capped by an acceptor (aldehyde) and a donor (dimethylamino), as a function of the switch from the polyene limit (I) to the cyanine limit (II) and to the zwitterionic limit (III) [from ref 84].

Bodart *et al.* found that α strongly increases when reducing Δr, and is largest for vanishing Δr, as a result of a more homogeneous electronic potential.[258] de Melo and Silbey[256] calculated a significant γ increase in the presence of solitons or polarons along the polyene chains; this can be rationalized by the fact that the solitons and polarons lead locally to a depression in the Δr value.

A most insightful approach has been recently reported by Marder and co-workers who investigated polyenes end-capped by acceptor (aldehyde) and donor (dimethylamino) groups.[259,280,83,84] These authors have calculated at the Hartree–Fock AM1 level[259,260,83] and at the INDO/SDCI correlated level,[84] how the degree of bond-length alternation is altered by the presence of an external electric field (aimed at simulating the influence of solvent molecules or, more generally, the dielectric medium) and how the modified geometry in turn affects the molecular polarizabilities. The interesting aspect here is that one is able: (i) *to follow in a continuous manner the evolution of γ* as one goes from the polyene limit [form I below; $\Delta r \sim 0.1$ Å] to the cyanine limit [form II; $\Delta r \sim 0$ Å], and then to the zwitterionic limit [form III; $\Delta r \sim 0.1$ Å] as a function of the external electric field:

$$(CH_3)_2N - (CH=CH)_3 - CH=O \qquad \qquad I$$

$$\downarrow E = 5\times10^9 \text{ V/m}$$

$$(CH_3)N^{\delta+} \cdots (CH \doteq CH)_3 \doteq CH \doteq O^{\delta-} \qquad II$$

$$\downarrow E = 10^{10} \text{ V/m}$$

$$(CH_3)N^+ = (CH-CH)_3 = CH-O^- \qquad III$$
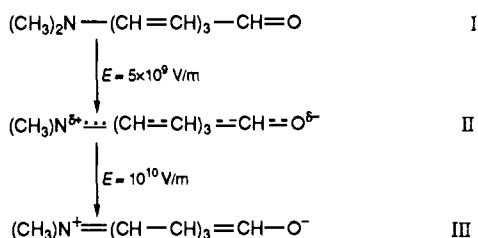
and (ii) *to unify the concepts describing these three sets of compounds.*[84]

The evolution of the static $\langle \gamma \rangle$ obtained by Meyers *et al.*[84] at the INDO/SDCI level is sketched in Figure 11. For the usual gas-phase Δr value of 0.11 Å, *i.e.*, the polyene limit I, $\langle \gamma \rangle$ is calculated to be positive. The $\langle \gamma \rangle$ value strongly increases with the reduction of Δr driven by the external field. A peak in the positive $\langle \gamma \rangle$ value is obtained for Δr on the order of 0.05 Å ($\langle \gamma \rangle$ is then over twice as big as for Δr equal to 0.11 Å). For Δr values smaller than 0.05 Å, $\langle \gamma \rangle$ decreases, passes by zero (Δr around 0.03 Å) and reaches a negative peak for

zero bond-length alternation, *i.e.*, the cyanine limit II. When one goes toward the zwitterionic limit III, $\langle \gamma \rangle$ tends to become positive again. Note that the magnitude of the negative peak is larger than those of the positive peaks.

These results call for the following remarks:

(i) They illustrate the *essential influence of molecular geometry on the polarizabilities.*

(ii) They point out the very different evolution of α and γ vs Δr. While α keeps increasing when Δr tends to zero, γ presents a second-derivative-like evolution. The often-used scaling arguments that try to link γ to α are therefore very misleading in the present context.

(iii) They stress the need for taking the dielectric medium properly into account to achieve a coherent evaluation of the nonlinear optical response and also the possibility of optimizing the γ response by adequately controlling the medium. (We point out that we have recently started to calculate the influence of the dielectric medium at the *ab initio* level, by following a reaction-field approach; we obtain excellent agreement between the NLO coefficients obtained in that framework and experimental data collected in different solvents for polyene derivatives such as retinal and aromatics such as *p*-nitroaniline.[50])

(iv) It should be borne in mind that the increase in γ value obtained when Δr starts decreasing from its gas-phase value is simultaneously related to a reduction in the 1B transition energy. The transparency domain of the molecule thus narrows toward the cyanine limit.

It must be emphasized that these theoretical results are supported by an increasing number of experimental data collected by Marder and co-workers.[83]

Garito and co-workers have theoretically examined the influence on the γ response of chain conformation, *all-trans vs trans-cisoid*, in the case of *short* polyenes.[76] They have found that the parameter determining γ is the overall length of the chain, *i.e.*, the distance between the two terminal carbons. An *all-trans* chain and a *trans-cisoid* chain (with a larger number of carbons) possessing equivalent lengths lead to the same γ value.

2. Chain-Length Influence

Numerous theoretical studies have been devoted to the investigation of the γ evolution as a function of chain length in polyenes.[48,53,56,60–62,77,78,82,92,254,256] The results provide power values (see section III) which range between 3 and 5.4 for the short chains; a saturation regime sets in after some 30 bonds. Schrock and Zyss and co-workers[261] have recently reported an experimental study on triblock copolymers containing model polyenes which range in size from 4 to 16 double bonds. These copolymers are synthesized via a ring opening metathesis polymerization (ROMP) scheme[262,263] which allows for a very good control of the sequence lengths. From EFISH measurements on the copolymers, the power law dependence of the static γ value with respect to chain length is estimated to correspond to 3.2. For the 16 double-bond polyene, the static γ is measured to reach about 3600 × 10⁻³⁶ esu.

We have carried out valence-effective Hamiltonian (VEH)/sum-over-states calculations of the static γ value in polyene chains containing 2–15 double bonds.[57] Comparison between the calculated and measured values is provided in Table 5 (note that in our original

Table 5. Comparison between the VEH/SOS[56b] and Experimental[261] Static Third-Order Polarizability (γ) Values (in 10^{-36} esu) for Polyenes as a Function of the Number N of Double Bonds

N	VEHSOS (γ)	experimental (γ)
2	0.09	
3	1.07	
4	6.12	50
5	21.25	99
6	55.59	180
7	120.20	280
8	226.44	400
9	384.33	570
10	601.33	830
11	882.53	1100
12	1229.03	1500
13	1639.88	1900
14	2110.82	2400
15	2637.76	2900

paper, the γ's were calculated via a Taylor series; they have been divided by a factor of 6 to convert them to a power series). As can be observed from Table 5, the agreement for the longer chains between theory and experiment is extremely good, even on a quantitative basis. The calculated power law dependence tends to 3.3 when N reaches 15 double bonds, to be compared to the 3.2 experimental value.

The coupled anharmonic oscillator approach provides a simple framework in which to understand the appearance of a saturation of the γ response. In that context, saturation is reached when the chain length reaches the coherence length of the $1B_u$ exciton.[60,61] This picture is actually similar to the phase space filling model proposed by Greene, Schmitt-Rink, and co-workers for polydiacetylenes[264] and by Charra and Messier for polythiophene.[265] This origin of the saturation in the γ response implies that the α and γ terms should saturate at about the same chain length since α in conjugated polyenes is dominated by virtual excitations to the $1B_u$ state. Kavanaugh and Silbey have recently investigated the chain length dependence of α, β, and γ within the coupled oscillator model and found nearly identical settings of saturation behavior.[64] Experimental evidence appear to indicate that this holds true for substituted oligothiophenes.[96] More work is, however, needed to fully confirm this picture.

It is also important to point out that disorder effects are expected to limit the γ value. They can manifest for instance in the form of torsions around some of the single carbon–carbon bonds, lifting the full planarity of the chain and as a consequence, decreasing the effective conjugation along the chain. Such disorder effects have been modeled by Hone and Sing who showed that they result in the saturation regime being reached sooner and corresponding to a lower γ value.[266] It is thus of prime importance to work with materials in which the conjugated chains are as well oriented (extended) as possible and defect-free. In addition to differences in methodologies and to experimental artifacts, differences in materials quality are one of the major sources of scattering in the nonlinear optical experimental data which are being reported (a feature which is similar to what happens in the field of conducting polymers).

3. Effect of Charge State

The charge state of the molecule can exert a pronounced influence on the nonlinear optical response. We have described above that positively charged symmetric cyanines (which carry an even number of electrons for an odd number of sites) provide dramatic increases in the γ response as a function of chain length in the case of molecules with up to 12 π-electrons. The INDO/SDCI sum-over-states results indicate a power law dependence with respect to N on the order of 7.6.[82] (We recall that this value might, however, be somewhat overestimated since some degree of bond-length alternation should appear in the middle of the molecule.)

In the case of polyenes, de Melo and Silbey[256] have analyzed via a perturbation treatment the influence, on the γ response, of the formation of charged solitons on odd-numbered polyene chains. They also considered the presence of (singly) charged polarons or (doubly) charged bipolarons on even-numbered chains. They examined polyenes containing up to about 20 carbons. The presence of these charged species lead to the appearance of new electronic levels within the otherwise forbidden energy gap of the polyene chain.[67] The power law evolution of γ on chain length is calculated to depend strongly on the charge state.[256] While the power value is calculated by de Melo and Silbey to be around 4.25 for a regular (neutral) polyene, it jumps to 4.8, 6.3, and 6.1 for chains carrying a charged soliton, polaron, or bipolaron, respectively. The largest γ values are calculated for the charged polaron and are *negative*.[238] Our interpretation is that this behavior might be due to the appearance of a singly occupied polaron level located only a few tenths of an electronvolt above the HOMO level; the resulting very low-lying $1B_u$ electronic transition involving mainly these two levels, could thus dominate the γ response through the negative $1A_g \rightarrow 1B_u \rightarrow 1A_g \rightarrow 1B_u \rightarrow 1A_g$ channel. We note that Beratan has also considered within a one-electron tight-binding model, the influence on γ of the appearance of gap states in conjugated organic polymers.[267]

As we mentioned above, the formation of a charged soliton, polaron, or bipolaron has the consequence of decreasing the Δr value along the portion of the chain where the charge is localized.[67] Thus, the charge state exerts an influence on the γ response via its modification of both the electronic transitions and the molecular geometry. Again, it should be kept in mind that this results in narrowing the transparency domain of the compound. Evaluation of the γ response in polyenes carrying soliton pairs has recently been made by Dalton, Spangler, and their co-workers.[268]

B. Polyacetylene

all-trans-Polyacetylene, $(-CH=CH-)_n$, is considered to be the prototypical π-conjugated polymer. Interest in the material has sharply increased since the 1970s, when appropriate synthetic routes toward film formation were developed[269] and, most importantly, when it was discovered that the intrinsically semiconducting material (bandgap of about 1.8 eV) can be made highly conducting through redox chemistry.[270] Electrical conductivities at room temperature as large as that of copper can now be achieved.[271,272]

Proper characterization of the nonlinear optical characteristics of polyacetylene has long been hampered
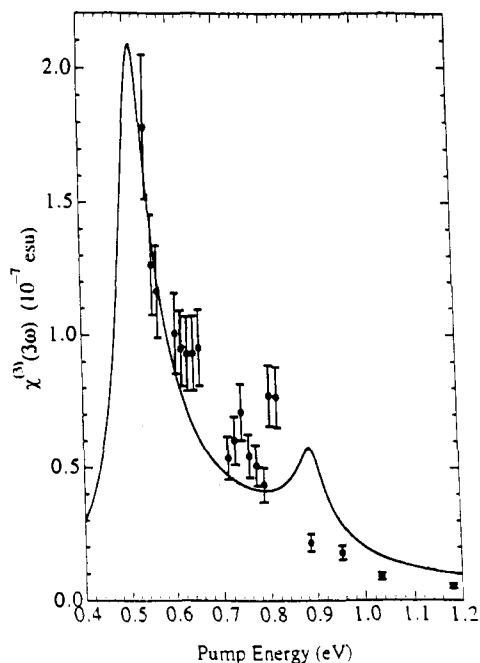
Figure 12. Illustration of the measured $\chi^{(3)}(3\omega)$ for an oriented sample of *trans*-polyacetylene as a function of pump energy (adapted from ref 275).
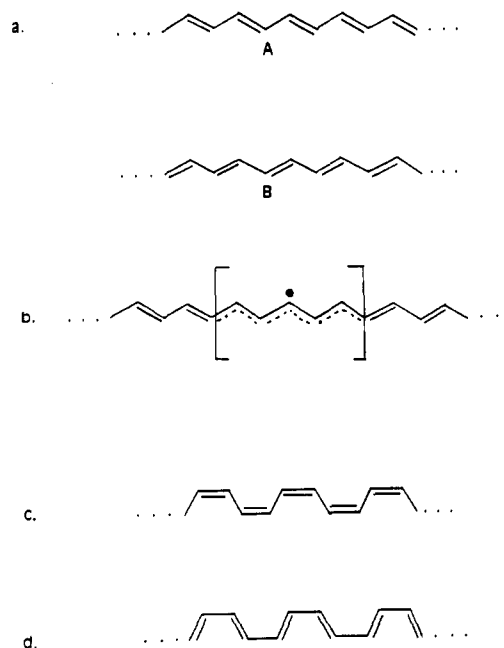

Figure 13. Part a shows sketches of the energetically degenerate A and B phases of *trans*-polyacetylene; b, schematic representation of a neutral soliton in *trans*-polyacetylene; c, molecular structure of the *cis-transoid* conformer of polyacetylene; d, molecular structure of the *trans-cisoid* conformer of polyacetylene.

by the relatively poor quality of the prepared films and therefore the large amount of disorder. Major improvements in materials quality have come from the works carried out at Durham[273] by Feast and co-workers and BASF.[271] Up to the mid-1980s, only single-frequency measurements of the polyacetylene $\chi^{(3)}$ susceptibility were available.[274] The situation dramatically improved with the work of Kajzar and co-workers[275] and in particular the THG free-electron laser measurements by Fann *et al.*,[147] which were carried out over a frequency range going from about 0.4 to 1.1 eV. The $\chi^{(3)}$ *vs* $\hbar\omega$ data showed two distinct peaks, at *ca.* 0.6 and 0.9 eV. These peaks can be interpreted as three-photon and two-photon resonance enhancements with the $1B_u$ state and the mA_g state, respectively.

More recently, Heeger and co-workers have carried out a THG measurement over a wide frequency range (0.5 to 1.2 eV) on both *all-trans*- and *cis*-polyacetylene.[276] Over the investigated spectral range, the $\chi^{(3)}$-$(-3\omega;\omega,\omega,\omega)$ susceptibility of the *trans* compound is found to be at least 1 order of magnitude larger than that of the *cis* compound (even when the latter is fully on resonance and the former not). These authors have also measured the THG $\chi^{(3)}$ component parallel to the chain axis in *trans*-polyacetylene samples prepared using the best techniques currently available and stretched up to a draw ratio of 10 (*i.e.*, elongation of the sample by 1000%). This leads to a highly-oriented material (the same kind of material as that which upon iodine doping, typically leads to an electrical conductivity of about ((1–3) × 10⁴ S/cm[272]). The THG $\chi^{(3)}$ dispersion is then measured to be significantly larger than in previous instances, Figure 12. A strong resonance appears at *ca.* 0.55 eV and amounts to about 2 × 10⁻⁷ esu. It is considered by Heeger and co-workers to correspond simultaneously to a three-photon resonance to the $1B_u$ state and a two-photon resonance to a relaxed $2A_g$ state.[276] Off-resonance $\chi^{(3)}$ values are on the order of 10⁻⁸–10⁻⁹ esu. The spectrum of Figure 12

suggests the presence of another resonance (at *ca.* 0.80 eV), which can be related to the two-photon resonance to the mA_g state.

The very significant $\chi^{(3)}$ enhancement obtained in structurally-ordered and strongly-oriented polyacetylene samples, illustrates the importance of designing synthetic strategies resulting in highly-processible polymers. This is definitely required in order to achieve the high performance values needed for use in photonics, as discussed in section I. The major role to be played by polymer chemistry and processing cannot be underestimated.

The origin of the $\chi^{(3)}$ difference between the *trans*- and *cis*-polyacetylenes is still controversial, especially since it is not expected on the basis of the results on polyenes.[76] Heeger and co-workers have stressed the *degenerate* ground-state nature of *trans*-polyacetylene.[276] It is therefore worthwhile to indicate that the ground state of the polymer *all-trans* conformer is said to be degenerate because it can correspond to either of two geometric structures which are obtained from one another by a simple exchange of the single and double carbon–carbon bonds, see Figure 13. These geometric structures possess exactly the same total energy and are usually referred to as phase A and phase B of *trans*-polyacetylene. They are valence bond isomers of one another; they are *not* resonance forms, in which case all the carbon–carbon bonds would be equal. The importance consequence of the degenerate character of the ground state is that *trans*-polyacetylene supports nonlinear excitations in the form of solitons.[65,277] (For a description of solitons in chemical terminology, the reader is referred to ref 67.) The soliton can be viewed as a topological (geometry relaxed) defect making the boundary between a phase A segment and a phase B segment along a *trans*-polyacetylene chain (Figure 13b). Note that a neutral soliton (S•) is a radical and carries

a spin $1/2$ while a positively (S$^+$) or negatively (S$^-$) charged soliton is spinless. On the other hand, cis-polyacetylene does not present any degenerate ground state. Exchange of the single and double bonds lead from the cis-transoid conformer to the trans-cisoid conformer or vice-versa, see Figure 13c,d. These two conformers possess different total energies, the cis-transoid form being more stable by about 10 kJ/mol per C_2H_2 unit.[278]

Su and Schrieffer were the first to point out[66] that the one-photon strongly allowed $1B_u$ state of trans-polyacetylene tends to relax toward the formation of a pair of oppositely charged solitons: $1B_u \rightarrow S^+S^-$. Note that this feature allows one to understand that a photocurrent is observed as soon as there is excitation into the $1B_u$ state.[279] A number of authors have also indicated that the $2A_g$ state of trans-polyacetylene can be envisioned as leading to the appearance of a pair of neutral solitons: $2A_g \rightarrow S^{\cdot}S^{\cdot}$.[280,281] The models of third-order NLO response usually discussed are based on a rigid lattice approximation which does not take into account either excited-state geometry relaxations or ground-state quantum lattice fluctuations (zero-point vibrations); in other words, all the states are depicted on the basis of a rigid ground-state geometry. Heeger and co-workers[276] have theoretically examined the influence of considering an optical channel in which the intermediate state is the relaxed neutral soliton pair $S^{\cdot}S^{\cdot}$ state, i.e., the $1A_g \rightarrow 1B_u \rightarrow (2A_g)S^{\cdot}S^{\cdot} \rightarrow 1B_u \rightarrow 1A_g$ channel. They have found this channel to provide a significant enhancement of the third-order response over that from the rigid lattice model.[276] Note that the transition from the $1B_u$ state to the relaxed $(2A_g)S^{\cdot}S^{\cdot}$ state is made possible through strong zero-point motions (quantum lattice fluctuations) of the trans-polyacetylene chain; these motions reduce the optimal Δr value by about 15% relative to the rigid lattice case and can be modeled as corresponding to the virtual formation of soliton pairs.[282] The lack of possibility of soliton formation in cis-polyacetylene is then advocated as the reason for the lower $\chi^{(3)}$ measured for that conformer. Much further work is needed to confirm or disprove the validity of this approach. It would in particular be extremely useful to obtain truly off-resonance $\chi^{(3)}$ measurements on well-characterized trans- and cis-polyacetylenes.

C. Polydiacetylenes

The polydiacetylenes have the following general chemical structure:

$$[-C{\equiv}C-CR_1{=}CR_2-]_n$$

They constitute a very special class of conjugated polymers in that, since the end of the 1960s and the pioneering work of Wegner and co-workers, they can be grown in the form of large, almost defect-free single crystals.[283,284] They can also be obtained as single crystalline thin films, Langmuir–Blodgett films, or in solution.[285] A large number of polydiacetylenes can be synthesized depending on the nature of the R_1 and R_2 side groups. Much studied polydiacetylenes include the p-toluenesulfonate, PTS, derivative where R_1 and R_2 are $CH_2OSO_2C_6H_4CH_3$, and the n-BCMU derivatives where R_1 and R_2 correspond $(CH_2)_nOCONHCH_2$-$COOC_4H_9$. Note that such bulky side groups are needed to insure the formation of single crystals.
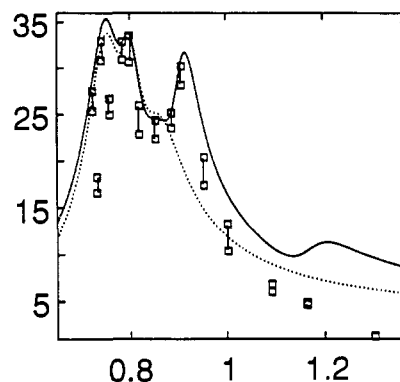
Figure 14. Spectral dispersion of the magnitude of the third-order susceptibility $\chi^{(3)}(3\omega)$, in arbitrary units, measured for the poly-4BCMU polydiacetylene (adapted from ref 62). The solid and dotted lines correspond to various theoretical fits.

Together with polyene derivatives such as carotenoids, polydiacetylenes have been among the first organic materials investigated for their $\chi^{(3)}$ response in the mid-1970s.[126] The recent literature has been surveyed by Etemad and Soos[241,242] who have also addressed the technological potentialities of the polydiacetylenes. (We refer the reader to these reviews for a thorough description of these materials.)

Polydiacetylenes present a very sharp one-photon absorption around 2 eV, which corresponds to a $1B_u$ state with excitonic character. Degenerate four-wave mixing experiments indicate a strong resonance enhancement when the optical frequency is tuned toward the $1B_u$ exciton energy. DFWM $\chi^{(3)}$ values approaching 10^{-8} esu have been measured.[286] The spectral dispersion of both the magnitude and phase of the THG $\chi^{(3)}$ has been reported for the 4-BCMU polydiacetylene[62] between 0.6 and 1.3 eV. Over that energy range, there occur three distint resonance peaks, see Figure 14. Starting from the low-energy side, these are currently interpreted as three-photon resonance to the $1B_u$ exciton, a three-photon resonance to the nB_u (conduction band) state, and a two-photon resonance to the mA_g state. Note that the middle resonance had been earlier attributed to the two-photon resonance to the $2A_g$ state; however, more recent calculations by Mazumdar and co-workers show the contributions of the $2A_g$ state to the nonlinear optical response to be negligible.[78,79]

D. Polyarylenes and Polyarylene Vinylenes

Since the mid-1980s, the polyarylenes (in particular, polythiophene, i.e., poly-2,5-thienylene, and its 3-alkyl derivatives) and the polyarylene vinylenes [especially poly(p-phenylenevinylene), its 2,5-dialkoxy derivatives, and poly(thienylenevinylene)] have attracted a great deal of attention because of their superior processibility and environmental stability and their large $\chi^{(3)}$ responses. On the experimental side, major contributions have come namely from the groups of Friend, Heeger, Kaino, Kajzar, Kobayashi, Meijer, Prasad, Sasabe, Stegeman, Taliani, and their co-workers.[95,96,287-295]

In the case of poly(alkylthiophenes),[295] the optical nonlinearities as measured by THG in the near-IR, have been shown to be comparable to those of polydiacetylenes. Dispersion measurements of both the magnitude and phase of $\chi^{(3)}(3\omega)$ for poly(3-butylthiophene) and

poly(3-decylthiophene) have been measured in the range 0.65–1.3 eV by Torruellas *et al.*[295] In their original paper, these authors fitted the resonances they measured on the basis of four significantly contributing states: $1A_g$, $2A_g$, $1B_u$, and mA_g. Guo *et al.*[58] have now shown that an equally good fit can be obtained by taking the $1A_g$, $1B_u$, mA_g, and nB_u states that have been discussed previously. The INDO/MRDCI calculations we have recently performed[80] (which unlike the models used by Torruellas *et al.* and Guo *et al.* do not rely on any adjustable parameters such as the values of transition dipole moments) confirm that the most reasonable assignment should take the nB_u state rather than the $2A_g$ state, into consideration.

We note that in terms of the relative locations of the $2A_g$ and $1B_u$ states, the situation between short polyenes and thiophene oligomers is markedly different. While in polyene chains containing as few as 6 π-electrons, *i.e.*, hexatriene, the $2A_g$ state lies below the $1B_u$ state,[75–77] the relative locations of these two states are reversed in short thiophene oligomers. For instance, in the case of bithiophene, the $2A_g$ state is measured to be as much as 0.8 eV *above* the $1B_u$ state.[296] A common feature is, however, that in both types of compounds the $2A_g$ state stabilizes more strongly than the $1B_u$ state as a function of chain length.[76,80,297] Indeed, in α-hexathiophene, Taliani and co-workers have observed the $2A_g$ state to be only very slightly above the $1B_u$ state by about 0.1 eV.[298] It is not clear yet what is the exact situation in polythiophene, where the two-photon absorption is dominated by the mA_g state. For poly(3-octylthiophene) in solution in THF, the mA_g state is located 0.6 eV above the $1B_u$ state.[299] The large transition energy observed for the $1B_u$ state (2.9 eV) is, however, indicative of significant twists along the polymer chains in solution;[299] the rotation barriers are indeed relatively small, on the order of 10 kJ/mol per ring.[300] In the case of conjugated compounds, the appearance of conformational twists has been calculated to increase the $2A_g$ state energy to a larger extent than the $1B_u$ state energy.[301] The 0.6 eV difference measured in solution between the mA_g state and the $1B_u$ state might thus correspond to an upper limit.[299]

Polythiophene is a conjugated polymer which, together with polyacetylene, has been shown to provide evidence of geometry relaxation effects when it is excited across the bandgap.[302] In this case, since polythiophene is a nondegenerate ground-state system, the relaxation takes the form of polarons or bipolarons, *i.e.*, radical-ions or diions which are associated to a local geometry modification toward a quinoid-like structure.[67] Vardeny *et al.*[303] have observed the decay of the polaronic states to be in the picosecond time range. The formation of (bi)polarons leads, as is the case for solitons, to the appearance of new electronic levels within the originally forbidden gap of the polymer. There thus occur significant shifts in the distribution of oscillator strengths and thus important contributions to the $\chi^{(3)}$ response. We discussed in section III the $\chi^{(3)}$ excited-state enhancement due to photoexcited polarons, as measured by Taliani and co-workers.[99,100]

Poly(*p*-phenylenevinylene) and its 2,5-dialkoxy derivatives as well as poly(thienylenevinylene) can be synthesized via soluble precursor routes which provide films of very good optical quality.[304–306] The poly(*p*-
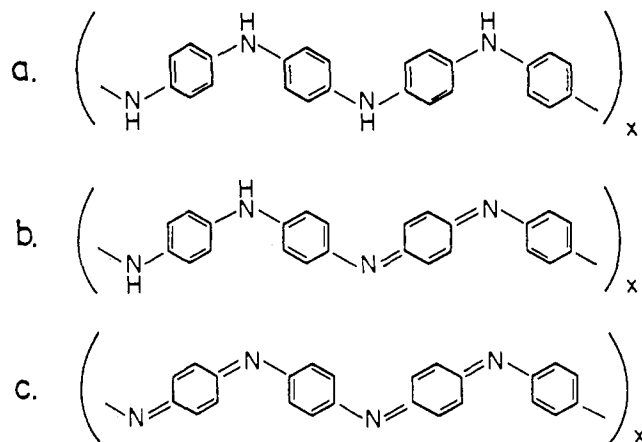
Figure 15. Molecular structures of the three polyaniline base forms: (a) the leucoemeraldine fully-reduced form, (b) the emeraldine semioxidized form, and (c) the pernigraniline fully oxidized form.

phenylenevinylenes) have more recently triggered an enormous interest since they can be used as the active element in polymeric (flexible) light-emitting diodes.[307,308] As in the case of polyacetylene described above, significant improvements in the third-order nonlinear optical response by almost 1 order of magnitude have been recently reported by Friend and co-workers[309] due to the availability of materials which are better ordered and contain fewer structural defects. Typical $\chi^{(3)}$ values which have been published in the literature range between 10^{-11} and 10^{-9} esu. The intrinsic limit for perfectly-ordered chains might not have been reached yet.

In poly(*p*-phenylenevinylene), the $2A_g$ state is located above the $1B_u$ state. This is considered to be one of the reasons for the efficient luminescence properties since the $1B_u$ excitation cannot relax down to a two-photon state (or an electric dipole forbidden state) more prone to nonradiative decay.[310,311]

The $\chi^{(3)}$ resonances of the polyaniline family of polymers have also been investigated. Polyanilines constitute a fascinating class of conjugated polymers[312–314] since: (i) their properties strongly depend on their oxidation state; and (ii) high electrical conductivity can be induced not only via a usual redox process but also via Brønsted acid–base chemistry. Three polyaniline base forms can be isolated (Figure 15): (i) the leucoemeraldine fully reduced form; (ii) the emeraldine semioxidized form; and (iii) the pernigraniline fully oxidized form. It is the emeraldine base form which undergoes an insulator to metal transition upon protonation of the imine nitrogen sites leading to the emeraldine salt form; the electrical conductivity increases by some 13 orders of magnitude from about 10^{-10} S/cm up to several times 10^3 S/cm at room temperature.[312–316] Note that the pernigraniline base form is also of interest since it presents a degenerate ground state and thus supports the formation of solitons.[314–317]

In the case of polyanilines, improvement in material quality has been recently achieved via the use of surfactant counterions.[318] Halvorson *et al.*[319] have investigated the THG dispersion spectrum of the three base forms and compared their results to those previously reported by Osaheni *et al.*[320] on polyanilines
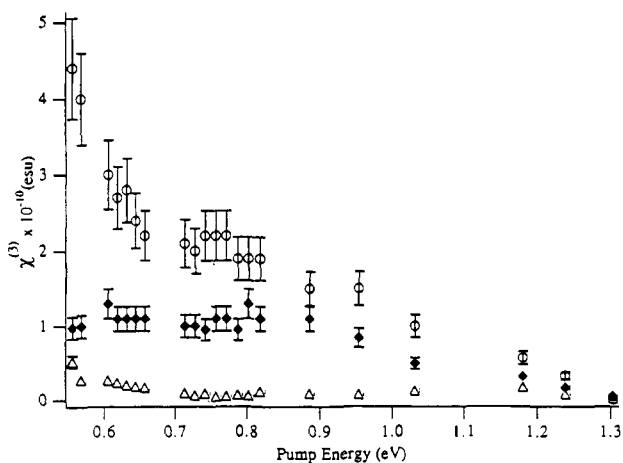
Figure 16. Measured $\chi^{(3)}(3\omega)$ susceptibilities for the three polyaniline forms: leucoemeraldine (triangles); emeraldine (circles); and pernigraniline (diamonds) (adapted from ref 319).

synthesized via the more traditional route. Halvorson *et al.* obtain an increase in the $\chi^{(3)}$ THG values by 1 order of magnitude, a feature which again stresses the importance of materials quality.

The results of Halvorson *et al.* on the three polyaniline forms are sketched on Figure 16. It is observed that the largest $\chi^{(3)}$ values are obtained for emeraldine base; they range between about 2×10^{-11} esu off-resonance and 4.5×10^{-10} esu at 0.55 eV on three-photon resonance.[319] The $\chi^{(3)}$ response of the pernigraniline form, *i.e.*, the one with the degenerate ground state, is lower. (According to Halvorson *et al.*,[319] the intermediate soliton A_g state mechanism, that could be enabled by quantum lattice fluctuations, is in any case not significant in pernigraniline because of nonlinear zero-point motions much smaller than in *trans*-polyacetylene.)

1. Influence of Molecular Geometry

The polyarylenes and polyarylene vinylenes lend themselves to an informative theoretical study of the effect of aromaticity *vs* quinoidicity on the $\chi^{(3)}$ or γ response. It was generally considered that the quinoid geometric structure should be more highly polarizable than the aromatic geometric structure. Two main arguments were usually proposed to justify this standpoint:

(i) A quinoid geometry should lead to a π-electron cloud which is more delocalized along the chain than is the case in an aromatic geometry; this appears to be confirmed at the second-order level for push–pull quinodimethanes.[321]

(ii) First-order polarizabilities α have been calculated to be larger for quinoid compounds than the corresponding aromatic compounds;[322] use of simple scaling arguments between α and γ then suggests a higher third-order response in quinoid systems.

We have recently undertaken a detailed theoretical study of the static γ-tensor components in phenylenevinylene and thienylenevinylene compounds as well as their quinoid counterparts.[49] The molecules under investigation are presented in Figure 1. The main results coming from coupled perturbed Hartree–Fock *ab initio* calculations with extended basis sets, have been collected in Table 2. We observe that the switch
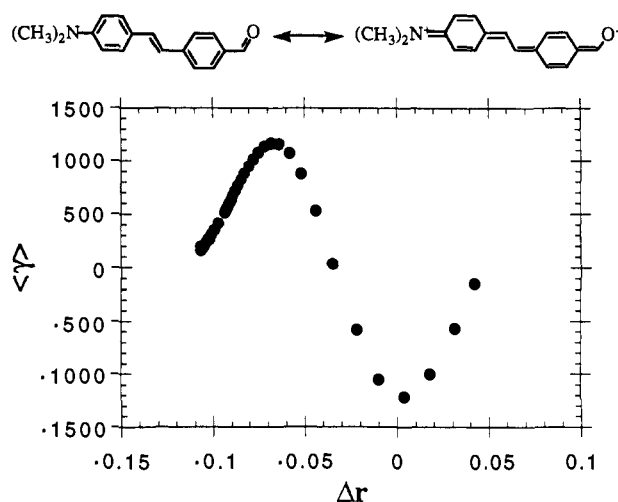
Figure 17. Evolution of the AM1/finite-field static γ value, in 10^{-36} esu, of a push–pull aromatic/quinoid compound as a function of the degree of bond-length alternation, in angstroms (adapted from ref 259).

from an arylethenyl type of structure to a quinoid structure does not lead to any significant increase in the $\langle\gamma\rangle$ value. In fact, there occur opposite evolutions between components: we obtain a larger longitudinal γ_{zzzz} value in the arylethenyl structure (with the 3-21G+pd basis set: 26×10^{-36} esu in styrene *vs* 17×10^{-36} esu for quinodimethane) but, on the other hand, a significant increase in the γ_{zzyy} and γ_{zzxx} component in the quinoid structure.[49] Furthermore, we stress that the different evolutions calculated for $\langle\alpha\rangle$ and $\langle\gamma\rangle$ values as a function of a switch to a quinoid structure illustrate that one has to be very cautious when applying scaling laws to extrapolate γ values from α values.

Given these results, it might actually be much more efficient to deal with semiquinoid structures, *i.e.*, compounds having geometries that are intermediate between an aromatic and a quinoid character. In the same context as that discussed for polyenes above, Gorman and Marder[259] have analyzed the evolution of γ as a function of molecular geometry in push–pull aromatic–quinoid compounds. In Figure 17, we present the results they have obtained in the case of the following kind of molecules:
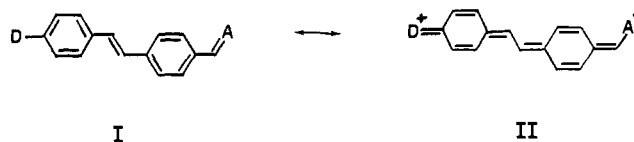
The results are qualitatively similar to those in the case of polyenes; the largest static γ value is obtained for a geometry corresponding to equal contributions from resonance forms I and II above. The molecular geometry is then what can be referred to as semiquinoid-like.

We have also observed a very large γ response in the case of the crystal violet cation[323,324] whose molecular structure is depicted in Figure 18. The formal positive charge located on the central carbon of the molecule is actually strongly delocalized over the phenylene rings and amino groups, which results in the appearance of a semiquinoid geometry; for instance, the central carbon–phenylene carbon bonds are only 1.43 Å long

$X \equiv N(CH_3)_2$
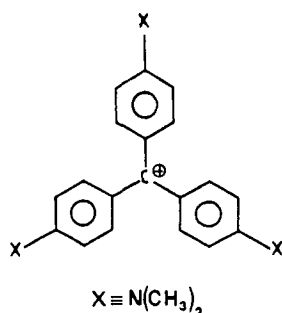
Figure 18. Molecular structure of the crystal violet cation.

(i.e., a length intermediate between that of a single sp^2-sp^2 bond, ca. 1.51 Å, and that of a double bond). The static γ value calculated at the semiempirical finite field level[323,324] is 350×10^{-36} esu. This value is comparable to that measured[325] and calculated[326] in the case of the C_{60} fullerene, i.e., a molecule containing about three times as many π electrons as crystal violet. (We note in passing that crystal violet also presents a remarkable second-order response which is originating in octopolar contributions;[327] the static β value is calculated to be around 300×10^{-30} esu while hyper-Rayleigh-scattering measurements at $1.064~\mu m$ show a resonantly enhanced β on the order of $(3-5000) \times 10^{-30}$ esu, in full agreement with the results of dynamic calculations.[323,324])

Obviously, fine control of molecular geometry can help in enhancing the nonlinear optical response of aromatic–quinoid-ring based compounds.

2. Influence of Charge State

In the case of π-conjugated systems, we have described in section III that charge state and molecular geometry are intimately connected and result in what condensed matter physicists refer to as strong electron–phonon coupling. Oxidation or reduction of conjugated polymers, besides leading to a very large increase in electrical conductivity, also results in significant modifications of the lattice (macromolecular) geometry, as demonstrated by IR, Raman, and NMR measurements.[328] Lefrant and co-workers have for instance shown from resonance Raman scattering experiments that the geometry of polyarylene compounds switched upon doping (i.e., upon oxidation or reduction) from aromatic-like to quinoid-like,[329] thereby fully confirming the conclusions of quantum-chemical investigations.[330]

In the case of polythiophene for example, oxidation leads to the formation of polarons or bipolarons. While the singly-charged polarons result in moderate semi-quinoid-like local geometry modifications, the doubly-charged bipolarons provoke a local lattice relaxation toward a very pronounced quinoid geometry.[330,331] The experimental results reported on the evolution of third-order optical response of conjugated chains as a function of oxidation state have so far been contradictory: Prasad and co-workers have observed the third-order susceptibility to decrease as polarons and/or bipolarons start appearing on polythiophene chains[332] while Nickel et al. have recently reported $\chi^{(3)}$ enhancement by soliton-pair generation in doped bisanthracenyl polyenes.[268] (Part of the difficulty in obtaining a correct assessment of the doping influence is due to the very different resonances that occur in the undoped and doped systems.)

E. σ-Conjugated Polymers

Polysilane and polygermane high polymers, which contain only silicon or germanium atoms, respectively, along the polymer backbone, display very interesting electrical and optical properties which originate in σ-electron conjugation effects.[333] Catenated silicon or germanium linkages constitute highly polarizable, yet thermally and environmentally stable alternatives to π-conjugated polymers; they have been shown to present interesting nonlinear optical properties.[136,334–338] Much as in π-conjugated systems, the transition energies in polysilanes and polygermanes depend on the substituents, the chain length, and the chain conformation;[333,339,340] there is usually very good optical transparency throughout the visible regime. These compounds are often soluble in common organic solvents and form high optical quality films. In addition, they are imageable with UV light to high resolution; this feature could prove useful in the generation of patterned waveguides and nonlinear optical devices. These materials typically present off-resonance THG $\chi^{(3)}$ values which are on the order of 10^{-12} to 10^{-11} esu.[136,334–338]

A very detailed investigation of the modulus and phase of the THG $\chi^{(3)}$ susceptibility of polydihexylsilane has been recently reported by Hasegawa et al. over a wide photon energy range extending from 0.56 to 2.15 eV.[341] In that energy range, there occur three resonance peaks, at 1.1, 1.5, and 2.1 eV. The first peak is attributed to a three-photon resonance to the lowest $1B_u$ exciton state at 3.3 eV while the third peak is interpreted as a two-photon resonance to the $2A_g$ state located at about 4.2 eV (i.e., significantly above the $1B_u$ state). The middle peak at 1.5 eV is considered to originate in three-photon resonances to nB_u states around the conduction band threshold.[57,341] The theoretical description of the dispersion in the THG spectrum obtained for σ-conjugated systems such as polysilanes appears thus to be very similar to that we have discussed above in the case of π-conjugated systems.

The work of Hasegawa et al.[341] is illustrative of the fact that various measurements of the nonlinear optical properties constitute a very intimate probe of the electronic structure of a system. The characteristics of the resonance features allow one to uncover the location of states that are not visible in linear absorption spectrum, due to either selection rules (two-photon A_g states) or very weak direct transition moments with the ground state; in poly(dihexylsilane), the linear absorption is totally dominated by the $1B_u$ transition and transitions to the nB_u states are hardly observed.

F. Ladder Polymers

Ladder polymers constitute a group of π-conjugated polymers that have recently been investigated in terms of their nonlinear optical properties, primarily for two reasons. First, their rigid-rod-type molecular conformation exhibits very high mechanical strength and stability. This is the case for the poly(p-phenylenebenzobisthiazole) (PBZT) and poly(p-phenylenebenzobisoxazole) (PBO) compounds:
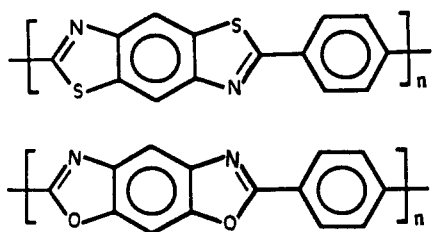
Second, in the case of systems where the rings are completely fused such as
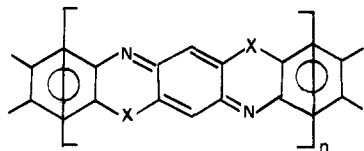
there is no possibility for ring torsions to occur, a feature which maintains ideal electronic conjugation.

The $\chi^{(3)}$ response of ladder polymers has been studied among others by groups of Prasad and Reinhardt,[22] Jenekhe and Meth,[73,141–143,342] and Dalton.[343] A review chapter that mostly focuses on ladder polymers has recently been published by Dalton and co-workers.[343] The $\chi^{(3)}$ susceptibilities obtained on ladder polymers can reach value on the order of 10^{-11}–10^{-10} esu off-resonance and about 10^{-9}–10^{-8} esu on resonance. Recent data by Jenekhe et al.[73a] indicate that the paraphenylenebenzobisthiazole and -benzobisoxazole polymers display very similar THG $\chi^{(3)}$ responses. The nature of the heteroatoms present in those two polymers thus appears not to influence significantly the nonlinear optical properties.

G. Higher Dimensional Structures

The systems we have discussed so far can be viewed as quasi-one-dimensional structures for which the third-order nonlinear response is dominated by the tensor component along the chain axis, γ_{zzzz}. Other structures have been investigated which are more two-dimensional-like as in the case of macrocycles or three-dimensional-like as in the fullerenes. It is obvious that in these instances, the γ value will depend on contributions coming from a larger number of components.

1. Macrocycles

Phthalocyanines (Figure 19) are among the most attractive macrocyclic systems. These are very stable organic materials undergoing no noticeable degradation in air up to 400–500 °C. This exceptional thermal stability together with a large chemical versatility makes it feasible to obtain high-quality thin films of a great variety of phthalocyanines by successive sublimation. These and other unique properties they exhibit have warranted the vast amount of basic and applied research concerning phthalocyanines.[344,345] Industrially, they have been studied for their use as dyes and pigments and for their electrocatalytic activity and suitability for semiconductor devices.[345–347] More recently, phthalocyanines have been of particular interest in many fields concerning energy conversion (photovoltaic and solar cells),[345,348] electrophotography,[349] photosensitizers,[350] gas sensors,[351] rectifying devices,[352] low dimensional metals,[353] electrochromism,[354] optical data stor-
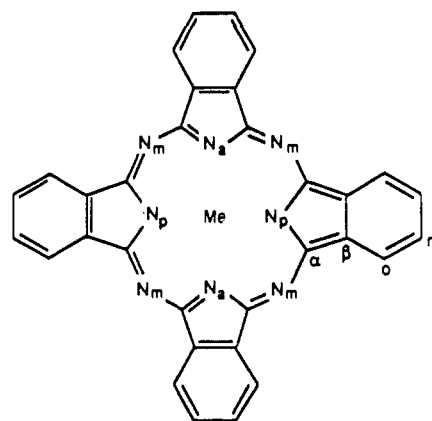
Figure 19. Molecular structure of phthalocyanine. Me denotes a metal atom, N_p a pyrrole nitrogen, and N_a and N_m indicate pyrrole aza and meso-bridging aza nitrogens, respectively.
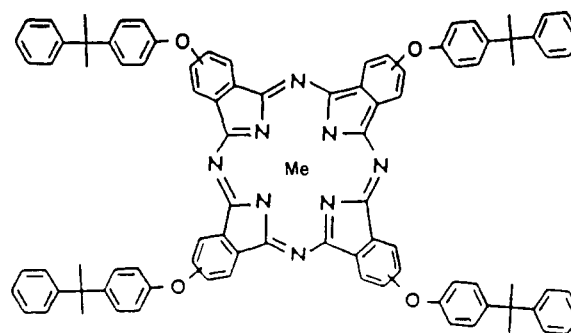
Figure 20. Molecular structure of tetrakis(cumylphenoxy)-phthalocyanines where the metal is Co, Ni, Cu, Zn, Pd, or Pt.

age,[355] Langmuir–Blodgett films,[356] liquid crystals,[357] as well as nonlinear optics.[358–365]

The groups of Bubeck, Garito, Perry, Prasad, and Sasabe have been among those that have actively investigated the $\chi^{(3)}$ response of macrocycles, especially phthalocyanines.[197,218,332,358–365] In particular, the sharp Q band, characteristics of phthalocyanine-type molecules, has attracted much interest. For instance, Wu et al.[365] have studied in detail the saturable absorption behavior of silicon-naphthalocyanines.

Another attribute of these compounds is their ease of complexation by a large variety of metals, which places them at the interface between organics and organometallics and allows for a fine tuning of the macrocycle electronic properties as influenced by the coordinated metal. Shirk et al.[366] have examined, via DFWM at 1.064 μm, a number of metal tetrakis-(cumylphenoxy)phthalocyanines (Figure 20) where the metal is Co, Ni, Cu, Zn, Pd, or Pt. Depending on the metal, they obtain $\langle\gamma\rangle$ values ranging between 1×10^{-32} and 1×10^{-31} esu, the largest value coming from the Pt compound and corresponding to a $\chi^{(3)}$ value of 2×10^{-10} esu; by comparison, in the same conditions, the metal-free molecules display a $\langle\gamma\rangle$ value on the order of 2×10^{-33} esu. The metal thus significantly enhances the third-order response by factors of 5 to 50. The variations in γ's are attributed to differences in the electronic structure of the metal phthalocyanines since there appear new low-lying electronic states into the electronic manifold; these states correspond to metal-to-ligand or ligand-to-metal charge transfer states as well as d–d transitions on the metal ion itself.[367,368]

Table 6. VEH/SOS Static Third-Order Polarizability γ (in 10^{-36} esu) Components for C_{60}, C_{70}, and the $C_{60}H_{62}$ Polyene

	C_{60}	C_{70}	$C_{60}H_{62}$
γ_{zzzz}	218.4	491.6	4×10^5
$\langle \gamma \rangle$	207.6	852.9	8×10^4

Sasabe and co-workers have studied the influence of the stacking mode in thin films of metal phthalocyanines.[362,363] In the case of vanadylphthalocyanine and TiO phthalocyanine, when there occurs a phase transition from a cofacial type of packing to a slipped-stack arrangement, the THG $\chi^{(3)}$ values at 1.907 μm increase by factors of 2 and 5, respectively, to reach values near 10^{-10} esu. This phase transition is also related to a significant modification of the linear absorption.

Neher et al.[361] have carried out DFWM experiments on phthalocyanine thin films. They were able to vary the relative distance between the macrocycles by dissolving or copolymerizing phthalocyanines in polystyrene or by building up Langmuir–Blodgett of phthalocyanine monomers or polymers. The linear and nonlinear optical properties of the films were observed to depend strongly on the distance and therefore electronic coupling between the macrocycles. Increased electronic coupling leads to a spectral broadening of the optical absorption bands and to a reduction of the response time down to the picosecond range.

Such results illustrate the influence that aggregation processes can have on the linear and nonlinear optical response when dealing with thin films or solutions of chromophores.

2. Fullerenes

The discovery of the carbon-cage fullerenes has stirred an enormous scientific interest.[369,370] In the framework of nonlinear optics, early DFWM measurements for C_{60} in benzene solution[371] and for C_{70} in toluene solution[372] generated much excitement. Indeed, the results were interpreted in such a way that the off-resonance γ values were estimated to be on the order of 10^{-30} esu; this leads to macroscopic $\chi^{(3)}$'s around 10^{-8} esu, i.e. similar to those of the best trans-polyacetylene samples.

However, more recently, Wang and Cheng[373] have performed EFISHG measurements on fullerenes, both in toluene solution and in form of fullerene-DEA [where DEA denotes (N,N-diethylaniline)] charge-transfer complexes. They deduced the γ values, after a standard local field treatment, to be $(7.5 \pm 2) \times 10^{-34}$ esu and $(1.3 \pm 0.3) \times 10^{-33}$ esu for C_{60} and for C_{70}, respectively (in toluene solution). Kafafi et al. have carried out DFWM measurements on C_{60} and found the $\chi^{(3)}$ value to be 7 $\times 10^{-12}$ esu,[374] while THG measurements on sublimed C_{60} films provide $\chi^{(3)}(-3\omega;\omega,\omega,\omega)$ values of 6.1 and 8.2 $\times 10^{-11}$ esu at 1.3 and 1.064 μm, respectively.[375] These figures are 3–4 orders of magnitude smaller than the experimental data reported in refs 371–372 and generally appear to be more reasonable.

On the basis of AM1-optimized geometries, we have performed a VEH/sum-over-states calculation on the static and dynamic γ response of the C_{60} and C_{70} molecules.[98] The main static γ values are collected in Table 6, where comparison is provided to the results obtained for the corresponding $C_{60}H_{62}$ polyene under

the same theoretical model. The calculated static $\langle \gamma \rangle$ values, 2.0 × 10^{-34} esu for C_{60} and 8.6 × 10^{-34} esu for C_{70}, are in very good agreement with the experimental data of Wang and Cheng[373] and Kafafi et al.[374]

From Table 6, we observe that the VEH/SOS approach provides a γ value for the $C_{60}H_{62}$ polyene which is over 2 orders of magnitude larger than that of the fullerenes. This result clearly illustrates the strong enhancement of the nonlinear optical response due to electron delocalization in one dimension, allowing for charge separation over large distances. In contrast, the 3D spherical structure of the fullerenes limits the charge separation even though electron delocalization is also large in these compounds. However, one potential advantage of fullerenes, whose nonlinear optical properties continue to be intensely examined, is the absence of carbon–hydrogen bonds and therefore of the vibrational harmonics associated to them.

VI. Synopsis

The principal application of the organic materials discussed in the previous sections is in the area of all-optical signal processing. The potential of these materials can be judged by recalling the list of requirements for the third-order nonlinear optical materials relevant to optical signal processing that was presented at the beginning of this review, and by considering the figure of merit given in eq 12 that defines the optical switching performance of a third-order nonlinear optical material. The figure of merit informs us that a combination of (i) a large magnitude for the third-order electric susceptibility tensor, $\chi^{(3)}(\lambda)$, (ii) small linear and nonlinear absorptivities, $\alpha'(\lambda)$, and (iii) a short lifetime for the third-order polarization response, τ, is desired at the operating light wavelength, λ, for the given device. In the case where λ is not near resonance, wavelengths for an one-, two-, and three-photon electronic transitions within these materials (which is not a common occurrence), two of the three objectives relating to the figure of merit are met almost automatically: small linear and nonlinear absorptivities, and short response times on the order of 10^{-15}–10^{-14} s. The critical question is whether the magnitude of the real component of $\chi^{(3)}(\lambda)$ is large enough for the given device. The magnitude required for the given device application depends on the optical path length and the light intensity (electric field strength) within the device. Of course, it is preferred that the optical path length and light intensity be kept as short and low as possible.

The preferred operating wavelength for all-optical switching devices is 1.5 μm because it is optimal for transmission through silica-based optical fibers. This operating wavelength means that the candidate third-order nonlinear optical material should have no strongly absorbing: (i) one-photon transitions (electronic and/or vibrational overtones) near 1.5 μm (0.8–0.85 eV), (ii) two-photon transitions near 0.75 μm (1.65 eV), and (iii) three-photon transitions near 0.375 μm (3.3 eV). The nonlinear, two- and three-photon absorptivities are dependent on the light intensity used for optical switching, such that the lower this intensity the lower the nonlinear absorption. Almost all of the organic materials discussed in this review have some three-photon absorption at 0.375 μm. Fortunately, three-

photon absorption is much weaker than one- and two-photon absorption.

There are two strategies that can be followed with regard to minimizing the one- and two-photon absorption by the organic material. The most direct strategy is to develop a material where the first strong one-photon absorption occurs at wavelengths shorter than 0.75 μm. In the case of a semiconducting polymer, this means that the bandgap must correspond to an energy larger than 1.65 eV. The second strategy is to develop a material where the first strong one-photon absorption occurs at wavelengths shorter than 1.5 μm, and the bandwidths of the first absorbing state and higher energy states are so narrow that a two-photon absorption is more difficult to achieve. This second strategy is technically more demanding than the first because narrow absorption bandwidths generally imply crystalline structures, weak electron–phonon coupling (absence of vibronic structures), and operation at low temperatures. In the case of polymers with conjugated bonding networks, their electronic band structures make it difficult to avoid two- and three-photon resonances. It is noted that in this discussion of linear and nonlinear absorption, we have focused solely on the intrinsic absorptive loss by the material. We assume that the loss due to scattering can be kept to a minimum through improvements in the processing of the materials. The next question is whether the third-order electric susceptibilities for the candidate materials are large enough for all optical switching at light intensities <1 MW/cm^2, and device path lengths on the order of centimeters. A third-order electric suceptibility >10^{-8} esu is needed to meet these light-switching and path-length requirements. None of the organic materials so far (except perhaps for the best polyacetylene samples) have an off-resonant third-order susceptibility of this magnitude. Thus, trade-offs between the linear and nonlinear absorptivities, the response time, and the magnitude of the third-order electric susceptibility will have to be made as the resonance enhancement of the susceptibility is explored, as well as other approaches. Trade-offs concerning the response time are possible because of parallel processing alternatives to serial processing.

A very intriguing alternative approach to achieving all-optical switching is to use nonlinear phase shifts obtained from phase-mismatched second-harmonic generation, as recently demonstrated by Stegeman and co-workers.[376] Of course, this technique is limited to second-order noncentrosymmetric materials. The advantage with that approach is that a significant second-order nonlinear optical response can be attained at lower light intensities than the third-order response, and thus nonlinear absorption processes can be greatly reduced.

In conclusion, we hope that this review has shown that the field of organic materials for cubic nonlinear optical applications is very exciting and promises many fascinating applications. It also demonstrates that a lot of work is needed, however, in order for the potentialities to turn into realities. In this respect, chemists have an essential role to play.

VII. Acknowledgments

VIII. References

(1) Gibbs, H. M. Optical Bistability: Controlling Light with Light; Academic Press: New York, 1985.

(2) Bowden, C. M.; Giftan, M.; Robl, H. R. Optical Bistability; Plenum: New York, 1981.

(3) Fisher, R. Optical Phase Conjugation; Academic: New York, 1983.

(4) Hinton, H. S. IEEE Spectrum February 1992, 42.

(5) (a) Stegeman, G. I.; Wright, E. M. Opt. Quantum Electron. 1990, 22, 95. (b) Stegeman, G. I.; Zanoni, R.; Seaton, C. T. In ref 15, p 53.

(6) (a) Stegeman, G. I.; Miller, A. In Physics of All-Optical Switching Devices; Midwinter, J. E., Ed.; Academic: Orlando, in press. (b) Stegeman, G. I. Proc. SPIE—Int. Soc. Opt. Eng., in press.

(7) Zernike, F.; Midwinter, J. E. Applied Nonlinear Optics; Wiley: New York, 1973.

(8) Weis, R. S.; Gaylord, T. K. Appl. Phys. A. 1985, 37, 191.

(9) Lines, M. E.; Glass, A. M. Principles and Applications of Ferroelectrics and Related Materials; Clarendon: Oxford, 1977.

(10) Klein, M. B.; Dunning, G. J.; Valley, G. C.; Lind, R. C.; O'Meara, T. R. Opt. Lett. 1986, 11, 575.

(11) Valley, G. C.; Klein, M. B. Opt. Eng. 1983, 22, 704.

(12) Chemla, D. S., Zyss, J., Eds. Nonlinear Optical Properties of Organic Molecules and Crystals; Academic: New York, 1987; Vols. 1 and 2.

(13) Williams, D. J. Angew. Chem., Int. Ed. Engl. 1984, 690.

(14) Prasad, P. N.; Williams, D. J. Introduction to Nonlinear Optical Effects in Molecules and Polymers; Wiley: New York, 1991.

(15) Heeger, A. J., Orenstein, J., Ulrich, D. R., Eds. Nonlinear Optical Properties of Polymers, Mat. Res. Soc. Symp. Proc.; Materials Research Society: Pittsburgh, 1988; Vol. 109.

(16) (a) Messier, J., Kajzar, F., Ulrich, D., Eds. Nonlinear Optical Effects in Organic Polymers; NATO-ARW Series; Kluwer: Dordrecht, 1989; Vol. E162. (b) Messier, J., Kajzar, F., Prasad, P. N., Eds. Organic Molecules for Nonlinear Optics and Photonics; NATO-ARW Series; Kluwer: Dordrecht, 1991; Vol. E194.

(17) (a) Khanarian, G., Ed. Nonlinear Optical Properties of Organic Materials; SPIE-Int. Soc. Opt. Eng.: Washington, 1988; Vol. 971. (b) Singer, K. D., Ed. Nonlinear Optical Properties of Organic Materials IV; SPIE-Int. Soc. Opt. Eng.: Washington, 1991; Vol. 1560.

(18) Brédas, J. L., Chance, R. R., Eds. Conjugated Polymeric Materials: Opportunities in Electronics, Optoelectronics, and Molecular Electronics; NATO-ARW Series; Kluwer: Dordrecht, 1990; Vol. E182.

(19) Prasad, P. N., Ulrich, D. R., Eds. Nonlinear Optical and Electroactive Polymers; Plenum: New York, 1987.

(20) Marder, S. R., Sohn, J. E., Stucky, G. D., Eds. Materials for Nonlinear Optics; American Chemical Society: Washington, 1991.

(106) Lorentz, H. A. *Theory of Electrons*; Leipzig, 1990; pp 138–306.
(107) Hellwarth, R. W. *Prog. Quant. Electr.* **1977**, *5*, 1.
(108) Kleinman, D. A. *Phys. Rev.* **1962**, *126*, 1977.
(109) Cyvin, S.; Rauch, J. E.; Decius, J. C. *J. Chem. Phys.* **1965**, *43*, 4083.
(110) Wu, C. K.; Agostini, P.; Petite, G.; Fabre, F. *Opt. Lett.* **1983**, *8*, 67.
(111) Jerphagnon, J.; Kurtz, S. K. *Phys. Rev. B* **1970**, *1*, 1739.
(112) Van Herzeele, H. *Appl. Opt.* **1990**, *29*, 2246.
(113) Thalhammer, M.; Penzkofer, A. *Appl. Phys. B* **1983**, *32*, 137.
(114) Kajzar, F.; Messier, J. *Phys. Rev. A* **1985**, *32*, 2352.
(115) Terhune, R. W.; Maker, P. D.; Savage, C. M. *Phys. Rev. Lett.* **1962**, *8*, 404.
(116) (a) Bey, P. P.; Giuliani, J. F.; Rabin, H. *Phys. Rev. Lett.* **1967**, *19*, 819. (b) Ward, J. F.; New, G. H. C. *Phys. Rev.* **1969**, *185*, 57.
(117) Harris, S. E.; Miles, R. B. *Appl. Phys. Lett.* **1971**, *19*, 385.
(118) Kung, A. H.; Young, J. F.; Bjorklund, G. C.; Harris, S. E. *Phys. Rev. Lett.* **1972**, *29*, 985.
(119) Kung, A. H.; Young, J. F.; Harris, S. E. *Appl. Phys. Lett.* **1973**, *22*, 301.
(120) Miles, R. B.; Harris, S. E. *IEEE J. Quantum Electron.* **1973**, *9*, 470.
(121) Bloom, D. M.; Bekkers, G. W.; Young, J. F.; Harris, S. E. *Appl. Phys. Lett.* **1975**, *26*, 687.
(122) Bloom, D. M.; Young, J. F.; Harris, S. E. *Appl. Phys. Lett.* **1975**, *27*, 390.
(123) Kung, A. H.; Young, J. F.; Harris, S. E. *Appl. Phys. Lett.* **1976**, *28*, 239.
(124) Hermann, J. P.; Ricard, D.; Ducuing, J. *Appl. Phys. Lett.* **1973**, *23*, 178.
(125) Hermann, J. P.; Ducuing, J. *J. Appl. Phys.* **1974**, *45*, 5100.
(126) Sauteret, C.; Hermann, J. P.; Frey, R.; Pradère, F.; Ducuing, J.; Baughman, R. H.; Chance, R. R. *Phys. Rev. Lett.* **1976**, *36*, 956.
(127) Meredith, G. R.; Buchalter, B.; Hanzlik, C. *J. Chem. Phys.* **1983**, *78*, 1533.
(128) Meredith, G. R.; Buchalter, B.; Hanzlik, C. *J. Chem. Phys.* **1983**, *78*, 1543.
(129) Cheng, L. T.; Tam, W.; Meredith, G. R.; Rikken, G. L. J. A.; Meijer, E. W. *Proc. SPIE—Int. Soc. Opt. Eng.* **1990**, *1147*, 61.
(130) Mattoussi, H.; Berry, G. C. *Polym. Prepr. (ACS)* **1991**, *32*, 690.
(131) Kajzar, F.; Messier, J.; Rosilio, C. *J. Appl. Phys.* **1986**, *60*, 3040.
(132) Miller, R. D. *Bull. Soc. Chim. Belg.* **1989**, *98*, 691.
(133) Shukla, P.; Cotts, P. M.; Miller, R. D.; Ducharme, S.; Asthana, R.; Zavislan, J. *Mol. Cryst. Liq. Cryst.* **1990**, *183*, 241.
(134) Callender, C. L.; Carere, C. A.; Albert, J.; Zhou, L. L.; Worsfold, D. J. *J. Opt. Soc. Am. B* **1992**, *9*, 518.
(135) Hasegawa, T.; Iwasa, Y.; Kishida, H.; Koda, T.; Tokura, Y.; Tachibana, H.; Kawabata, Y. *Phys. Rev. B* **1992**, *45*, 6317.
(136) Baumert, J. C.; Bjorklund, G. C.; Jundt, D. H.; Jurich, M. C.; Looser, H.; Miller, R. D.; Rabolt, J.; Sooriyakumaran, R.; Swalen, J. D.; Twieg, R. J. *Appl. Phys. Lett.* **1988**, *53*, 1147.
(137) (a) Taliani, C.; Ruani, G.; Zamboni, R.; Kazjar, F.; Yang, L.; Dorsinville, R.; Alfano, R. R.; Tubino, R. In ref 16b, p 301. (b) Zamboni, R.; Taliani, C.; Ruani, G.; Pal, A. J.; Kajzar, F. *Mat. Res. Soc. Symp. Proc.* **1990**, *173*, 613. (c) Kajzar, F.; Ruani, G.; Taliani, C.; Zamboni, R. *Synth. Met.* **1990**, *37*, 223.
(138) Kajzar, F.; Messier, J. *Thin Solid Films* **1985**, *132*, 11.
(139) Charra, F.; Nunzi, J. M. In ref 16b, p 359.
(140) LeMoigne, J.; Hilberer, A.; Kajzar, F. *Makromol. Chem.* **1991**, *192*, 515.
(141) Yang, C. J.; Jenekhe, S. A.; Vanherzeele, H.; Meth, J. S. *Polym. Prepr. (ACS)* **1991**, *32*, 165.
(142) Vanherzeele, H.; Meth, J. S.; Jenekhe, S. A.; Roberts, M. F. *J. Opt. Soc. Am. B* **1992**, *9*, 524.
(143) Jenekhe, S. A.; Roberts, M.; Agrawal, A. K.; Meth, J. S.; Vanherzeele, H. *Mat. Res. Soc. Symp. Proc.* **1991**, *214*, 55.
(144) Frazier, C. C.; Guha, S.; Chen, W. P.; Cockerham, M. P.; Porter, P. L.; Chauchard, E. A.; Lee, C. H. *Polymer* **1987**, *28*, 553.
(145) Nalwa, H. S. *Appl. Organomet. Chem.* **1991**, *5*, 349.
(146) Aramaki, S.; Torruellas, W.; Zanoni, R.; Stegeman, G. I. *Opt. Commun.* **1991**, *85*, 527.
(147) Fann, W. S.; Benson, S.; Madey, J. M. J.; Etemad, S.; Baker, G. L.; Kajzar, F. *Phys. Rev. Lett.* **1989**, *62*, 1492.
(148) Charra, F.; Messier, J.; Sentein, C. *Synth. Met.* **1991**, *41–43*, 3169.
(149) (a) Heflin, J. R.; Zhou, Q. L.; Wong, K. Y.; Zamani-Khamiri, O.; Garito, A. F. *Proc. SPIE—Int. Soc. Opt. Eng.* **1990**, *1337*, 186. (b) Zhou, Q. L.; Heflin, J. R.; Wong, K. Y.; Zamani-Khamiri, O.; Garito, A. F. In ref 16b, p 239.
(150) Hosoda, M.; Wada, T.; Yamada, A.; Garito, A. F.; Sasabe, H. *Proc. SPIE—Int. Soc. Opt. Eng.* **1990**, *1337*, 99.
(151) Hoshi, H.; Nakamura, N.; Maruyama, Y.; Nakagawa, T.; Suzuki, S.; Shiromaru, H.; Achiba, Y. *Jpn. J. Appl. Phys.* **1991**, *30*, 1397.
(152) Neher, D.; Stegeman, G. I.; Tinker, F. A.; Peyghambarian, N. *Opt. Lett.* **1992**, *17*, 1491.
(153) Levine, B. F.; Bethea, C. G. *J. Chem. Phys.* **1975**, *63*, 2666.
(154) Huijts, R. A.; Hesselink, G. L. J. *Chem. Phys. Lett.* **1989**, *156*, 209.
(155) Kajzar, F.; Messier, J. *J. Opt. Soc. Am. B* **1987**, *4*, 1040.
(156) LeMoigne, J.; Thierry, A.; Chollet, P. A.; Kajzar, F.; Messier, J. *J. Chem. Phys.* **1988**, *88*, 6647.
(157) Persoons, A.; Van Wonterghem, B.; Tackx, P. *Proc. SPIE—Int. Soc. Opt. Eng.* **1991**, *1409*, 220.
(158) Heflin, J. R.; Cai, Y. M.; Garito, A. F. *J. Opt. Soc. Am. B* **1991**, *8*, 2132.
(159) Hellwarth, R. W. *J. Opt. Soc. Am.* **1977**, *67*, 1.
(160) Bloom, D. M.; Liao, P. F.; Economou, N. P. *Opt. Lett.* **1978**, *2*, 58.
(161) Pepper, D. M.; Fekete, D.; Yariv, A. *Appl. Phys. Lett.* **1978**, *33*, 41.
(162) Jain, R. K.; Klein, M. B.; Lind, R. C. *Opt. Lett.* **1979**, *4*, 328.
(163) Caro, R. G.; Gower, M. C. *Appl. Phys. Lett.* **1981**, *39*, 855.
(164) Moran, M. J.; She, C. Y.; Carman, R. L. *IEEE J. Quantum Electron.* **1975**, *11*, 259.
(165) Owyoung, A. *Opt. Commun.* **1976**, *16*, 266.
(166) McMichael, I.; Yeh, P.; Khoshnevisan, M. *Proc. SPIE—Int. Soc. Opt. Eng.* **1986**, *613*, 32.
(167) Saltiel, S. M.; Van Wonterghem, B.; Parthenopoulos, D. A.; Dutton, T. E.; Rentzepis, P. M. *Appl. Phys. Lett.* **1989**, *54*, 1842.
(168) Saltiel, S. M.; Van Wonterghem, B.; Rentzepis, P. M. *Opt. Lett.* **1989**, *14*, 183.
(169) Cao, X. F.; Jiang, J. P.; Hellwarth, R. W.; Yu, L. P.; Chen, M.; Dalton, L. *Proc. SPIE—Int. Soc. Opt. Eng.* **1990**, *1337*, 114.
(170) Tackx, P.; Persoons, A. *OSA Tech. Dig. Ser.* **1990**, *15*, 214.
(171) Yu, L.; Polis, D. W.; Sapochak, L. S.; Dalton, L. R. In ref 16b, p 273.
(172) Hattori, T.; Okawa, H.; Wada, T.; Sasabe, H. *Opt. Lett.* **1992**, *17*, 1560.
(173) Persoons, A.; Tackx, P. *IQEC '92 Tech. Dig. Ser.* **1992**, *9*, 556.
(174) Smith, P. W.; Tomlinson, W. J.; Eilenberger, D. J.; Maloney, P. J. *Opt. Lett.* **1981**, *6*, 581.
(175) Bunning, T. J.; Natarajan, L. V.; Schmitt, M. G.; Epling, B. L.; Crane, R. L. *Appl. Opt.* **1991**, *30*, 4341.
(176) Zhao, M.; Cui, Y.; Samoc, M.; Prasad, P. N.; Unroe, M. R.; Reinhardt, B. A. *J. Chem. Phys.* **1991**, *95*, 3991.
(177) Fleitz, P. A.; Sutherland, R. L.; Natarajan, L. V.; Pottenger, T.; Fernelius, N. C. *Opt. Lett.* **1992**, *17*, 716.
(178) Yariv, A.; Pepper, D. M. *Opt. Lett.* **1977**, *1*, 16.
(179) Bloom, D. M.; Bjorklund, G. C. *Appl. Phys. Lett.* **1977**, *31*, 592.
(180) Abrams, R. L.; Lind, R. C. *Opt. Lett.* **1978**, *3*, 205.
(181) Abrams, R. L.; Lind, R. C. *Opt. Lett.* **1978**, *2*, 94.
(182) Caro, R. G.; Gower, M. C. *IEEE J. Quantum Electron.* **1982**, *18*, 1376.
(183) Rao, D. N.; Chopra, P.; Ghoshal, S. K.; Swiatkiewicz, J.; Prasad, P. N. *J. Chem. Phys.* **1986**, *84*, 7049.
(184) Rao, D. N.; Swiatkiewicz, J.; Chopra, P.; Ghoshal, S. K.; Prasad, P. N. *Appl. Phys. Lett.* **1986**, *48*, 1187.
(185) Maloney, C.; Byrne, H.; Dennis, W. M.; Blau, W.; Kelly, J. M. *Chem. Phys.* **1988**, *121*, 21.
(186) Prasad, P. N.; Swiatkiewicz, J.; Pfleger, J. *Mol. Cryst. Liq. Cryst.* **1988**, *160*, 53.
(187) Zhao, M. T.; Samoc, M.; Singh, B. P.; Prasad, P. N. *J. Phys. Chem.* **1989**, *93*, 7916.
(188) Samoc, M.; Prasad, P. N. *J. Chem. Phys.* **1989**, *91*, 6643.
(189) Maloney, C.; Blau, W. *J. Opt. Soc. Am. B* **1987**, *4*, 1035.
(190) Winter, C. S.; Oliver, S. N.; Rush, J. D.; Hill, C. A. S.; Underhill, A. E. In ref 16b, p 383.
(191) Chance, R. R.; Shand, M. L.; Hogg, C.; Silbey, R. *Phys. Rev. B* **1980**, *22*, 3540.
(192) Dennis, W. M.; Blau, W.; Bradley, D. J. *Opt. Eng.* **1986**, *25*, 538.
(193) Nunzi, J. M.; Charra, F. *Spec. Publ. R. Soc. Chem.* **1991**, *91*, 249.
(194) Nunzi, J. M.; Charra, F. In ref 16b, p 345.
(195) Carter, G. M. *J. Opt. Soc. Am. B* **1987**, *4*, 1018.
(196) Bolger, J.; Harvey, T. G.; Ji, W.; Kar, A. K.; Molyneux, S.; Wherett, B. S.; Bloor, D.; Norman, P. *J. Opt. Soc. Am. B* **1992**, *9*, 1552.
(197) Bubeck, C.; Grund, A.; Kaltbeitzel, A.; Neher, D.; Mathy, A.; Wegner, G. In ref 16b, p 335.
(198) Du, W.; Chen, K. *Proc. SPIE—Int. Soc. Opt. Eng.* **1992**, *1626*, 55.
(199) Davey, A. P.; Cardin, D. J.; Byrne, H. J.; Blau, W. In ref 16b, p 391.
(200) Norwood, R. A.; Sounik, J. R.; Popolo, J.; Holcomb, D. R. In ref 17b, p 54.
(201) Spangler, C. W.; Saindon, M. L.; Nickel, E. G.; Sapochak, L. S.; Polis, D. W.; Dalton, L. R.; Norwood, R. A. *Proc. SPIE—Int. Soc. Opt. Eng.* **1991**, *1497*, 408.
(202) Zhang, Z.; Wang, D.; Ye, P.; Li, Y.; Wu, P.; Zhu, D. *Opt. Lett.* **1992**, *17*, 973.
(203) Rodenberger, D. C.; Heflin, J. R.; Garito, A. F. *IQEC '92 Tech. Dig. Ser.* **1992**, *9*, 120.
(204) Grischkowsky, D. *Phys. Rev. Lett.* **1970**, *24*, 866.
(205) Grischkowsky, D.; Armstrong, J. A. *Phys. Rev. A* **1972**, *6*, 1566.
(206) Soileau, M. J.; Williams, W. E.; Van Stryland, E. W. *IEEE J. Quantum Electron.* **1983**, *19*, 731.
(207) Marburger, J. H. In Sandom, J. H.; Stenholm, S. *Progress of Quantum Electronics*; Pergamon: New York, 1977; p 35.
(208) Sheik-Bahae, M.; Said, A. A.; Van Stryland, E. W. *Opt. Lett.* **1989**, *14*, 955.
(209) Williams, W. E.; Soileau, M. J.; Van Stryland, E. W. *Opt. Commun.* **1984**, *50*, 256.
(210) Soileau, M. J.; Guha, S.; Williams, W. E.; Van Stryland, E. W.; Vanherzeele, H. *Mol. Cryst. Liq. Cryst.* **1985**, *127*, 321.
(211) Soileau, M. J.; Van Stryland, E. W.; Guha, S. *Mol. Cryst. Liq. Cryst.* **1987**, *143*, 139.
(212) Winter, C. S.; Oliver, S. N.; Rush, J. D. *Opt. Commun.* **1988**, *69*, 45.
(213) Van Stryland, E. W.; Vanherzeele H.; Woodall, M. A.; Soileau, M. J.; Smirl, A. L.; Guha, S.; Boggess, T. F. *Opt. Eng.* **1985**, *24*, 613.

(214) Van Stryland, E. W.; Wu, Y. Y.; Hagan, D. J.; Soileau, M. J.; Mansour, K. *J. Opt. Soc. Am. B* 1988, *5*, 1980.
(215) Sheik-Bahae, M.; Hagan, D. J.; Van Stryland, E. W. *Phys. Rev. Lett.* 1990, *65*, 96.
(216) Sheik-Bahae, M.; Said, A. A.; Wei, T. H.; Wu, Y. Y.; Hagan, D. J.; Soileau, M. J.; Van Stryland, E. W. *Proc. SPIE—Int. Soc. Opt. Eng.* 1990, *1148*, 41.
(217) Soileau, M. J.; Wei, T. H.; Sheik-Bahae, M.; Hagan, D. J.; Sence, M.; Van Stryland, E. W. *Mol. Cryst. Liq. Cryst.* 1991, *207*, 97.
(218) Perry, J. W.; Khundkar, L. R.; Coulter, D. R.; Alvarez, D.; Marder, S. R.; Wei, T. H.; Sence, M. J.; Van Stryland, E. W.; Hagan, D. J. In ref 16b, p 369.
(219) Tutt, L. W.; Kost, A. *Nature* 1992, *356*, 225.
(220) Yang, L.; Dorsinville, R.; Wang, Q. Z.; Ye, P. X.; Alfano, R. R.; Zamboni, R.; Taliani, C. *Opt. Lett.* 1992, *17*, 323.
(221) Sheik-Bahae, M.; Wang, J.; DeSalvo, R.; Hagan, D. J.; Van Stryland, E. W. *Opt. Lett.* 1992, *17*, 258.
(222) Qian, Q.; Wang, Z. *Proc. SPIE—Int. Soc. Opt. Eng.* 1992, *1979*, 662.
(223) Buckingham, A. D. *Proc. Phys. Soc. London Sect. B* 1956, *69*, 344.
(224) Kerr, J. *Philos. Mag.* 1875, *50*, 377.
(225) Mayer, G.; Gires, R. *C. R. Acad. Sci.* 1963, *258*, 2039.
(226) Maker, P. D.; Terhune, R. W.; Savage, C. W. *Phys. Rev. Lett.* 1964, *12*, 507.
(227) Veduta, A. P.; Kirsanov, B. P. *Sov. Phys. JETP* 1968, *27*, 736.
(228) Duguay, M. A.; Hansen, J. *Appl. Phys. Lett.* 1969, *15*, 192.
(229) Shimizu, F.; Stoicheff, B. P. *IEEE J. Quantum Electron.* 1969, *5*, 544.
(230) Wong, G. K. L.; Shen, Y. R. *Phys. Rev. A* 1974, *10*, 1277.
(231) Ippen, E.; Shank, C. *Appl. Phys. Lett.* 1975, *26*, 92.
(232) Ho, P. P.; Alfano, R. R. *Phys. Rev. A* 1979, *20*, 2170.
(233) Ho, P. P. In *Semiconductors Probe by Ultrafast Laser Spectroscopy*; Alfano, R. R., Ed.; Academic: New York, 1984; p 409.
(234) Kobayashi, T.; Terasaki, A.; Hattori, T.; Kurokawa, K. *Appl. Phys. B* 1988, *47*, 107.
(235) Guha, S.; Frazier, C. C.; Porter, P. L.; Kang, K.; Finberg, S. E. *Opt. Lett.* 1989, *14*, 952.
(236) Yang, L.; Dorsinville, R.; Wang, Q. Z.; Zou, W. K.; Ho, P. P.; Yang, N. L.; Alfano, R. R.; Zamboni, R.; Danieli, R.; Ruani, G.; Taliani, C. *J. Opt. Soc. Am. B* 1989, *6*, 753.
(237) Foggi, P.; Kamalov, V. F.; Righini, R.; Torre, R. *Opt. Lett.* 1992, *17*, 775.
(238) Guha, S.; Kang, K.; Porter, P.; Roach, J. F.; Remy, D. E.; Aranda, F. J.; Rao, D. V. G. L. N. *Opt. Lett.* 1992, *17*, 264.
(239) Xuan, N. P.; Ferrier, J. L.; Gazengel, J.; Rivoire, G. *Opt. Commun.* 1984, *51*, 433.
(240) Choy, M. M.; Byer, R. L. *Phys. Rev. B* 1976, *14*, 1693.
(241) Etemad, S.; Soos, Z. G. In *Spectroscopy of Advanced Materials*; Clark, R. J. H., Hester, R. E., Eds.; Wiley: New York, 1991; p 87.
(242) Etemad, S.; Baker, G. L.; Soos, Z. G. In *Nonlinear Optical Properties of Organic Molecules and Crystals*; Zyss, J., Ed.; Vol. 3, to be published.
(243) Kuhn, H. *J. Chem. Phys.* 1949, *17*, 1198.
(244) André, J. M. Etude comparative des méthodes de Hückel et de l'électron libre (Comparative Study of the Hückel and Free-Electron Methods). Ms. Sc. Thesis, Université Catholique de Louvain, Leuven, Belgium, 1965.
(245) Bodart, V. P.; Delhalle, J.; André, J. M. In ref 18, p 509.
(246) Tolbert, L. M. *Acc. Chem. Res.* 1992, *25*, 561.
(247) Malhotra, S. S.; Whiting, M. C. *J. Chem. Soc.* 1960, 3812.
(248) Kohler, B. E. *J. Chem. Phys.* 1990, *93*, 5838.
(249) Rustagi, K. C.; Ducuing, J. *Opt. Commun.* 1974, *10*, 258.
(250) Kuhn, C. *Synth. Met.* 1991, *41–43*, 3681.
(251) Matsumoto, S.; Kubodera, K.; Kurihara, T.; Kaino, T. *Opt. Commun.* 1990, *76*, 147.
(252) Dirk, C. W.; Kuzyk, M. G. *Chem. Mater.* 1990, *2*, 4. Dirk, C. W.; Kuzyk, M. G. *Proc. SPIE—Int. Soc. Opt. Eng.* 1989, *1147*, 18.
(253) Zhou, Q. L.; Shi, R. F.; Zamani-Khamari, O.; Garito, A. F. *Nonlinear Opt.*, in press.
(254) (a) Soos, Z. G.; Ramasesha, S. *Phys. Rev. B* 1984, *29*, 5410. (b) Ramasesha, S.; Soos, Z. G. *J. Chem. Phys.* 1984, *80*, 3278.
(255) (a) Mazumdar, S.; Dixit, S. N. *Phys. Rev. Lett.* 1983, *51*, 292. (b) Mazumdar, S.; Campbell, D. K. *Phys. Rev. Lett.* 1985, *55*, 2067.
(256) (a) de Melo, C. P.; Silbey, R. *Chem. Phys. Lett.* 1987, *140*, 537. (b) de Melo, C. P.; Silbey, R. *J. Chem. Phys.* 1988, *88*, 2567.
(257) Beljonne, D.; Brédas, J. L. *J. Opt. Soc. Am. B*, submitted for publication.
(258) Bodart, V.; Delhalle, J.; André, J. M. In *Electronic Properties of Polymers and Related Compounds*; Kuzmany, H., Mehring, M., Roth, S., Eds.; Springer Series in Solid State Sciences; Springer Verlag: Berlin, 1985; Vol. 63, p 148.
(259) Gorman, C. B.; Marder, S. R. *Proc. Natl. Acad. Sci. U.S.A.* 1993, in press.
(260) Marder, S. R.; Perry, J. W. *J. Am. Chem. Soc.* 1993, *115*, 2524.
(261) Craig, G. S. W.; Cohen, R. E.; Schrock, R. R.; Silbey, R. J.; Pucetti, G.; Ledoux, I.; Zyss, J. *J. Am. Soc.* 1993, *115*, 860.
(262) Gorman, C. B.; Crubbs, R. R. In *Conjugated Polymers*; Brédas, J. L., Silbey, R., Eds.; Kluwer: Dordrecht, 1991; p 1.
(263) Schrock, R. R. *Acc. Chem. Res.* 1990, *24*, 1580.

(264) (a) Greene, B. I.; Orenstein, J.; Millard, R. R.; Williams, L. R. *Phys. Rev. Lett.* 1987, *58*, 2750. (b) Greene, B. I.; Mueller, J. F.; Orenstein, J.; Rapkine, D. H.; Schmitt-Rink, S.; Thakur, M. *Phys. Rev. Lett.* 1988, *61*, 325. (c) Greene, B. I.; Orenstein, J.; Schmitt-Rink, S. *Science* 1990, *247*, 679.
(265) Charra, F.; Messier, J. In ref 18, p 409.
(266) Hone, D.; Singh, C. *Phys. Rev. B* 1992, *45*, 3455.
(267) Beratan, D. N. *J. Phys. Chem.* 1989, *93*, 3915.
(268) Nickel, E. G.; Spangler, C. W.; Tang, N.; Hellwarth, R.; Dalton, L. *Nonlinear Opt.* 1993, in press.
(269) (a) Shirakawa, H.; Ikeda, S. *Polym. J.* 1971, *2*, 231. (b) Ito, T.; Shirakawa, H.; Ikeda, S. *J. Polym. Sci. Polym. Chem. Educ.* 1974, *12*, 11.
(270) (a) Chiang, C. K.; Fincher, C. R., Jr.; Park, Y. W.; Heeger, A. J.; Shirakawa, H.; Gau, S. C.; MacDiarmid, A. G. *Phys. Lett.* 1977, *39*, 1098. (b) Shirakawa, H.; Louis, E.; MacDiarmid, A.; Chaing, C.; Heeger, A. J. *J. Chem. Soc., Chem. Commun.* 1977, 758.
(271) (a) Naarmann, H. *Synth. Met.* 1987, *17*, 223. (b) Naarmann, H.; Theophilou, N. *Synth. Met.* 1987, *17*, 22.
(272) Basescu, N.; Liu, Z. X.; Moses, D.; Heeger, A. J.; Naarman, H.; Theophilou, N. *Nature* 1987, *327*, 403.
(273) (a) Edwards, J. H.; Feast, J. W. *Polym. Commun.* 1980, *21*, 595. (b) Edwards, J. H.; Feast, J. W.; Bott, D. C. *Polymer* 1984, *25*, 395.
(274) Sinclair, M.; Moses, D.; Akagi, K.; Heeger, A. J.; Yu, J.; Su, W. P. *Synth. Met.* 1989, *28*, D655.
(275) (a) Kajzar, F.; Etemad, S.; Baker, G. L.; Messier, J. *Synth. Met.* 1987, *17*, 563. (b) Kajzar, F.; Etemad, S.; Baker, G. L.; Messier, J. *Solid State Commun.* 1987, *63*, 1113.
(276) (a) Halvorson, C.; Hagler, T. W.; Moses, D.; Cao, Y.; Heeger, A. J. *Synth. Met.* 1993, *55–57*, 3961. (b) Hagler, T. W.; Heeger, A. J. *Chem. Phys. Lett.* 1992, *189*, 333.
(277) Heeger, A. J.; Kivelson, S.; Schrieffer, J. R.; Su, W. P. *Rev. Mod. Phys.* 1988, *60*, 781.
(278) Karpfen, A.; Petkov, J. *Theor. Chim. Acta* 1979, *53*, 65.
(279) (a) Etemad, S.; Mitani, M.; Ozaki, M.; Chung, T. C.; Heeger, A. J.; MacDiarmid, A. G. *Solid State Commun.* 1981, *40*, 75. (b) Blanchet, G. B.; Fincher, C. R.; Heeger, A. J. *Phys. Rev. Lett.* 1983, *51*, 2132.
(280) (a) Hayden, G. W.; Mele, E. J. *Phys. Rev. B* 1985, *32*, 6527. (b) Hayden, G. W.; Mele, E. J. *Phys. Rev. B* 1986, *34*, 2988.
(281) Campbell, D. K.; TinkaGammel, J.; Lin, H. Q.; Loh, E. Y. *Synth. Met.* 1992, *50*, 631.
(282) (a) Su, W. P. *Solid State Commun.* 1982, *42*, 497. (b) Fradkin, E.; Hirsch, J. E. *Phys. Rev. B* 1983, *27*, 1680.
(283) Wegner, G. *Z. Naturforsch. B* 1969, *24*, 824.
(284) Wegner, G. In *Molecular Metals*; Hatfield, W. E., Eds.; Plenum: New York, 1979; p 209.
(285) Bloor, D., Chance, R. R., Eds. *Polydiacetylenes: Synthesis, Structure and Electronic Properties*; NATO-ARW Series; Martinus-Nijhof: Dordrecht, 1985; Vol. E102.
(286) Carter, G. M.; Hryniewicz, J. V.; Thakur, M. K.; Chen, Y. J.; Meyler, S. E. *App. Phys. Lett.* 1986, *49*, 998.
(287) Ziemelis, K.; Hussain, A. T.; Bradley, D. D. C.; Friend, R. H.; Riihe, J.; Wegner, G. *Phys. Rev. Lett.* 1991, *66*, 2231.
(288) Gelsen, O. M.; Bradley, D. D. C.; Murata, H.; Takada, N.; Toutsui, T.; Saito, S. *J. Appl. Phys.* 1992, *71*, 1064.
(289) Sinclair, M.; McBranch, D.; Hagler, T. W.; Heeger, A. J. *Synth. Met.* 1992, *50*, 593.
(290) Kaino, T.; Kurihara, T.; Kubodera, K.; Kanbara, H. In ref 20, p 704.
(291) Kajzar, F.; Messier, J.; Sentein, C.; Elsenbaumer, R. L.; Miller, G. G. *Proc. SPIE—Int. Soc. Opt. Eng.* 1989, *1147*, 36.
(292) Kajzar, F.; Ruani, G.; Taliani, C.; Zamboni, R. *Synth. Met.* 1990, *37*, 223.
(293) (a) Yoshizawa, M.; Yasuda, A.; Kobayashi, T. *Appl. Phys. B* 1991, *53*, 296. (b) Kobayashi, T.; Yoshizawa, M. *Synth. Met.* 1991, *41–43*, 3129. (c) Kobayashi, T. *Synth. Met.* 1992, *50*, 565. (d) Kobayashi, T.; Yoshizawa, M.; Stamm, U.; Taiji, M.; Hasegawa, M. *J. Opt. Soc. Am. B* 1990, *7*, 1558. (e) Cheng, X.; Ichimura, K.; Fichou, D.; Kobayashi, T. *Chem. Phys. Lett.* 1991, *185*, 286.
(294) Hattori, T.; Okawa, H.; Wada, T.; Sasabe, H. *Opt. Lett.* 1992, *17*, 1560.
(295) Torruellas, W. E.; Neher, D.; Zanoni, R.; Stegeman, G. I.; Kajzar, F.; Leclerc, M. *Chem. Phys. Lett.* 1990, *175*, 11.
(296) Birnbaun, D.; Kohler, B. E. *J. Chem. Phys.* 1992, *96*, 2492.
(297) (a) Tavan, P.; Schulten, K. *J. Chem. Phys.* 1986, *85*, 6602. (b) Tavan, P.; Schulten, K. *Phys. Rev. B* 1987, *86*, 4337.
(298) Periasamy, N.; Danieli, R.; Ruani, G.; Zamboni, R.; Taliani, C. *Phys. Rev. Lett.* 1992, *68*, 919.
(299) Pfeffer, N.; Raimond, P.; Charra, F.; Nunzi, J. M. *Chem. Phys. Lett.* 1993, *201*, 357.
(300) Brédas, J. L.; Heeger, A. *Macromolecules* 1990, *23*, 1150.
(301) Brédas, J. L.; Meyers, F.; Heeger, A. J. In ref 16b, p 23.
(302) Vardeny, Z.; Ehrenfreund, E.; Brafman, O.; Nowak, M.; Schaffer, H.; Heeger, A. J.; Wudl, F. *Phys. Rev. Lett.* 1986, *56*, 671.
(303) Vardeny, Z.; Grahn, H. T.; Heeger, A. J.; Wudl, F. *Synth. Met.* 1989, *28*, C299.
(304) Gagnon, D. R.; Capistran, J. D.; Karasz, F. E.; Lenz, R. W.; Antoun, S. *Polymer* 1987, *28*, 567.
(305) Colaneri, N. F.; Bradley, D. D. C.; Friend, R. H.; Burn, P. L.; Holmes, A. B.; Spangler, C. W. *Phys. Rev. B* 1990, *42*, 11671.

(306) Shi, S.; Wudl, F. In ref 18, p 83.
(307) Burroughes, J. H.; Bradley, D. D. C.; Brown, A. R.; Marks, R. N.; MacKay, K.; Friend, R. H.; Burn, P. L.; Holmes, A. B. *Nature* **1990**, *347*, 539.
(308) Gustafson, G.; Cao, Y.; Treacy, G. M.; Klavetter, N.; Colaneri, N.; Heeger, A. J. *Nature* **1992**, *357*, 477.
(309) Halliday, D. A.; Burn, P. L.; Bradley, D. D. C.; Friend, R. H.; Gelsen, O. M.; Holmes, A. B.; Kraft, A.; Martens, J. H. F.; Pichler, K. *Adv. Mater.* **1993**, *5*, 40.
(310) Soos, Z. G.; Etemad, S.; Galvao, D. S.; Ramasesha, S. *Chem. Phys. Lett.* **1992**, *194*, 341.
(311) Soos, Z. G.; Ramasesha, S.; Galvao, D. S.; Kepler, R. G.; Etemad, S. *Synth. Met.* **1992**, *54*, 35.
(312) MacDiarmid, A. G.; Chiang, J. C.; Halpern, M.; Huang, W. S.; Mu, S. L.; Somasiri, N. L. D.; Wu, W.; Yaniger, S. I. *Mol. Cryst. Liq. Cryst.* **1985**, *121*, 173.
(313) (a) MacDiarmid, A. G.; Epstein, A. J. *Faraday Discuss. Chem. Soc.* **1989**, *88*, 317. (b) Epstein, A. J.; MacDiarmid, A. G. *Makromol. Chem., Macromol. Symp.* **1991**, *51*, 217.
(314) Brédas, J. L. In *Proceedings of the Nobel Symposium on Conjugated Polymers and Related Materials*; Salaneck, W. R., Lundström, I., Rånby, B., Eds.; Oxford Science Publications: Oxford, 1993; p 187.
(315) Heeger, A. J.; Smith, P. In *Conjugated Polymers*; Brédas, J. L., Silbey, R., Eds.; Kluwer: Dordrecht, 1991; p 141.
(316) Epstein, A. J. In *Conjugated Polymers*; Brédas, J. L., Silbey, R., Eds.; Kluwer: Dordrecht, 1991; p 211.
(317) dos Santos, M. C.; Brédas, J. L. *Phys. Rev. Lett.* **1989**, *62*, 2499.
(318) Cao, Y.; Smith, P.; Heeger, A. J. *Synth. Met.* **1992**, *48*, 91.
(319) Halvorson, C.; Cao, Y.; Moses, D.; Heeger, A. J. *Synth. Met.* **1993**, *55–57*, 3941.
(320) Osaheni, J. A.; Jenekhe, A. S.; Vanherzeele, H.; Meth, J. S.; Sun, Y.; MacDiarmid, A. G. *J. Phys. Chem.* **1992**, *96*, 2830.
(321) Garito, A. F.; Wong, K. Y.; Zamani-Khamiri, O. In ref 19, p 13.
(322) (a) Brédas, J. L.; Dory, M.; Thémans, B.; Delhalle, J.; André, J. M. In ref 17a, p 42. (b) Brédas, J. L. In *Photoresponsive Materials*; Tazuke, S., Ed.; Materials Research Society International Symposium Series; Materials Research Society: Pittsburgh, PA, 1989; Vol. 12, p 33.
(323) Brédas, J. L.; Meyers, F. In *Organics Materials for Nonlinear Optics III*; Ashwell, G. J., Bloor, D., Eds.; Royal Society Chemistry: London, 1993; p 129.
(324) Brédas, J. L.; Dehu, C.; Meyers, F.; Persoons, A.; Zyss, J. *Nonlinear Optics* **1993**, in press.
(325) Wang, Y.; Cheng, L. T. *J. Phys. Chem.* **1992**, *96*, 1530.
(326) Shuai, Z.; Brédas, J. L. *Phys. Rev. B* **1992**, *46*, 16135.
(327) Zyss, J. *Nonlinear Opt.* **1991**, *1*, 3.
(328) Zerbi, G.; Gussoni, M.; Castiglioni, C. In *Conjugated Polymers*; Brédas, J. L., Silbey, R., Eds.; Kluwer: Dordrecht, 1991; p 435.
(329) Pelous, Y.; Froyer, G.; Hérold, C.; Lefrant, S. *Synth. Met.* **1989**, *29*, E17.
(330) Brédas, J. L.; Thémans, B.; Fripiat, J. G.; André, J. M.; Chance, R. R. *Phys. Rev. B* **1984**, *29*, 6761.
(331) Brédas, J. L.; Wudl, F.; Heeger, A. J. *Solid State Commun.* **1987**, *63*, 577.
(332) Prasad, P. N. In ref 15, p 271.
(333) Miller, R. D.; Michl, J. *J. Chem. Rev.* **1989**, *89*, 1359.
(334) Miller, R. D.; Schellenberg, F. M.; Baumert, J. C.; Looser, Y. H.; Shukla, P.; Torruellas, W.; Bjorklund, G. C.; Kano, S.; Takahashi, Y. In ref 20, p 636.
(335) Kajzar, F.; Messier, J.; Rosilio, C. *J. Appl. Phys.* **1986**, *60*, 3040.
(336) McGraw, D. J.; Siegman, A. E.; Miller, R. D. *Appl. Phys. Lett.* **1989**, *84*, 1713.
(337) Yang, L.; Wang, Q. Z.; Ho, P. P.; Dorsenville, R.; Alfano, R. R.; Zou, W. K.; Yang, N. L. *Appl. Phys. Lett.* **1988**, *53*, 1245.
(338) Schellenberg, F.; Byer, R. L.; Miller, R. D. *Chem. Phys. Lett.* **1990**, *166*, 331.
(339) Trefonas, P.; West, R.; Miller, R. D.; Hofer, D. *J. Polym. Sci. Polym. Lett. Educ.* **1983**, *21*, 823.
(340) Miller, R. D.; Rabolt, J. F.; Sooriyakumaran, R.; Fleming, W.; Fickes, G. N.; Farmer, B. L.; Kuzmany, H. In *Inorganic and Organometallic Polymers*; Zeldin, M.; Wynne, K. J.; Allcock, H. R. Eds.; ACS Symposium Series No. 360, American Chemical Society: Washington, DC, 1987; Chapter 4 and references cited therein.
(341) Hasegawa, T.; Iwosa, Y.; Sunamura, H.; Koda, T.; Tokura, Y.; Tachibana, H.; Matsumoto, M.; Abe, S. *Phys. Rev. Lett.* **1992**, *69*, 668.
(342) Roberts, M. F.; Jenekhe, S. A. *Chem. Mater.* **1990**, *2*, 629.
(343) Yu, L.; Polis, D. W.; McLean, M. R.; Dalton, L. R. In *Electroresponsive Molecular and Polymeric Systems*; Skotheim, T. A., Ed.; Marcel Dekker: New York, 1991; Vol. 2, p 113.
(344) (a) Robertson, J. M. *J. Chem. Soc.* **1935**, 615. (b) Robertson, J. M. *J. Chem. Soc.* **1936**, 1195. (c) Linstead, R. P.; Robertson, J. M. *J. Chem. Soc.* **1936**, 1736. (d) Robertson, J. M.; Woodward, I. *J. Chem. Soc.* **1937**, 219.
(345) See, for example: Simon, J.; André, J. J. *Molecular Semiconductors*; Springer: Berlin, 1985; Chapter III.
(346) (a) Lever, A. B. P.; Hempstead, M. R.; Leznoff, C. C.; Lin, W.; Melnik, M.; Nevin, W. A.; Seymour, P. *Pure Appl. Chem.* **1986**, *58*, 1467. (b) Lever, A. B. P. *Adv. Inorg. Chem. Radiochem.* **1965**, *7*, 27.
(347) (a) Meier, H. *Organic Semiconductors*; Verlag Chemie: Weinheim, 1974. (b) Pope, M.; Swenberg, C. E. *Electronic Processes in Organic Crystals*; Clarendon: Oxford, 1982.
(348) (a) Loutfy, R. O.; Sharp, J. H. *J. Chem. Phys.* **1979**, *71*, 1211. (b) Tang, C. W. *Appl. Phys. Lett.* **1986**, *48*, 183.
(349) Loutfy, R. O.; Hor, A. M.; Hsiao, C. K.; Baranyi, G.; Kazmaier, P. *Pure Appl. Chem.* **1988**, *60*, 1047.
(350) Kato, M.; Nishioka, Y.; Kaifu, K.; Kawamura, K.; Ohno, S. *Appl. Phys. Lett.* **1985**, *46*, 196.
(351) (a) Collins, R. A.; Mohamed, K. A. *J. Phys. D* **1988**, *21*, 154. (b) Temofonte, T. A.; Schoch, K. F. *J. Appl. Phys.* **1989**, *65*, 1350. (c) Sadaoka, Y.; Jones, T. A.; Göpel, W. *Sensors Actuators B* **1990**, *1*, 148.
(352) Abe, K.; Sato, H.; Kimura, T.; Ohkatsu, Y.; Kusano, T. *Makromol. Chem.* **1989**, *190*, 2693.
(353) For recent reviews, see: (a) Marks, T. J. *Science* **1985**, *227*, 881. (b) Marks, T. J. *Angew. Chem., Int. Ed. Engl.* **1990**, *29*, 857. (c) Hoffman, B. M.; Ibers, J. A. *Acc. Chem. Res.* **1983**, *16*, 15. (d) Palmer, S. M.; Stanton, J. L.; Martinsen, J.; Ogawa, M. Y.; Hener, W. B.; Van Wallendael, S. E.; Hoffman, B. M.; Ibers, J. A. *Mol. Cryst. Liq.* **1985**, *125*, 1. (e) Hanack, M.; Datz, A.; Fay, R.; Fischer, K.; Keppeler, U.; Koch, J.; Metz, J.; Mezger, M.; Schneider, O.; Schulze, H. J. In *Handbook of Conducting Polymers*; Skotheim, T. A., Ed.; Marcel Dekker: New York, 1986; p 133.
(354) (a) Corker, G.; Grant, B.; Clecak, C. *J. Electrochem. Soc.* **1979**, *126*, 1339. (b) Collins, G. C. S.; Schiffrin, D. J. *J. Electrochem. Soc.* **1985**, *132*, 1835. (c) Riou, M.-T.; Clarisse, C. *J. Electroanal. Chem.* **1988**, *249*, 181.
(355) Kuder, J. E. *J. Imag. Sci.* **1988**, *32*, 51.
(356) (a) Roberts, G. G.; Petty, M. C.; Baker, S.; Fowler, M. T.; Thomas, N. J. *Thin Solid Films* **1985**, *132*, 113. (b) Cook, M. J.; Dunn, A. J.; Daniel, M. F.; Hart, R. C. O.; Richardson, R. M.; Roser, S. J. *Thin Solid Films* **1988**, *159*, 395. (c) Palacin, S.; Lesieur, P.; Stefanelli, I.; Barraud, A. *Thin Solid Films* **1988**, *159*, 83.
(357) (a) Van der Pol, J. F.; Neeleman, E.; Zwikker, J. W.; Nolte, R. J. M.; Drenth, W.; Aerts, J.; Visser, R.; Picken, S. J. *Liq. Cryst.* **1989**, *6*, 577. (b) Simon, J.; Sirlin, C. *Pure Appl. Chem.* **1989**, *61*, 1625.
(358) (a) Casstevens, M. K.; Samoc, M.; Pfleger, J.; Prasad, P. N. *J. Chem. Phys.* **1990**, *92*, 2019. (b) Prasad, P. N.; Caststevens, M. K.; Samoc, M. *Proc. SPIE—Int. Soc. Opt. Eng.* **1989**, *1056*, 117.
(359) Simon, J.; Bassoul, P.; Norvez, S. *New J. Chem.* **1989**, *13*, 13.
(360) Coulter, D. R.; Miskowski, V. M.; Perry, J. W.; Wei, T. H.; Van Stryland, E. W.; Hagan, D. J. *Proc. SPIE—Int. Soc. Opt. Eng.* **1989**, *1105*, 42.
(361) (a) Bubeck, C.; Neher, D.; Kaltbeitzel, A.; Duda, G.; Arndt, T.; Sauer, T.; Wegner, G. In ref 16a, p 185. (b) Neher, D.; Kaltbeitzel, A.; Wolf, A.; Bubeck, C.; Wegner, G. In ref 18, p 387.
(362) Hosoda, M.; Wada, T.; Yamamoto, T.; Kaneko, A.; Garito, A. F.; Sasabe, H. *Jpn. J. Appl. Phys.* **1992**, *31*, 1071.
(363) Hosoda, M.; Wada, T.; Garito, A. F.; Sasabe, H. *Jpn. J. Appl. Phys.* **1992**, *31*, L249.
(364) Wada, T.; Hosoda, M.; Sasabe, H. In *Molecular and Biomolecular Electronics*; Birge, R. R., Ed.; American Chemical Society: Washington, in press.
(365) Wu, J. W.; Heflin, J. R.; Norwood, R. A.; Wong, K. Y.; Zamani-Khamiri, O.; Garito, A. F.; Kabyanaraman, P.; Sounik, J. *J. Opt. Soc. Am. B* **1989**, *6*, 707.
(366) Shirk, J. S.; Lindle, J. R.; Bartoli, F. J.; Kafafi, Z. H., Snow, A. W. In ref 20, p 626.
(367) Schaffer, A. M.; Gouterman, M.; Davidson, E. R. *Theor. Chim. Acta* **1973**, *30*, 9.
(368) Stillman, M. J.; Nyokong, T. In *Phthalocyanines*; Leznoff, C., Lever, A. B. P., Eds.; VCH: New York, 1989; p 133.
(369) (a) Krätschmer, W.; Lamb, L. D.; Fostiropoulos, K.; Huffman, D. R. *Nature* **1990**, *347*, 354. (b) Krätschmer, W., Fostiropoulos, K.; Huffman *Chem. Phys. Lett.* **1990**, *170*, 167.
(370) (a) Kroto, H. W.; Heath, S. C.; Curl, R. F.; Smalley, R. E. *Nature* **1985**, *318*, 162. (b) Heath, J. R.; Curl, R. F.; Smalley, R. E. *J. Chem. Phys.* **1987**, *87*, 4236. (c) Yang, S. H.; Pettiette, C. L., Conceiao, J.; Cheshnovsky, O.; Smalley, R. E. *Chem. Phys. Lett.* **1987**, *139*, 233. (d) Miller, J. S. *Adv. Mater.* **1991**, *3*, 262.
(371) Blau, W. J.; Byrne, H. J.; Cardin, D. J.; Dennis, T. J.; Hare, J. P.; Kroto, H. W.; Taylor, R.; Walton, D. R. M. *Phys. Rev. Lett.* **1991**, *67*, 1423.
(372) Yang, S.; Gong, Q.; Xia, Z.; Zhou, Y.; Wu, Y.; Qiang, D.; Sun, Y.; Gu, Z. *Appl. Phys. B*, in press.
(373) Wang, Y.; Cheng, L. T. *J. Phys. Chem.* **1992**, *96*, 1530.
(374) (a) Kafafi, Z. H.; Lindle, J. R.; Pong, R. G. S.; Bartoli, F. J.; Lingg, L. J.; Milliken, J. *Chem. Phys. Lett.* **1992**, *188*, 492. (b) Kafifi, Z. H.; Bartoli, F. J.; Lindle, J. R.; Pong, R. G. S. *Phys. Rev. Lett.* **1992**, *68*, 2705.
(375) Kajzar, F.; Taliani, C.; Zamboni, R.; Rossini, S.; Danieli, R. *Synth. Met.* **1993**, *54*, 21.
(376) Assanto, G.; Stegeman, G. I.; Sheik-Bahae, M.; Van Stryland, E. W. *Appl. Phys. Lett.* **1993**, *62*, 1323.